

Performance Evaluation of Microbial Fuel Cell for Removing Chromium from Textile Wastewater

Thesis Submitted in Partial Fulfillment of the Requirements for the Degree of

MASTER OF SCIENCE IN CHEMICAL ENGINEERING

by

Abdullah Al Moinee

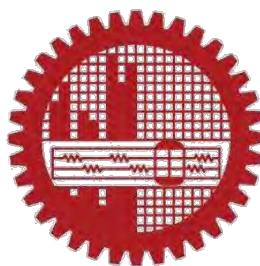
0417022017 P

SUPERVISED BY:

Dr. Nahid Sanzida

Associate Professor

Department of Chemical Engineering, BUET



Department of Chemical Engineering


BANGLADESH UNIVERSITY OF ENGINEERING AND TECHNOLOGY

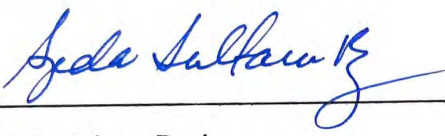
March 2020


CERTIFICATION

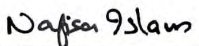
This is to certify that the thesis entitled '**Performance Evaluation of Microbial Fuel Cell to Remove Chromium from Textile Wastewater**' which is submitted by **Abdullah Al Moinee**, 0417022017P to the Department of Chemical Engineering, BUET, has been accepted as satisfactory in partial fulfillment for the award of degree of **Master of Science in Chemical Engineering** on **March 16, 2020**.


BOARD OF EXAMINERS

1. 

Dr. Nahid Sanzida
Associate Professor
Department of Chemical Engineering, BUET, Dhaka
Chairman
(Supervisor)
2. 

Dr. Syeda Sultana Razia
Professor and Head of the Department
Department of Chemical Engineering, BUET, Dhaka
Member (Ex-Officio)
3. 

Dr. Md. Ali Ahammad Shoukat Choudhury
Professor
Department of Chemical Engineering, BUET, Dhaka
Member
4. 

Dr. Nafisa Islam
Assistant Professor
Department of Chemical Engineering, BUET, Dhaka
Member
5. 

Dr. Sheikh Md. Enayetul Babar
Professor
Department of Biotechnology and Genetic Engg. Discipline
Khulna University
Member (External)

DECLARATION

This is to certify that the thesis (ChE 6000) entitled ‘Performance Evaluation of Microbial Fuel Cell to Remove Chromium from Textile Wastewater’ which is submitted by me in partial fulfillment for the award of degree of Master of Science in Chemical Engineering to the Department of Chemical Engineering, Bangladesh University of Engineering and Technology (BUET) comprises only my original work and has not been submitted for the award of any other degree.

March 16, 2020.

Abdullah Al Moinee

Abdullah Al Moinee

Student ID: 0417022017 P

Department of Chemical Engineering,

Bangladesh University of Engineering and Technology (BUET),

Dhaka – 1000

ACKNOWLEDGEMENT

First and foremost, I would like to express my profound gratitude to the Almighty for His boundless blessings and gracious guidance throughout my life.

Sustaining the sense of sincere gratitude, I feel greatly obliged to revere and thank my supervisor, Dr. Nahid Sanzida, Associate Professor, Department of Chemical Engineering, Bangladesh University of Engineering and Technology, for her wonderful guidance, encouragement, and aspiration from the beginning to the end of the thesis. It was a great privilege to be supervised and mentored by a brilliant researcher and I am very grateful for all her supports and suggestions throughout the years. The research interactions had always been an invaluable learning experience by dint of her meticulous discussions, perpetual guidelines, constructive remarks, technical management, congenial cooperation, and inspirational instructions.

It is a matter of immense pride to convey my esteemed gratitude to the Boards of Postgraduate Studies (BPGS), ChE, BUET for their constructive criticism and intellectual inspection that added significant meaning to this study. I place on record my sincere gratitude to Committee for Advanced Studies and Research (CASR), BUET for encouraging me to think critically and work inherently for shaping the salient standards.

I would like to convey my gratitude to the personnel of the laboratories of the Department of Chemical Engineering (ChE), BUET, for their ever technical support. I register my sincere gratitude to Mr. Omar Faruk for remaining always to the aid of this research and strengthening the thesis by means of valuable knowledge and indispensable instructions. I acknowledge profuse thanks to Mr. Mahbubur Rahman Khan for corroborating in constructing the experimental design. I am truly very thankful to Engr. Toriqul Islam, Mr. Jashim Uddin, Engr. Sudarshan Sarker and the fellow researchers for their inspiration and coherent cooperation.

The research work had been aided by significant technical supports of the Department of Glass and Ceramic Engineering (GCE). In this regards, I owe my earnest thanks to Mr. Rana and Ms. Saima Haque for reinforcing this research work by sharing their perspicuous knowledge during analytical experiments.

I am grateful to Mr. Rafiq and Mr. Amar for their support and cooperation to perform experimental works on the wastewater of their Effluent Treatment Plant. I would also like to thank the chemist, microbiologists, and engineers for their convivial cooperation.

It's my fortune to gratefully acknowledge the contribution of all the experts for the availability of their invaluable knowledge through their books, research papers, and articles referenced by this thesis.

Most importantly, I would like to thank my parents and brother for being the enormous source of inspiration when their belief, patience, and prayer always encourage and fuel the flow of this research work.

Abdullah Al Moinee

March, 2020

ABSTRACT

Textile industry is one of the largest industries in Bangladesh. The industries discharge a large volume of wastewater containing organic pollutants and heavy metals. Heavy metal contamination in water is a serious threat to environment and human health. Chromium is a strictly regulated heavy metal in wastewater due to its high toxicity at low concentration. Heavy metals are difficult to remove in conventional wastewater treatment approaches because they are bio-accumulating, non-biodegradable, and more persistent than organic pollutants. Advanced treatment methods e.g. membrane filtration or ion exchange, can be applied but they often require a high energy input and a large amount of chemicals for pre- or post-treatment. Microbial fuel cell (MFC) is full of promise to take the edge off environment pollution. MFC can be used without these external and expensive requirements of wastewater treatment. The microbial metabolism enables MFC to produce bio-electricity simultaneously while removing chromium from waste water. This research work evaluated the performance of MFC for bioelectricity generation as well as removing chromium from textile wastewater. In order to develop an energy-efficient and cost-effective cell, the performance was analyzed by power density and coulombic efficiency. On the other hand, the removal percentages of total chromium and chemical oxygen demand (COD) provided waste removal efficiency of the MFC. This research progressed with a gradual development of an experimental setup by considering the optimum effect of electrode materials, aeration, salt bridge, and nutrient. The novelty and significance of this system is that it uses an uncomplicated and economical salt bridge which replaces costly membranes like Nafion. As a result, the lab-scale MFC operations demonstrated successful microbial bioremediation of chromium. The commonly investigated removal mechanism for heavy metals in MFCs is reduction at the cathode. However, this thesis work emphasized the anodic removal of chromium to highlight the microbial mechanism for removing chromium from textile wastewater. The fully developed MFC resulted in 53.75% removal of chromium from the anodic chamber where the initial concentration of Cr was less than 1 mg/L. The analytical assessment of SEM – EDX and XRD provided the surface morphology, mass percentage, and elemental identification of chromium in the anode. The analytical experiments of anode also confirmed the active presence of microbes for removing chromium from textile wastewater.

TABLE OF CONTENTS

	PAGE NO
Certification	i
Declaration	ii
Acknowledgement	iii
Abstract	v
Table of Contents	vi
List of Figures	ix
List of Tables	xii
CHAPTER 1	
INTRODUCTION	1
1.1 Introduction	2
1.2 Present State of Research	3
1.3 Research Aim and Objectives	5
1.4 Scope of the Research	6
1.5 Thesis Structure	7
1.6 Research Contribution	8
CHAPTER 2	
LITERATURE REVIEW	9
2.1 Textile Industries and Water Pollution in Bangladesh	10
2.2 Basic Principles of Microbial Fuel Cell (MFC)	14
2.3 Chromium removal mechanism of Microbial Fuel Cell	18
2.3.1 Microbial Approaches to Transfer Electrons	18
2.3.2 Electrochemical Phenomena of Microbial Fuel Cell	20
2.3.3 Metabolic Interactions between Microbes and Metals	22
2.3.4 Biochemical Phenomena of Microbial Fuel Cell	23
2.3.5 Effects of Carbon Dioxide on Microbial Growth	26
2.4 Electrode Materials to remove Chromium in MFC	26
2.5 Governing Factors of MFC Performance	28

CHAPTER 3

EXPERIMENTAL WORK	30
3.1 Architecture of Cell Chambers	31
3.1.1 Feed of Cell Compartment	32
3.1.2 Cell Electrodes	34
3.1.3 Salt Bridge of MFC.....	36
3.1.4 Electrical System	37
3.2 Operation Principles	38
3.2.1 Operating Conditions	38
3.2.2 Operations in Cell Chambers	38
3.2.3 Series of Experimental Steps	39
3.3 Parameters of Cell Performance	41
3.4 Analytical Methodologies	45
3.4.1 Scanning Electron Microscopy-Energy Dispersive X-Ray	45
3.4.2 X – Ray Diffraction (XRD) Analysis	48

CHAPTER 4

RESULTS AND DISCUSSIONS	50
4.1 Experimental Cases for MFC Operation	51
4.2 Evaluation of Electrical Parameters	53
4.2.1 Graphical Representations for Generation of Current	56
4.2.2 Graphical Representations of Voltage Outcome	57
4.2.3 Graphical Relationship between Current and Voltage	59
4.2.4 Graphical Representations for Power Density	61
4.2.5 Graphical Representations for Recovered Energy	64
4.2.6 Coulombic Efficiency of MFC	67
4.3 Removal Percentages of COD and Total Chromium	67
4.4 Discussions	69
4.4.1 Advantage of Aeration in Cathode Chamber	69
4.4.2 Impact of Nutrient in Anode Chamber	70
4.4.3 Effect of Electrode Materials on Cell Performance	70
4.4.4 Comparative Analyses for Removing Chromium	72
4.5 Analyses of SEM – EDX	74
4.5.1 Quantitative Analyses of SEM – EDX	89
4.6 Analyses of X – Ray Diffraction (XRD)	91

CHAPTER 5	
CONCLUSIONS AND RECOMMENDATIONS	98
5.1 Conclusions	99
5.2 Prospects and Recommendations	100
REFERENCES	101
APPENDIX	114

LIST OF FIGURES

	PAGE NO
Figure 1.1: An overview of different applications of MFC-based technology [18]	4
Figure 2.1: Percentage of sector wise industries in Bangladesh [6]	10
Figure 2.2: Location of textile industrial areas in Dhaka [13]	12
Figure 2.3: Major elements of a microbial fuel cell (MFC) reactor [47]	14
Figure 2.4: Pathway for ATP production in MFC	15
Figure 2.5: General principle of microbial fuel cell [50]	16
Figure 2.6: Transfer of electrons to anode in microbial fuel cell [67]	19
Figure 2.7: Bio-electrochemical phenomena of MFC for removing metals [12]	24
Figure 2.8: Microbial limiting factors to effect cell performance [44]	25
Figure 3.1: Schematic diagram of microbial fuel cell	31
Figure 3.2: Collection containers of textile wastewater	32
Figure 3.3: Preparation of synthetic wastewater	33
Figure 3.4: Graphite electrodes	34
Figure 3.5: Al-Foil electrodes	34
Figure 3.6: Carbon cloth electrode	35
Figure 3.7: Salt bridge of double chambered microbial fuel cell	36
Figure 3.8: Multi-meter	37
Figure 3.9: Air pump	37
Figure 3.10: Complete experimental setup of microbial fuel cell	39
Figure 3.11: Experimental setup after a complete batch operation	40
Figure 3.12: Experimental arrangements for COD measurements	43
Figure 3.13: Digestion and H ₂ SO ₄ solution for COD	43
Figure 3.14: HACH COD vials of raw and treated samples	43
Figure 3.15: HACH reactor and spectrophotometer (DR 6000)	43
Figure 3.16: HACH vials and PERMACHEM (ChromaVer3) for measurements of total chromium	44
Figure 3.17: Treated carbon cloths (10 days of batch operation in anodic chamber of wastewater)	45
Figure 3.18: Raw and treated carbon cloths in SEM-EDX laboratory.....	45
Figure 3.19: Laboratory setup for SEM – EDX analyses	46

Figure: 3.20: Schematic diagram of SEM (Scanning Electron Microscopy) Analyses [107]	46
Figure 3.21: 2D images generation (SEM) and elemental analyses (EDX) of sample carbon cloth	47
Figure 3.22: Samples of treated carbon clothes for XRD analyses	48
Figure 3.23: Laboratory setup of XRD (X – Ray Diffraction) analyses	48
Figure 3.24: Schematic diagram of XRD (X – Ray Diffraction) analyses [108]	49
Figure 4.1: Current generation for 12 hours of batch operation for Industry 1 from Experiment no. 1 to Experiment no. 7	56
Figure 4.2: Current generation for 10 days (240 hours) of batch operation for synthetic wastewater (Experiment no. 8)	56
Figure 4.3: Current generation for 10 days (240 hours) of batch operation for wastewater of Industry 2 (Experiment no. 9)	57
Figure 4.4: Voltage output for 12 hours of batch operation for Industry 1 from Experiment no. 1 to Experiment no. 7	57
Figure 4.5: Voltage output for 10 days (240 hours) of batch operation for synthetic wastewater (Experiment no. 8)	58
Figure 4.6: Voltage output for 10 days (240 hours) of batch operation for wastewater of Industry 2 (Experiment no. 9)	58
Figure 4.7: Relationship between current and voltage output for 12 hours of batch operation for Industry 1 from Experiment no. 1 to Experiment no. 7 ..	59
Figure 4.8: Relationship between current and voltage output for 240 hours (10 days) of batch operation for synthetic wastewater (Experiment no. 8) ...	59
Figure 4.9: Relationship between current and voltage output for 240 hours (10 days) of batch operation for wastewater of Industry 2 (Experiment no. 8)	60
Figure 4.10: Power density for 12 hours of batch operation for Industry 1 from Experiment no. 1 to Experiment no. 7	61
Figure 4.11: Power density for 10 days (240 hours) of batch operation for synthetic wastewater (Experiment no. 8)	63
Figure 4.12: Power density for 10 days (240 hours) of batch operation for wastewater of Industry 2 (Experiment no. 9)	63
Figure 4.13: Recovered energy for 12 hours of batch operation for Industry 1 from Experiment no. 1 to Experiment no. 7	64

Figure 4.14: Recovered energy for 10 days (240 hours) of batch operation for synthetic wastewater (Experiment no. 8)	66
Figure 4.15: Recovered energy for 10 days (240 hours) of batch operation for wastewater of Industry 2 (Experiment no. 9)	66
Figure 4.16: Removal percentage of COD from Experiment no. 1 to Experiment no. 9	68
Figure 4.17: SEM analyses of raw carbon cloth	74
Figure 4.18: SEM analyses of treated carbon cloth for synthetic wastewater	75
Figure 4.19: SEM analyses of treated carbon cloth for textile wastewater	76
Figure 4.20 a: EDX report of raw carbon cloth	77
Figure 4.20 b: EDX report of raw carbon cloth	78
Figure 4.20 c: EDX report of raw carbon cloth	79
Figure 4.21 a: EDX report 1 of treated carbon cloth for synthetic wastewater	80
Figure 4.21 b: EDX report 1 of treated carbon cloth for synthetic wastewater	81
Figure 4.22 a: EDX report 1 of treated carbon cloth for textile wastewater ...	82
Figure 4.22 b: EDX report 1 of treated carbon cloth for textile wastewater ..	83
Figure 4.22 c: EDX report 1 of treated carbon cloth for textile wastewater	84
Figure 4.23 a: EDX report 2 of treated carbon cloth for synthetic wastewater	85
Figure 4.23 b: EDX report 2 of treated carbon cloth for synthetic wastewater	86
Figure 4.24 a: EDX report 2 of treated carbon cloth for textile wastewater ...	87
Figure 4.24 b: EDX report 2 of treated carbon cloth for textile wastewater ..	88
Figure 4.25 a: XRD report 1 of raw carbon cloth	92
Figure 4.25 b: XRD report 1 of treated carbon cloth for synthetic wastewater	93
Figure 4.25 c: XRD report 1 of treated carbon cloth for textile wastewater ..	94
Figure 4.25 d: XRD report 2 of treated carbon cloth for synthetic wastewater	95
Figure 4.25 e: XRD report 2 of treated carbon cloth for textile wastewater ..	96

LIST OF TABLES

	PAGE NO
Table 2.1: Typical compositions of the Textile Wastewater [8]	11
Table 4.1: Relative results of cell operations	52
Table 4.2: Combinations of cell components for different operational cases ...	52
Table 4.3: Current generation for 12 hours of batch operations from Experiment no. 1 to Experiment no. 7	53
Table 4.4: Voltage output for 12 hours of batch operations from Experiment no. 1 to Experiment no. 7	54
Table 4.5: Current and voltage outcome for 10 days of batch operations for the treatment of synthetic wastewater and textile wastewater	55
Table 4.6: Power density from 12 hours of batch operations for Experiment no. 1 to Experiment no. 7	61
Table 4.7: Power density from 10 days (240 hours) batch operations of synthetic wastewater (SWW) and textile wastewater (TWW)	62
Table 4.8: Recovered energy from 12 hours of batch operations for Experiment no. 1 to Experiment no. 7	64
Table 4.9: Recovered energy from 10 days (240 hours) batch operations of synthetic wastewater (SWW) and textile wastewater (TWW)	65
Table 4.10: Coulombic efficiency of microbial fuel cell in treating wastewater	67
Table 4.11: Experimental data for percentage of COD removal	67
Table 4.12: Experimental data for percentage of total chromium (Cr) removal	68
Table 4.13: Experimental Data for SEM – EDX analyses	90
Table 4.14: Experimental Data for XRD analyses	91

CHAPTER 1

INTRODUCTION

1.1 Introduction

Heavy metal contamination in water is a serious environmental and human health hazard. As a consequence of inadequately planned industrialization, large amount of wastewater containing organic matter and toxic heavy metals are discharged into the environment daily. Heavy metal pollution has even more adverse consequences than the organic contaminants [1-2]. Remarkably, heavy metals are characterized by high toxicity, non-biodegradability, and bio-accumulation [2-4]. Chromium is one of the most toxic heavy metals present in tannery as well as in textile effluents. Chromium is included on the US Environmental Protection Agency (USEPA) priority pollutant list [5]. Although the concentration of textile wastewater is relatively lower as compared to that of tannery, textile industries are more prevalent throughout the country posing greater threat to the community [6-7]. The production units of a textile industry such as woven fabric, knit fabric, stock and yarn can result in chromium contamination in wastewater streams. The concentrations of chromium in the wastewater discharged by these units of textile industries are usually less than 1 mg/L [8]. The conventional physical (e.g. sedimentation), chemical (e.g. chemical precipitation), and biological (e.g. activated sludge process) treatment methods are expensive, energy-intensive, and become ineffective if metal concentrations are below 1 – 100 mg/L [9]. Moreover, some of the methods need regeneration using hazardous reagent solution [10]. The damage of a water body due to heavy metals can be alleviated by adopting an environment favorable method for their removal [11]. In this regard, microbial fuel cells (MFCs) offer an alternative green and energy-efficient technique for removing heavy metals even at lower concentration [12-14]. Microbial fuel cell (MFC) is a sustainable process which utilizes the cellular activity of bacteria to initiate oxidation of substrate (such as organic wastes from industries, agriculture, or sewage) at anode and reduction of an oxidant (usually O₂) at cathode. Unlike a conventional fuel cell, MFCs can run at ambient temperature and atmospheric pressure. MFC is a type of bio-electrochemical systems that can be used for removing chromium from aqueous solution of wastewater. With a relatively low voltage application, exoelectrogenic bacteria can oxidize organic matter at the bioanode of an MFC [15]. Therefore, wastewater can be treated for removing chromium while electrons are produced coherently by microbial metabolism in the double-chambered microbial fuel cell (DC-MFC). In this thesis work, the cell compartments of DC-MFC are connected by a salt bridge for ionic equilibrium. Thus

the novelty of this research is that it uses the salt bridge which can replace the expensive membranes with functional and economical complexities [16]. This approach converts the chemical energy of organic matter in wastewater into electricity. The microbial metabolism and electricity are the driving forces for removing chromium in MFC. The removal efficiency depends on the proper configuration and construction materials of electrodes. In this research, the performances of three different types of electrodes are evaluated for developing an efficient experimental setup of microbial fuel cell (MFC).

1.2 Present State of the Research

Wastewater management is one of the most important fields of research in engineering and environmental biotechnology. Security for water and environment is gaining importance throughout the world. There are intense interests in evaluating and implementing an energy efficient, eco-friendly, and economically feasible process to treat the industrial effluent [16]. Microbial Fuel Cell (MFC) technology is emerging as one of the popular wastewater treatment technologies to provide clean water and green energy [17]. Researchers believe that this process can prove to be a blessing for both developed and developing countries. The widespread application of the process inspires more research to eradicate the major problems of wastewater management and renewable energy sources [18]. The inherent theories of electron transfer mechanisms, biochemistry, microbiology, electrochemistry, microbial electro-metallurgy and reaction kinetics, chemical and biochemical phenomena, and material characteristics of electrodes are the current fields of research interests [19]. Thus, MFC technology represents a multidisciplinary approach to the quest for alternative ways of wastewater treatment and renewable sources of energy.

Figure 1.1 shows several possible applications of MFC such as bioremediation (sediment MFC), desalination (microbial desalination cell), CO₂ sequestration (microbial carbon capture cells), hydrogen production (microbial electrolysis cell, MEC), solar power production (plant microbial fuel cell, PMFC), synthesis of chemicals (microbial electrosynthesis), biosensors (microfluidic MFC), etc. which have become the potential premises of research [19]. It is possible to utilize a wide range of organic or inorganic matter such as organic wastes, heavy metals, or soil sediments as a source of fuel generation. High conversion and removal efficiency has been achieved with such devices due to the direct or a single step conversion of substrate energy to

electricity [19-20]. The electricity can be utilized for remove and recover several harmful metals. Bioelectricity produced in MFC can be utilized for decentralized power generation, and bioelectricity-based economy. Additional revenue can be obtained in the form of waste treatment credit, metal recovery credit, renewable energy credit, and carbon dioxide credits.

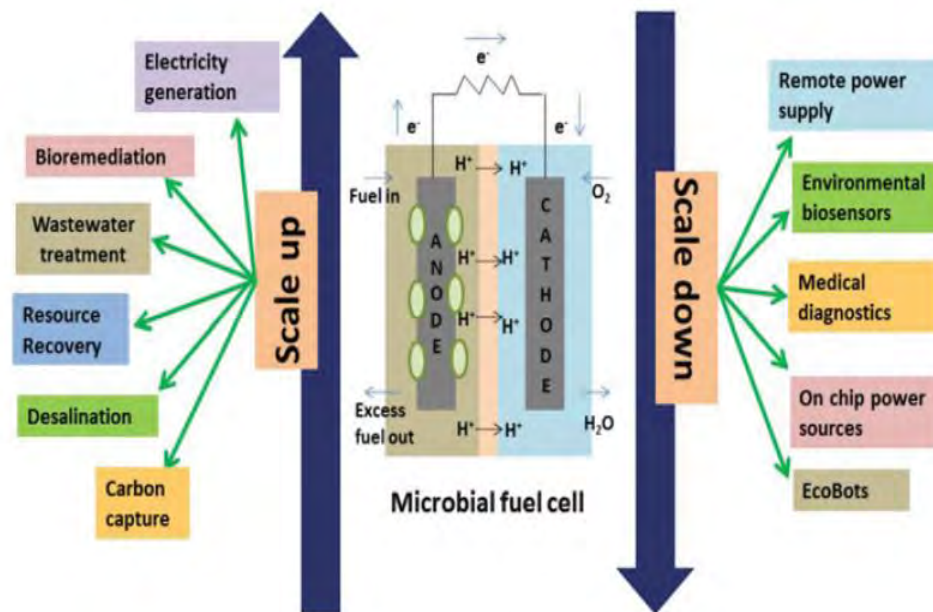


Figure 1.1: An overview of different applications of MFC-based technology [18]

Over the years, several advances have been made in developing innovative and analytical techniques to evaluate the performance of microbial fuel cells (MFCs). In spite of power outputs and COD removal efficiencies for MFCs, significant research is still required in order to make this technology viable. MFC studies have only been at a laboratory scale and completed in batch mode, which is impractical for many applications with constant flow rates.

Research is also required to determine the internal ohmic losses from wastewater conductivity, change in temperature and pH because these parameters play significant roles for optimal production [20-21]. The internal complexities, construction, and cost analyses of MFC systems make scale-up and practical implementation for wastewater treatment very difficult.

In addition to MFC design challenges, research results based upon actual wastewater treatment are lacking in the electrode fouling, high internal resistance and drop in

voltage, biofilm growth on electrode surfaces, and count of microbial population. Startup enrichment processes for biofilm development are critical for larger scale systems and require further research on optimal procedures. Bio-anodes and cathodes are typically designed using carbon cloth or graphite because of their ability to allow necessary biofilm development, low over potentials, and low costs; however, the electrical resistivity of graphite and carbon are very high [21]. Several diagnostic tools that are used to assess the performance of MFCs are researched in detail ranging from electrochemical workstation to molecular biological tools. Mathematical modeling of the process is also investigated which would help in scaling up and scaling down the MFC.

At present, the power outputs of MFCs are too low for scaling up the process which restricts its application and practical applicability but the low power outputs can pave a path of hope for scaling down this process. Engineers and scientists are researching to have a better understanding of all the components and their limitations to overcome the bottlenecks.

1.3 Research Aim and Objectives

The aim of this study is to develop a cost effective microbial fuel cell framework that utilizes the bioelectricity to treat the textile wastewater and remove chromium efficiently.

The major objectives to achieve the overall aim of this research are as follows:

1. To set up a microbial fuel cell and evaluate different performance parameters.
e.g.
 - power density
 - coulombic efficiency
 - percentage (%) of total chromium reduction
 - percentage (%) chemical oxygen demand (COD) removal
2. To study different configurations of MFC for constructing a cell to maximize the current flow and waste removal efficiencies.

1.4 Scope of the Research

This research work considered a double-chambered microbial fuel cell (DC MFC) where the chambers are connected by a salt bridge. Absorbent cotton has been used to seal the openings of the salt bridge instead of expensive ion exchange membranes. The salt bridge consists of only saturated NaCl salt and the length of the bridge remains constant for all the experiments.

Anaerobic condition was maintained in the compartment of wastewater only by polyethylene sheets. However, the chamber was initially not purged with nitrogen gas. The common and traditional methods of voltammetry and ideal galvanic cell are employed for analyzing MFCs though the operating conditions vary significantly. Therefore, it is a prerequisite to consider the differences while evaluating the cell performances [22].

This research work emphasized the microbial removal of chromium and so reported the analytical techniques for detecting chromium deposition on anode. The availability, cost, time, and experimental constraints were responsible for using carbon cloth only as anode. The electrochemical removal of chromium by graphite cathode was not assessed analytically.

Microbial Fuel Cell (MFC) requires terminal electron acceptors at cathode chamber. The aeration of cathode chamber was maintained by air pump that oxygenates the water. Though permanganate and hexacyanoferrate are widely used as terminal electron acceptors the work depended only on the oxygen to accept electrons. Employing the external reagents as the electron acceptors in the cathode compartment documented higher power density than that generated by depending on oxygen [18]. So, the role of terminal electron acceptors in cathodic reactions can be considered as serious challenges in MFC performances.

This experiment aimed at evaluating the performance of oxygen as the only acceptor of electrons to study the influence of natural electron acceptors. Besides, the expensive chemicals show toxicity in many cases which may deteriorate the growth of biofilms and cellular metabolism of microbes. Therefore, external electron acceptors were not applied in this research considering the microbial activities and cost effectiveness of the cell.

Moreover, this work took decisions depending on only the direct transfer of electrons from microbes to anode. Though mediators are used extensively in anode chamber for supporting the electron transport system this work did not apply any mediator in the chamber. Mediators (e.g. thionine, humic acid, etc.) are widely applied for enhancing the performance of MFC [18] but most of them are toxic and expensive.

It is expected that the research would be used as a basis for further research to investigate the removal and recovery of other heavy metals from textile waste water using the MFC technology while addressing the challenges of effectiveness in using membranes [23] instead of salt bridges, variation in the pH of electrolytes, fluctuation in the temperature, applications of the low power density, and experimentation with different strains of microorganisms.

1.5 Thesis Structure

Chapter 1 introduces the background and provides motivation for this research work. It demonstrates the present state of research work, research gap, and research objectives.

Chapter 2 provides an overview of available literature on microbial fuel cell technology by discussing the impact of textile industries on water pollution in Bangladesh. The working principle of MFC in removing chromium, the characteristics of electrodes, and the governing factors of MFC performance are also discussed in this chapter.

Chapter 3 explains the architecture of experimental setup and operation principle of MFCs and presents the parameters and analytical methods to determine cell performance.

Chapter 4 describes the performance of MFCs for different cases and interprets the reasoning of power generation and water treatment through graphical representations. The analyses of SEM – EDX and XRD are also explained considering the surface morphology of electrodes and elemental identification of chromium.

Chapter 5 concludes the thesis by presenting contributions of this thesis work and stating recommendations for future research.

1.5 Research Contribution

- Moinee, A. Al., Sanzida, N. (2018). Unification of ETP (Effluent Treatment Plant) & MFC (Microbial Fuel Cell): Sustainable Development, Environmental Safety, & Renewable Energy. In proceedings of 58th *Convention of Institution of Engineers, Bangladesh* (IEB), Khulna, Bangladesh, pp. 15-21.

CHAPTER 2

LITERATURE REVIEW

CHAPTER 2

LITERATURE REVIEW

This chapter reviews the literature relevant to the environmental impact of textile industries and water pollution. The review provides a background for the thesis work by summarizing the previously published works. These summaries help to justify this research by indicating how microbial fuel cells (MFCs) offer a green and energy-efficient technique for the removal of heavy metals (e.g. Cr) even at lower concentration in comparison with the expensive and energy intensive conventional methods.

2.1 Textile Industries and Water Pollution in Bangladesh

Industrial revolution is a great engine to accelerate the economic growth of a developing country like Bangladesh. According to the report of United Nations (UN) the textile industries provide the single source of growth in Bangladesh's developing economy [24]. Bangladesh operates a thriving textile and clothing export industry and is one of the world's largest garment exporters. Approximately 25% of the major industries in Bangladesh are occupied by textile industries [5-6].

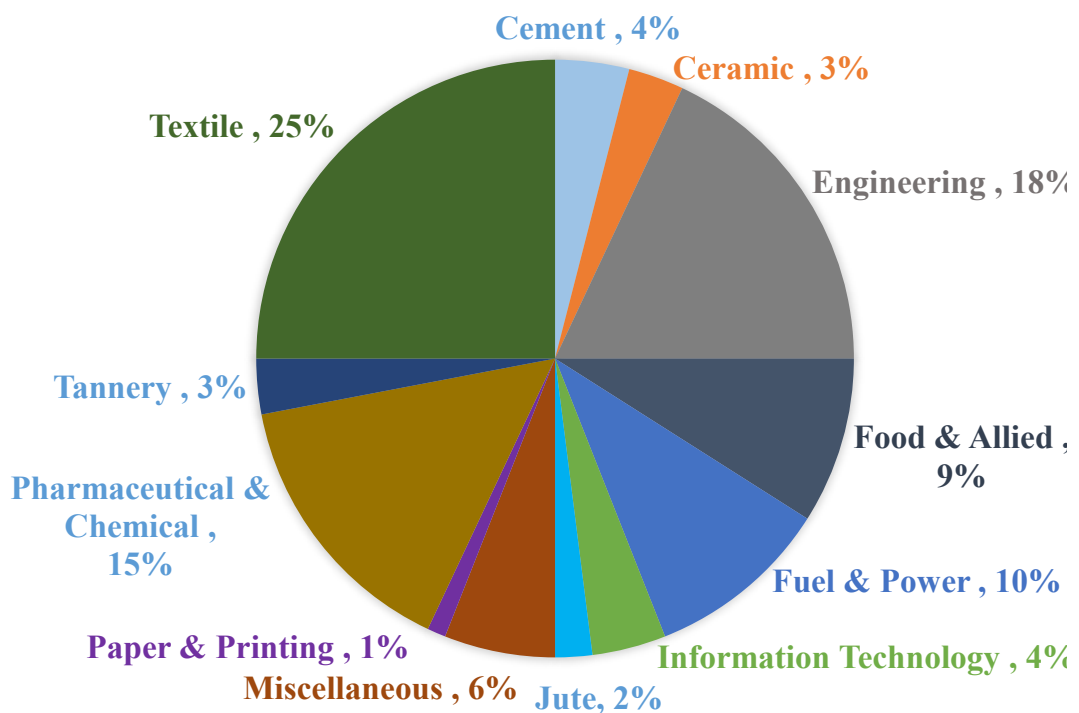


Figure 2.1: Percentage of sector wise industries in Bangladesh [7]

When the industrialization strengthens the economic growth of the country, it is a matter of great concern that the production processes of these industries pollute the water bodies of environment at an alarming rate. With the growth of the industries, the total pollution load is also increased. Eventually, great deterioration has come with the great success of economic growth [25]. Thus, one of major concern of the growth of industrialization is environmental pollution load from each industrial sector which greatly affects the environment as well as public health.

The textile sector has been an important part of Bangladesh's economy over the past few decades. In Bangladesh, the textile sector currently has an export value of nearly 28 billion USD per year which contributes about 82% of the country's total export earnings. It is projected that the annual ready-made garment (RMG) export value will be about 50 billion USD per year by 2021 [26]. However, the growth of Bangladeshi RMG sector is associated with different environmental issues, mostly caused by wastewater generated by textile industries. Despite significant economic contributions, Bangladesh textile industries cause a range of environmental problems, mostly the pollution of water resources [26-27]. Textile wastewater contains various chemicals such as oil, grease, caustic soda (NaOH), Glauber salt (Na₂SO₄), ammonia (NH₃), sulfide (S²⁻), heavy metals and other toxic substances [28]. Typical characteristics of wastewater produced by the textile industry include high temperature, a wide range of pH values, biochemical oxygen demand (BOD), chemical oxygen demand (COD), total dissolved solids (TDS), heavy metals and strong pigment [26, 29 – 32]. Table 2.1 shows typical compositions of wastewater from different units of textile industries [8]. Since wet process use a large quantity of water, they produce a large quantity of wastewater.

Table 2.1: Typical compositions of the Textile Wastewater [8]

Compositions Source	TSS (mg/L)	COD (mg/L)	BOD (mg/L)	Oil and Grease (mg/L)	Cr (mg/L)	Sulphide (mg/L)
Woven Fabric	300	1200	650	14	0.04	3.0
Knit Fabric	300	1000	350	53	0.24	0.20
Stock & Yarn	75	800	250	-	0.12	0.69

Since the wastewater contains suspended solids (SS), large amount of dissolved solids, unreacted dyestuffs, chemical and processing aids, it is considered a pollutant when discharged to surface water or municipal sewage system. Typical compositions of textile wastewaters generated during production and finishing processes are shown in Table 1 and the special parameters are based on type of dye containing Chromium (Cr). According to the Environment Conservation Rules (ECR) 1997, FEPA (Federal Environmental Protection Agency), and World Bank Group the permissible discharge limit of chromium for textile industries in Bangladesh is 0.05-0.5 ppm [33]. High volumes of textile wastewater may cause alteration of physical, chemical, and biological properties of the aquatic environment, and could be harmful to public health, livestock, wildlife, fish and other biodiversity [28, 34]. In addition, in many cases untreated textile effluents containing heavy metals are discharged into rivers or wetlands from nearby textile factories without proper treatment [25, 35], affecting the health of people who live along the polluted rivers.

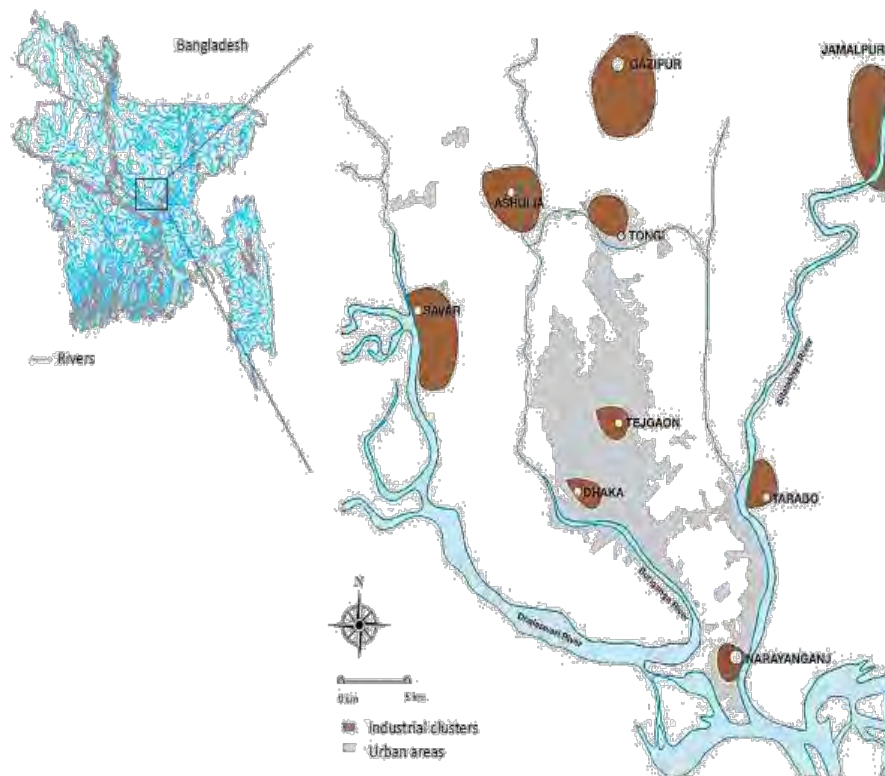


Figure 2.2: Location of textile industrial areas in Dhaka [1]

Industrial wastes and effluents containing heavy metals such as vanadium, molybdenum, zinc, nickel, mercury, lead, copper, chromium, cadmium, and arsenic are

being released in the vicinity of the industrial areas and this polluted river water is being used for irrigation purposes in paddy and vegetable cultivation fields near industrial areas in Gazipur and Keraniganj. Figure 2.2 shows the location of textile industrial areas in Dhaka. Dhamrai and Tongi have already shown the presence of heavy metals in textile dyes [36]. The incidence of illness among the people living in those areas is reported 16% higher on average than those living in a control area [37]. The polluted water causes disorder such as painful skin disease, dermatitis, diarrhea, food poisoning, cytotoxicity, and gastrointestinal problems in the short-term, and serious health implications such as respiratory problems when toxic materials accumulate in the body in the long-term [35–37]. Untreated textile effluent can contaminate groundwater and waterbodies, causing a high ‘grey water’ footprint and increase water stress, reduce dissolved oxygen in water and affect aquatic ecosystems and fisheries sector potentially which may indirectly cause climate change [25, 38-39].

According to the database of the Department of Inspection for Factories and Establishments, about 3000 garment factories are operating in Dhaka. According to an industrial survey conducted by Bangladesh Center for Advanced Studies (BCAS) in 2009, only about 40% industries have ETPs (Effluent Treatment Plants). In 10% industries, ETPs are under construction and about 50% industries have no ETP establishment. That is, more than 50% of waste generated by the industries eventually goes to the rivers untreated [40]. Wastewater from these textile industries in Bangladesh was estimated to be about 217 million m³ in 2016 [24], containing a wide range of pollutants, and will reach 349 million m³ by 2021 if the textile industries continue using conventional practices [25]. Whereas the conventional physical, chemical, and biological methods are expensive and energy-intensive, microbial interactions of MFCs bring about energy efficient removal of heavy metals even at lower concentration [12]. Contrary to organic pollutants, heavy metals do not usually cause biological degradation and thus are considered as a challenge for remedies [41–42]. Improving conventional technology, adopting cleaner production (CP) options, the reusing and recycling of treated water may reduce water consumption, effluent volume and water stresses, and may help preserving aquatic ecosystems. In this regard, MFCs can contribute to energy and environment simultaneously by harvesting bioelectricity during the removal process [13-14,43] of chromium, as the heavy metal of concern.

2.2 Basic Principles of Microbial Fuel Cell (MFC)

Microbial fuel cell technology has recently emerged as a promising technology to carry out heavy metal removal [3] by treating textile wastewater, while also producing electricity. A microbial fuel cell (MFC) is a bio-electrochemical system [44] that drives an electric current by utilizing catalytic (metabolic) activity of microorganisms [45]. Microorganisms, such as bacteria, can convert the chemical energy contained in organic matter into electrical energy by utilizing the bio-catalysis (metabolism) on organic matter and biodegradation i.e. treatment of biodegradable products, such as industrial and municipal wastewater [46].

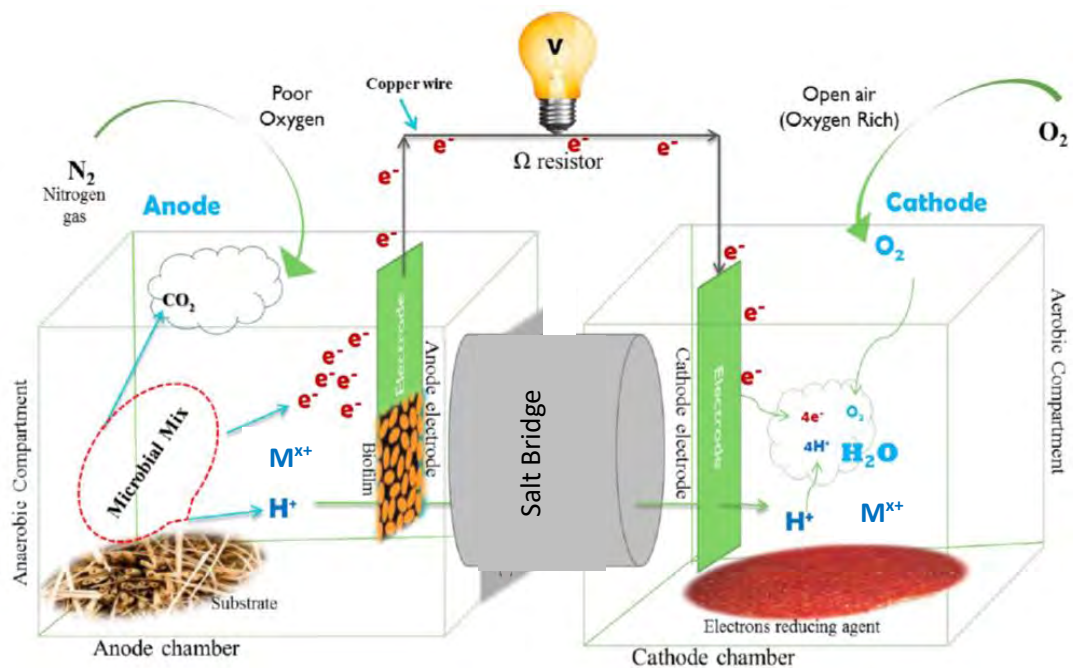


Figure 2.3: Major elements of a microbial fuel cell (MFC) reactor [47]

Figure 2.3 shows major elements of an MFC. It consists of an anaerobic chamber of anode and an aerobic chamber of cathode separated by a salt bridge or membrane. The chambers are comprised of glass, polycarbonate, or plexiglass, with a respective electrodes of carbon paper, carbon-cloth [47-49], graphite, graphite felt, Pt, Pt black, aluminum foil, or reticulated vitreous carbon. Wastewater is taken, as the growth media, in the anaerobic chamber where bacterial attachment occurs on anode electrode due to their metabolism. Microbes at the anode where electrons are released oxidize the organic fuel (e.g. wastewater) generating protons which pass to the cathode, and

electrons which move from the anode to an external conductive material (through copper wire) completing the circuit to generate a current. In order to maintain the continuity of current, substrate (e.g. glucose) can be added as nutrient which works as the source of carbon. Many organic substrates including carbohydrates, acetate, proteins, volatile acids, cellulose, and wastewater have been used as feed in MFC studies [47]. It can range from simple, pure, low molecular sugars to complex organic matter and heavy metal (M^{x+} , metal ion) containing waste water.

Microbial fuel cells rely on living biocatalysts (microbes) to facilitate the movement of electrons throughout their systems instead of the traditional chemically catalyzed oxidation of a fuel at the anode and reduction at the cathode. The principle involves collecting the electrons released by bacteria as they respire [49]. Cellular respiration is a collection of metabolic reactions that cells use to convert nutrients into adenosine triphosphate (ATP) which fuels cellular activity [50]. When an organic "fuel" enters the anode chamber, the bacteria set to work degrading the organic matter to generate the life sustaining ATP that fuels their cellular machinery.

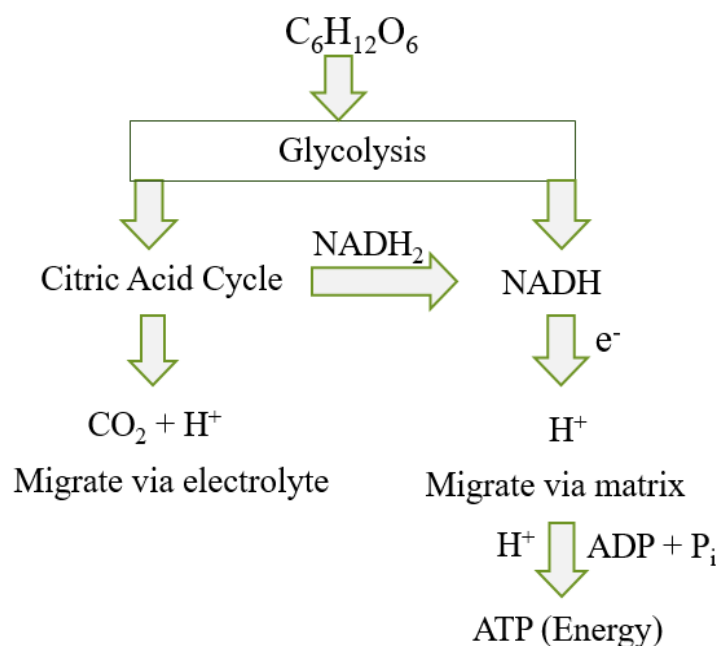


Figure 2.4: Pathway for ATP production in MFC

Figure 2.4 and 2.5 present the pathway and general principle for producing energy (ATP) for the survival of microbes. Aiming at biodegradation, microbial metabolism

process triggers the glycolysis process of organic substrate that eventually produces NADPH (Nicotinamide adenine dinucleotide phosphate + Hydrogen) i.e. NADH (Nicotinamide adenine dinucleotide + Hydrogen). NADH can be produced either directly from glycolysis or via citric acid cycle. The citric acid cycle results in carbon di-oxide and hydrogen ions that migrate via electrolyte. On the other hand, NADH releases electrons for producing hydrogen ions that migrate via the matrix of cell cytoplasm. The hydrogen ions in cytoplasm catalyze ADP and inorganic phosphate (P_i) to react and produce ATP as the survival energy for microbes.

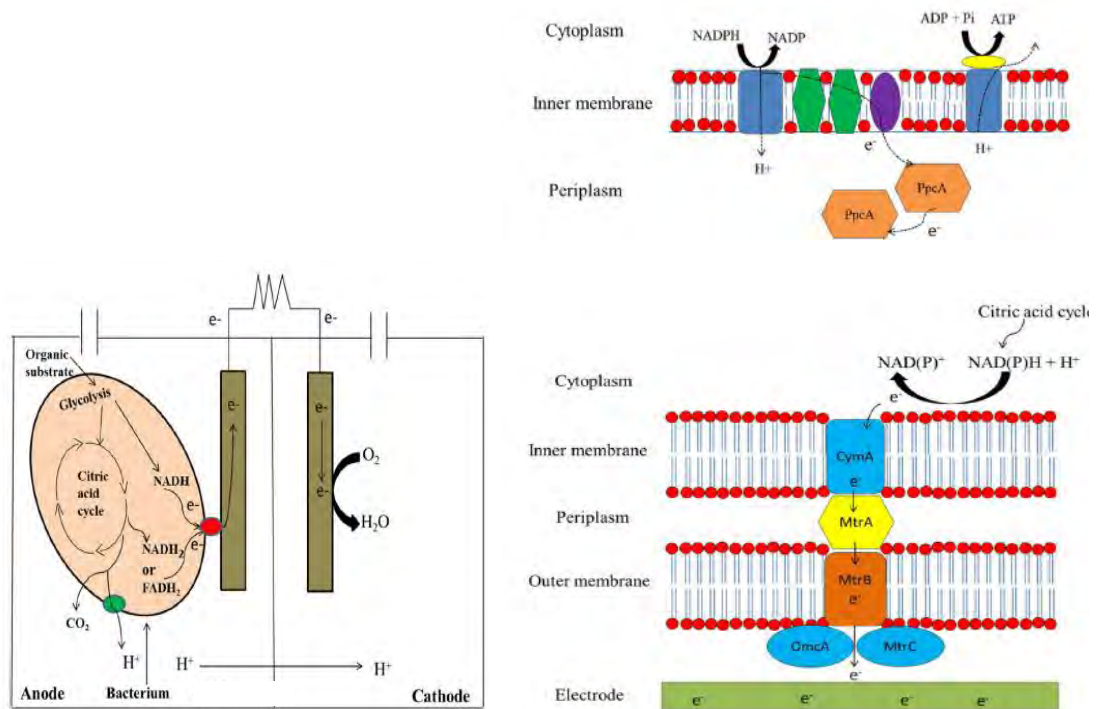
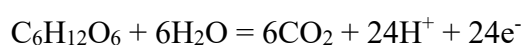


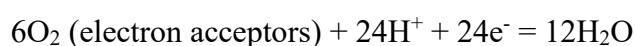
Figure 2.5: General principle of microbial fuel cell [50]

Bacterial respiration is basically one big redox reaction in which electrons are being moved around. The fact that bacteria can directly supply electrons or oxidize the substrates to produce electricity makes MFCs an ideal solution for wastewater treatment and domestic energy production. There are several biofilms on the anode surface that act to transfer electrons directly. Microorganisms (e.g. *Shewanella putrefaciens*, *Geobacter sulfurreducens*, *Rhodospirillum rubrum*) transfer electrons via highly conductive pili (nanowires) from the cellular membranes to electrode surface via c-type cytochromes [51]. When bacteria consume an organic substrate present in wastewater, like sugar under aerobic conditions, the products of cellular respiration are carbon

dioxide (CO₂) and water (H₂O). However, when placed in an environment void of oxygen (anaerobic condition), cellular respiration will produce protons and electrons instead, where CO₂ is entrapped within the chamber. It is therefore necessary to impart an anaerobic environment in the anode chamber of the MFC. The aeration of cathodic chamber maintains the pH by protonic balance. Thus, MFC reflects the path to step for sustainable development both for the production of bioelectricity and prevention of environment pollution. An ideal anode mechanism involves anaerobic oxidation of an organic substrate such as carbohydrate (supplied by wastewater). The wastewater chamber works as the oxidation half-cell and so the electrode in this compartment works as the anode. The pathway for producing metabolic energy (ATP) for the survival of microbes helps the MFC to degrade organics within the wastewater. The degradation eventually cleans the wastewater, removes the heavy metals, and produces electrons, hydrogen ions, and CO₂ [52]:



Electrons are diverted from the anode compartment by metabolic pathway, across an electrode, through external resistance (the load) into the oxygen-containing cathode compartment [53]:



Microbial fuel cells prove to be superior over other competing conventional wastewater treatment technologies, in many respects, which include enhanced conversion efficiency due to direct conversion of substrate's chemical energy into electricity, capability to treat even those wastewaters that are not suitable for anaerobic digestion processes, such as low-strength wastewater [54-55], ability to operate at ambient temperature, safe and quite performance [56], high conversion efficiency as compared to enzymatic fuel cells, ability to harvest up to 90 % of the electrons from the bacterial electron transport system compared to 50 % for typical fossil fuel power plants [3], and generation of 50–90 % less solids to be disposed of [57]. Besides, microbial fuel cells produce mainly carbon dioxide (CO₂) that has no useful energy content and comparatively less harmful, thus not requiring much further treatment [18]. Microbial fuel cells would not generate more CO₂ than typical biological wastewater treatment processes; hence, replacement of fossil fuel power plants by microbial fuel cells would result in a net reduction of CO₂ emissions [3]. In addition to this, the energy cost for

the removal process of chromium is reduced because the required energy was received from the bioelectricity produced by microbial metabolism. Besides, the residual substrate or nutrient can be utilized as fertilizer in agricultural lands [58]. This has proved the utility of microbial fuel cell (MFC) as a sustainable wastewater treatment system to remove heavy metals (e.g. Chromium) and their superior competency as compared with other wastewater treatment technologies.

2.3 Chromium Removal Mechanism of Microbial Fuel Cell

A microbial fuel cell (MFC) is a bio-electrochemical device that can treat wastewater generating electricity utilizing the electrons originated from the anaerobic oxidation of substrates (e.g. organic compounds or nutrients of microbes) readily obtained from the wastewater. Consequently, the metabolic process of oxidation is directed by microorganisms of the wastewater for generating energy for their cell growth. The microbes provide a series of enzymes in the media to degrade and oxidize the organics for obtaining energy and nutrients (e.g. carbon) they need to live and reproduce [59]. In general, microbial fuel cells are applied as functional half-cell. It means that only anode chamber (container of wastewater) is used to degrade pollutants/organics through bio-catalytic oxidation [60]. The function of cathode chamber is mainly as microbial fuel cell circuit closure or as the destination for electrons and protons.

2.3.1 Microbial Approaches to Transfer Electrons

During the anaerobic oxidation protons, electrons, and carbon dioxide are released and utilized in the wastewater media by different microbial mechanisms. This electron transfer, from the anode to the cathode, generates electricity by converting the chemical energy of the organic wastes and nutrients. Organisms that transfer electrons to the anode are electrode-reducing organisms. Figure 2.6 shows that they can pass electrons through (i) a mediator molecule in the solution, (ii) directly through the proteins in their outer membrane, or (iii) through appendages e.g. nanowires or pili within the thick biofilm formed by bacteria (e.g. exo-electrogenic microorganisms) around the anode [62-63]. Mediator-less MFCs are more efficient considering the toxicity of mediators, economic feasibility, and cell efficiency [64-65]. According to the microbial strategies, the microorganisms must transfer the electrons obtained by organic consumption so that they can utilize the energy (ATP) to survive and reproduce [66].

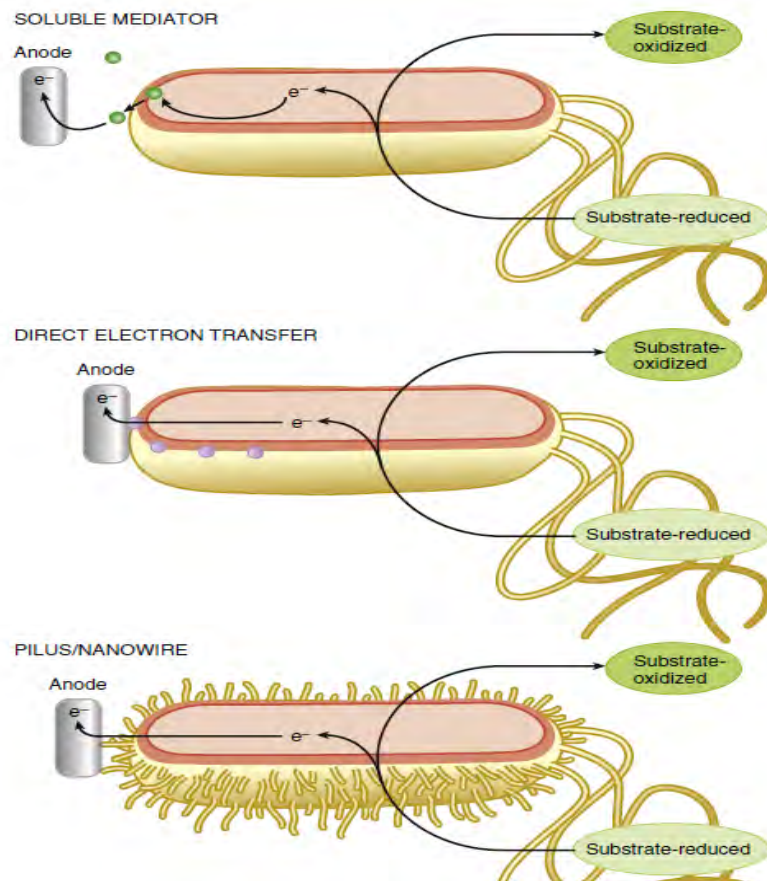


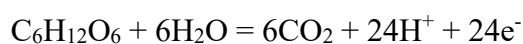
Figure 2.6: Transfer of electrons to anode in a microbial fuel cell [67]

In such case, the biochemical reaction needs electron acceptors with reasonable and effective oxidation potential [60]. In principle, any compound with high oxidation potential can serve as the electron acceptor in a microbial fuel cell [3]. The available oxidizing agents were biodegraded protons (H^+) of microbial metabolism and metal ions (M^{x+} , e.g. chromium) of wastewater in anaerobic anode chamber and oxygen in aerobic cathode chamber. To increase power density, an ideal electron acceptor is needed which is sustainable with no interference or toxic effects on the microbial community or any other elements of the system in any way. The specific movements of the available acceptors depend on different bio-electrochemical mechanisms of microorganisms (e.g. bacteria). The Microbial Mechanism of MFC is comprised of three types of reactions [3] in removing chromium from wastewater, generally, in the process for the production of electrons, their transfer, and consumption. These include bioelectrochemical, electrochemical, and chemical reactions. The bioelectrochemical reactions occur in the anode chamber, where the electrons are released during microbial metabolism. These electrons gather at the anode and, subsequently, travel through an

external load, trigger the catalytic adsorption of metal ions [68], and arrive at the cathode chamber where the electrochemical reactions take over.

2.3.2 Electrochemical Phenomena of Microbial Fuel Cell

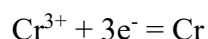
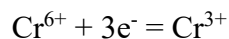
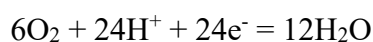
While the microorganism oxidizes organic compounds or substrates into carbon dioxide, the electrons are transferred to the anode [69] and hydrogen ions are migrated to the cathode through the salt bridge. The electrons captured by the anode are driven by an external power source to the cathode, the other electrode in the system. The overall metabolic activity of MFC is a big redox reaction. Anode represents the oxidation half-cell because electrons are released at anode by cellular metabolism.



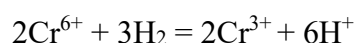
Eventually, cathode receives electrons, becomes the negative electrodes, and so works as reduction half-cell for MFC. So, the positive ions (protons and metal ions) are attracted by cathode. On the other hand, hypothetical positive holes are created which represents the absence of electrons in the particular positions on anode. Therefore, anode attracts the negative ions and repels the positive ions (H^+ , $\text{M}^{\text{x}+}$) to leave the compartment and migrate towards cathode. It will help to maintain a favorable pH (>7, basic) for wastewater which is essential for the survival of the microbes [70].

The wastewater of anode chamber contains organic pollutants and positive ions of heavy metals ($\text{M}^{\text{x}+}$, chromium). Wastewater and citric acid cycle provide positive hydrogen ions (H^+) to migrate through the electrolyte. Therefore, hydrogen ions and metal ions migrate through the salt bridge to provide electron acceptors for the reduction reactions that will take place at the cathode [67]. In electrolysis, the more reactive metal shows the least tendency as an ion to be preferentially discharged at the cathode. Chromium is more reactive than hydrogen. Thus chromium ions ($\text{M}^{\text{x}+}$) show least tendency to be reduced than hydrogen ions (H^+). So, hydrogen ions will be utilized before chromium ions in the aerobic compartment of cathode [71]. In MFCs, the aerobic cathode chamber can have three available electron acceptors i.e. protons, metal ions, and oxygen. Oxygen is the most common electron acceptor due to its high oxidation potential. Therefore, oxygen accepts the electrons and the oxide ions receive the hydrogen ions to combine and produce water (H_2O) [60].

So, the electrochemical reactions include reduction of oxygen to H₂O [72] and direct electrochemical reduction of chromium ions.



Concentration of chromium among the pollutants of textile [73] and tannery [74] wastewater is typically higher than that of other heavy metals e.g. manganese, iron, nickel, copper, zinc, cadmium, or lead [73-75]. Cr (VI) compounds are detrimental to the growth of microbes due to its higher chelation capacity than Cr (III) [Cr61]. Besides, Cr (VI) is carcinogenic and more toxic than Cr (III) [76-77]. Therefore, synthetic wastewater analyses tend to use salts of Cr (III) for the research. Moreover, Cr (VI) is not stable under anaerobic condition [69]. So, Cr (VI) is oxidized under anaerobic condition by the protons (H⁺) of wastewater for form molecular H₂ [78]. Then the cellular metabolism and electrolysis are catalyzed by the electrons and hydrogen ions (H⁺) produced from the unstable molecules of H₂.



These hydrogen ions (H⁺) migrate through the salt bridge. The salt bridge is used to maintain electrical neutrality within the internal circuit, preventing the cell from rapidly running its reaction to equilibrium. When sodium chloride salt bridge is used in MFC the saturated solution provides sodium ions (Na⁺) and chloride ions (Cl⁻). These ions maintain charge balance in the half cells. It is clear that the redox reactions of half cells accumulate negative ions (e.g. OH⁻, SO₄⁻) in anode and positive ions (e.g. H⁺, Cr³⁺) in cathode. If no salt bridge were present, the solution in one half cell would accumulate negative charge and the solution in the other half cell would accumulate positive charge as the reaction proceeded, quickly preventing further reaction, and hence production of electricity [79]. The salt bridge can provide necessary opposite ions for the half cells for obtaining charge balance and stable production of electricity. Besides, the liquid

junction potential decreases the electromotive force (emf) in membrane-based MFCs due to direct contact of two half cells. The liquid junction potential interferes with the exact measurement of the electromotive force of a fuel cell, so its effect should be minimized as much as possible for accurate measurement. The most common method of eliminating the liquid junction potential is to place a salt bridge (that provides indirect contact between half cells) consisting of a saturated solution [80].

2.3.3 Metabolic Interactions between Microbes and Metals

Prokaryotic and eukaryotic microbes are capable accumulating metals by binding them as cations to the cell surface in a passive process [81-82]. Even dead cells can bind metal ions. Depending on conditions, such binding may be selective or non-selective. In some cases, if the cell surface becomes saturated by a metal species, the cell may subsequently act as a nucleus in the formation of a mineral containing the metal [83-85].

Microbial metabolism can donate electrons to the anode directly through their outer membrane or appendages. They may excrete few negative ions as inorganic metabolic products e.g. sulfide (S^{2-}), carbonate (CO_3^{2-}), or phosphate (PO_4^{3-}), through non – enzymatic detoxification. The positive ions (M^{x+}) of toxic metal precipitate as a form of nanocrystals by combining with the negative ions [67]. The precipitation must decrease the concentration of dissolved metal species below their inhibitory level. The analytical studies i.e. SEM – EDX and XRD clearly show the bioaccumulation of chromium on anode. The evidence confirms that the metal ions were reduced from the textile wastewater due to microbial – metal interactions.

Working under the anaerobic condition and cellular metabolism of microbes enable reactions that otherwise would not be thermodynamically or kinetically favorable [12]. In the experiments, the wastewater was utilized in the anaerobic chamber of anode. Microorganisms colonize and create biofilms around the anode and the matrix let the electrons to be transmitted directly from cell wall interface to the anodic surface by dint of the electron transport system. Biofilms are layers of microbial cells growing on an interface and they can form highly complex structures adapted to a wide variety of environmental conditions [85].

2.3.4 Biochemical Phenomena of Microbial Fuel Cell

The optimal potential range promoted the biofilm growth around the anode in the anaerobic condition and corresponding power density of the MFCs [86]. The first colonist bacteria of a biofilm may adhere to the surface initially by the weak van der Waals forces and hydrophobic effects [87-88]. If the colonists are not immediately separated from the surface, they can anchor themselves more permanently using cell adhesion structures such as pili. Biofilm cells can get their nutrients either from the waste contaminants of water in anodic chamber or from the support material on which they grow attached [85].

When the soluble nutrients (called substrates) are provided by the liquid, a transport chain forms from the bulk liquid to the biofilm cells. In the initial stage of the operations, the organic wastes are available enough for the microbes to degrade for receiving survival energy and producing electricity. The presence of the organic wastes (as nutrients) provides the survival energy of microbes. The treatment eventually degrades the waste and removes the presence of organic pollutants which leads the microbes to a condition that lacks food (organic wastes) to survive. The situation triggers a microbial competition [85] and eventually power density decreases. Though the biofilms contribute to the generation of electricity towards a maximum, the value starts to decrease after a certain hours of operation during the batch due to the competition and lack of organic nutrients (consumable molecules) for producing electrons. As a result, the biofilms reduces in thickness due to the disturbance in nanowire to supply electrons. The working principle of MFCs is based on microbial physiology coupled with electrochemistry.

The bio-electrochemical phenomena of MFC related to metal (i.e. chromium) removal focuses on the carbon electrodes involved in sorption [12] and bio-electrochemical removal and recovery of metal ions due to cellular metabolism. Figure 2.7 illustrates that the dissolved metal ions of wastewater, microorganism, and electrode were reported to reduce and precipitate heavy metals (e.g. chromium) as metallic nanocrystals, principally at the cell wall interface, e.g. outer membrane c-type cytochromes of microbes [12]. The carbon electrodes provide the surface for adsorption, electrocoagulation, and biochemical interaction between metal and microbes.

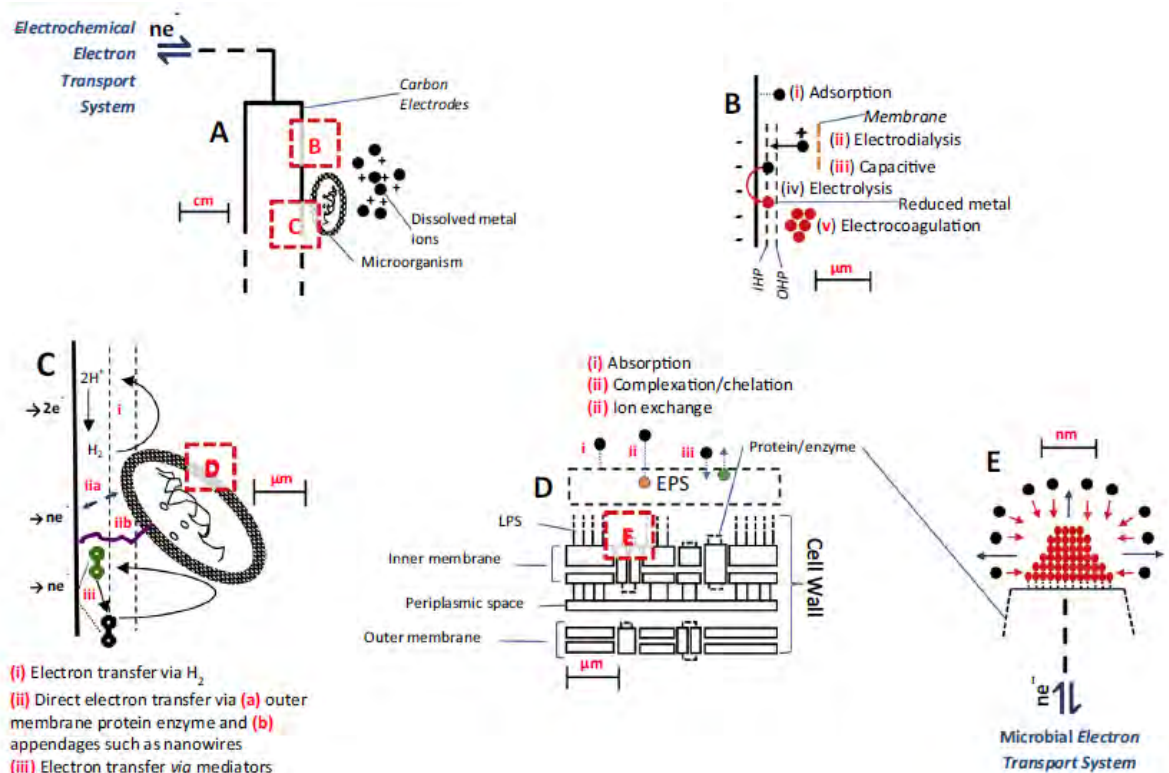


Figure 2.7: Bio-electrochemical phenomena of MFC for removing metals [12]

(A) “Macro” carbon electrodes involved in (B) sorption and bio-electrochemical removal of metal ions. (IHP - inner Helmholtz plane, OHP - outer Helmholtz plane) (C) Electron transfer systems (from biofilms to electrode) applied for metal removal. (D) “Micro” microbial metal ion biosorption on cell wall of microbes via extra polymeric substances (EPS) and (E) “nano” microbial electrodes, reported to reduce and precipitate metallic nanocrystals, at cell wall interface

Most microorganisms can create a matrix of biofilm through which electron transfer system works for attaching metal ions by ion-exchange, chelation, or absorption at the cell wall interface, leading to the biochemical removal of metals (e.g. chromium) at anode [89-90]. The cell wall provides necessary extra polymeric substances (EPS) and inner membrane provides necessary proteins and lipopolysaccharides (LPS) for metal ions. Thus, the cellular excretion enables the metal ions to be removed at anode as metallic nanoparticles (NPs) of salt compounds [91].

Here, bacteria are used as “nano-factories” for the bottom-up synthesis of various metallic NPs from ionic precursors in aqueous systems under ambient conditions. The remediation (depollution) of metal-containing waste streams can be combined with removal, recovery, and synthesis of novel (nano) materials [92].

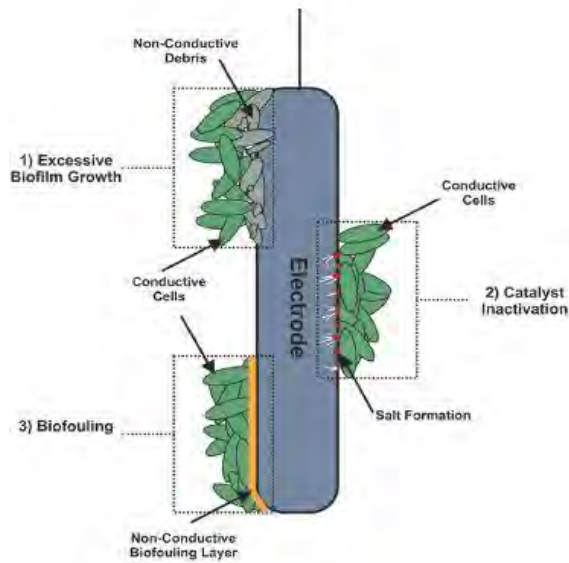


Figure 2.8: Microbial limiting factors to effect cell performance [44]

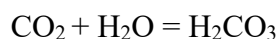
The key intrinsic factor currently limiting the power output of MFC technologies is the rate of electron transfer to the anode and the electrochemical properties of the material. Figure 2.8 presents that the microbial limiting factors include biofouling (leading to electrode surface blockage and ultimately a reduction in surface area), catalyst inactivation, and excessive biofilm growth – possibly leading to the production of non-conductive debris. The production of non-conductive debris such as polymeric substances and/ or dead cells, can isolate the electrochemically active biofilm from the electrode surface leading to a potential reduction in available surface area and ultimately a reduction in current generation [46]. Moreover, heavy metals can eventually affect the anode performance through their toxic inhibition to anodic microbes [90]. A study conducted in 2017, used cell viability counts and field emission scanning electron microscopy analysis to show that an increase in high polarization resistance correlated with the formation of a dead layer of cells [93]. Further, this study also revealed that the use of ultrasonic treatment was a verified method of controlling biofilm thickness and enhanced cell viability, maintaining stable power generation [93]. It was observed that when the predominant bacteria in an MFC set-up was *Geobacter anodireducens*, a two-layered biofilm developed over time, with an inner dead core and an outer layer of live cells. Results suggest that the outer layer was responsible for current generation and the dead inner-layer continued as an electrically conductive matrix [46].

The recent resurgence of the use of electrodes as electron donors or acceptors for microbial growth [94] opened a wide range of new possibilities, giving birth to what is known today as microbial-electrochemical technologies (METs). METs take the advantage of the synergistic alliance of electrochemical and biochemical phenomena and provide a bio-electrochemical system e.g. microbial fuel cells (MFCs) for removing chromium.

2.3.5 Effects of Carbon Dioxide on Microbial Growth

Carbon dioxide (CO₂), as one of the products of the anaerobic metabolism during biodegradation of chromium containing organic wastes, also contributes to the retardation and decrease in electricity generation. In this research work, CO₂ is entrapped in the anaerobic chamber of anode. Thus, carbon dioxide is unable to be released in the environment. Therefore, the gas is utilized by the microbial phenomena of MFC.

In the metabolic mechanism, carbon dioxide has negative effects on various biochemical pathways of MFC. In such ways, CO₂ can contribute to displace some or all of the oxygen available for bacterial metabolism, thus slowing the growth by a proportional amount [96]. Besides, acidic CO₂ are capable of contributing to the intracellular acidification and pH imbalance by producing carbonic acid which is adverse for the survival environment of microbes.



Thus, the metabolic interference of the cell can constitute a stress on the system resulting in a slowing of growth rate and the anaerobic bacteria may be inhibited by the carbon dioxide atmospheres [95].

2.4 Electrode Materials to Remove Chromium in MFC

The performance of MFC directly depends on the kinetics of the electrode reactions within the fuel cell, with the performance of the electrodes heavily influenced by the materials they are made from. The selection of the proper electrode material is crucial for the performance of MFCs in terms of bacterial adhesion, electron transfer and electrochemical efficiency. A wide range of materials have been tested to improve the performance of MFCs. In the past decade, carbon-based nanomaterials have emerged

as promising materials for both anode and cathode construction. Carbonaceous materials such as graphite rods and graphite brushes, carbon cloth, carbon paper, carbon felt and reticulated vitreous carbon are widely used in MFCs because of their high electrical conductivity, specific surface area, biocompatibility, chemical stability and low cost [63,96].

There are many studies to scale up the power production using different carbon-based materials such as graphite rod, carbon paper, carbon cloth, carbon felt or carbon fiber. Various transition metal oxides have been investigated as alternatives to conventional expensive metals like platinum for oxygen reduction reaction. To implement the MFC technology in practice, the cost of materials must be reduced and power densities must be maximized. In general, the electrodes of microbial fuel cells (MFCs) should possess the following properties:

Surface area and porosity: The output power of MFCs is greatly constrained by the surface area of electrodes. The ohmic losses are directly proportional to the resistance of the electrode. The easiest way to decrease the resistance is to increase the effective surface area while keeping the volume the same, hence enhancing the efficiency of the MFC. Furthermore, a high surface area provides more sites for reactions, enhancing electrode kinetics [97-98]. However, porosity will decrease the electrical conductivity of the material.

Electrical conductivity: Electrons released from microbes have to travel along an external circuit after passing through the anode. The high electrical conductivity of the electrode material makes the electron flow with less resistance. At the same time, the interfacial impedance should be low to facilitate the electron transfer [63].

Stability and durability: The reducing and oxidizing environment in an MFC may lead to the swelling and decomposition of the materials. The high surface roughness increases the durability of the material while it might increase the chances of fouling, thus may decrease the long-term performance of the MFC. Therefore, the material for electrodes should be durable as well as stable in an acidic and a basic environment [63].

Cost and accessibility: The cost of the electrode material influences the capital cost of the MFC to a large extent. To commercialize the MFC, the material should be low cost, sustainable and easily available. Some metals like platinum are highly expensive, non-

durable and nonsustainable as well. Non-precious metal materials such as composites might be an alternative to substitute precious metals in electrodes in the future. In addition, materials used for the anode must have biocompatible properties. A superior biocompatible material will increase the bacterial adhesion and hence the life of the MFC.

Most of the materials used as an anode can also be used as a cathode. However in addition a robust MFC cathode should have the following properties [63]:

- (a) High mechanical strength.
- (b) Catalytic property.
- (c) High electronic and ionic conductivity.

2.5 Governing Factors of MFC Performance

Operating MFC under optimized anodic condition (anaerobic) will allow anodic biocatalyst to grow properly and also to form an electrogenic biofilm on electrode surface during startup which improves the subsequent fuel cell performance in long-term operation. Numerous process parameters such as system pH, alkalinity, substrate nature, substrate concentration and organic loading rate (OLR) affect the activity of these electrochemically active microorganisms [18, 69]. The factors influencing the performance of MFC are discussed below.

Microorganisms: Electrochemically active microorganisms play vital role in MFC for removal of metal, wastewater treatment, and power generation. In the case of pure culture, the microbes are electrochemically active e.g. exoelectrogenic bacteria, which directly transport electrons outside the cell membrane [99]. There are a group of electrochemically active microbes present in the mixed culture. In general, wastewater, soil, fresh as well as marine sediments, and activated sludge have been widely employed as biocatalyst in MFC, because they are rich in mixed microorganisms. Pure bacterial culture typically grows very slowly due to strict anaerobic conditions in the anode compartment. Overall performance in terms of the power output of some pure culture is moderately low compared to a mixed culture. On the other hand, mixed culture inoculum takes longer startup time to achieve steady current generation as compared to pure culture [18].

Nutrient: Nutrient is one of the factors which affect the microbial activities in the anode compartment. It also determines the existence of dominant bacterial community when mixed culture is used as inoculum. A wide variety of nutrients has been used in MFCs from simple carbon source to complex carbon, nitrogen-rich biodegradable wastewater [100]. The pure nutrient such as acetate and glucose is used widely to maintain the homogeneity [101].

COD Concentration: Chemical oxygen demand (COD) considerably influence the performance of fuel cell operated both in batch feed and continuous mode of operation [100]. In MFC, electricity generation is directly proportional to the nutrient (substrate) concentration which can be measured in terms of COD. However, increasing concentration will increase power generation till it causes cellular inhibition. Hence, it is essential to determine the optimum concentration to achieve maximum power generation.

Feed pH: Apart from a biotic agent, several abiotic factors also influence the MFC performance. The pH plays a vital role in bioreactor performance [102]. Similarly, the electrolyte pH plays a vital key role in MFC's power output. In MFC operation, power output drastically reduces at the acidic pH range below 6 [69]. It means, low pH conditions have an adverse effect on electrochemically active bacterial population, which in turn leads to a drastic drop in power production. An ideal pH should be in the middle of 7–8 [103]. It is clear that pH will strongly influence the performance of MFC both in batch feed and continuous mode of operation.

CHAPTER 3

EXPERIMENTAL WORK

3.1 Architecture of Cell Chambers

A double-chambered microbial fuel cell (DC-MFC) was constructed for experimental operations. Each chamber was made of Perspex (Plexiglas, polymethyl methacrylate) and had a dimension of 10 cm × 10 cm × 15 cm.

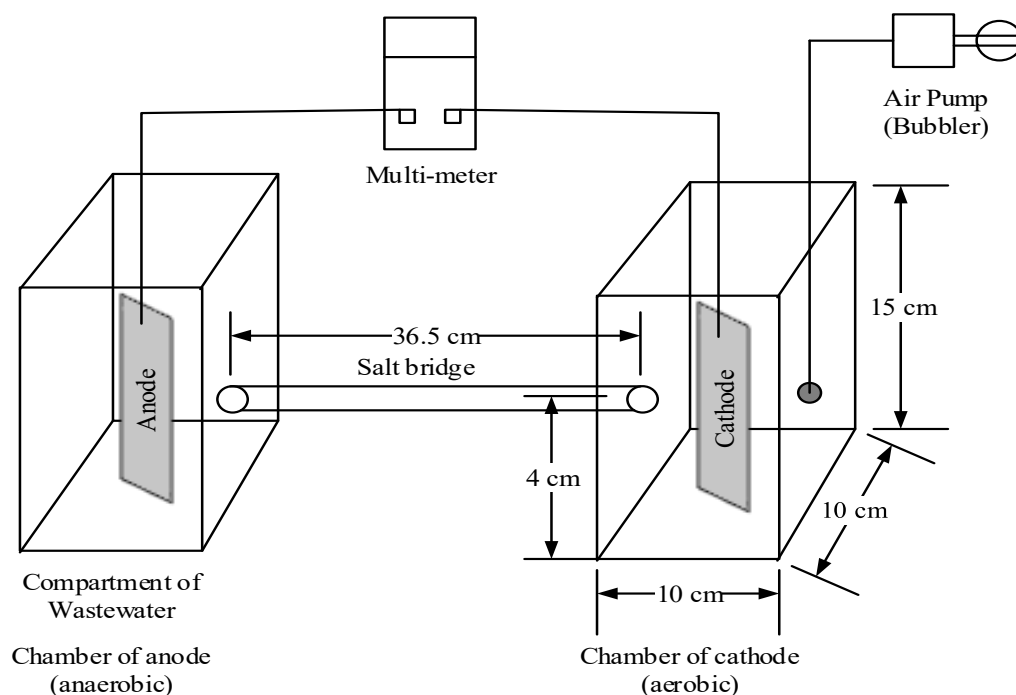


Figure 3.1: Schematic diagram of Microbial Fuel Cell

Microbial oxidation reaction occurs in the wastewater compartment. Therefore, this compartment acts as the chamber of anode and consequently reduction occurs in the chamber of cathode. The chamber of anode was isolated from air by polyethylene sheets to maintain anaerobic environment. An air pump was employed to create bubble and oxygenate the potable water of cathode for maintaining aerobic condition in cathode. The external circuit connected anode and cathode by insulated copper wire and multi-meter. The current and voltage was logged by the multi-meter periodically for batch operation in MFC. A salt bridge of saturated sodium chloride (NaCl) connected the chambers. The length of bridge was 36.5 cm. The sockets of bridge on chamber wall were on 4 cm above from the base. The outer diameter of the salt bridge was 0.8 inch and the inner diameter was 0.5 inch. The pipe fittings of salt bridge were made of stainless steel (SS).

3.1.1 Feed of Cell Chambers

Feed of Anode Chamber

Textile Wastewater: Textile wastewater (TWW) was collected from the Effluent Treatment Plant (ETP) of a textile industry located at Gazipur in Dhaka Division. Besides, Pran Industrial Park (PIP, Narsingdi, Dhaka) also provided wastewater from their ETP. The wastewater of PIP was used to identify efficient cell components and construct a cell for removing chromium from textile wastewater. Each of the containers had a volume of 5 L to collect the wastewater.



Figure 3.2: Collection containers of textile wastewater

Synthetic Wastewater: Synthetic wastewater is actually beneficial for optimizing the various parameters and experimental setup as real waste water contains many undesirable elements. Besides, synthetic wastewater (SWW) can keep the composition of the untreated wastewater constant to make valid comparisons [104] when industrial wastewater is variable in its composition.

Composition of the synthetic wastewater

The chamber of anode was initially inoculated by the industrial wastewater collected from the ETP of PIP. The concentration of total chromium, as the heavy metal of concern, was 0 mg/L in the wastewater of PIP. The United Nations Environment Program showed that the least concentrations of chromium in textile wastewater can vary from 0.24 mg/L to 0.04 mg/L in different sections (woven fabric, knit fabric, stock and yarn) [24, 25] of textile industry. One of the purposes of this thesis is to make the MFC effective at low (initial) metal concentration. Therefore, the concentration was maintained at 0.03 mg/L (< 0.04 mg/L) for chromium (metal of concern) as initial

amount of chromium to verify whether the developed setup of MFC was able to remove chromium from wastewater at lower concentration.



Figure 3.3: Preparation of synthetic wastewater

The cell was initially fed with 1.2 L of synthetic wastewater. The chemical analyses on required nutrients for microbial growth shows that the standard concentrations of carbon and nitrogen source in a standard growth media should be greater than 10^{-2} mol/L (0.12 g/L) and 10^{-3} mol/L (0.014 g/L) respectively [105]. Therefore, the concentration of glucose (source of carbon) was maintained at 0.20 g/L (>0.12 g/L) and the concentration of yeast extract (source of nitrogen) was maintained at 0.07 g/L (>0.014 g/L). The more contaminated the synthetic media the more nutrients become available for microbial degradation which would eventually enhance cell performance. Therefore, 0.15 mg/L milk powder was added as the basis of synthetic media which provides the carbohydrate, protein, and fat content for stable growth of microorganisms. The pH of the final solution was 7.2.

Feed of Cathode Chamber: Distilled water was used in the aerobic cathode compartment. The pH of the medium was between 6.4 to 7.4. The TDS i.e. total dissolved solid was less than 50 mg/L where the measure of total Chromium was 0 mg/L.

3.1.2 Cell Electrodes

Graphite Electrodes

During some of the experiments graphite electrodes were used as both anode and cathode to evaluate the performance of the cell. Each of the graphite electrodes had a dimension of $5.0\text{ cm} \times 2.5\text{ cm} \times 0.5\text{ cm}$.



Figure 3.4: Graphite electrodes

Aluminium Foil Electrodes

Aluminium foil was also used as anode and cathode to evaluate the performance of the cell. Each of the Al-foil electrodes had a dimension of $5.0\text{ cm} \times 2.5\text{ cm} \times 0.5\text{ cm}$.



Figure 3.5: Aluminium foil electrodes

Carbon Cloth Electrodes

Carbon cloths (fabrics of carbon) was used as anode to evaluate the efficiency of cell in removing chromium. The biochemical removal of metal occurs in anode chamber of wastewater. The surface area and porosity make carbon cloth more efficient than graphite or Al-Foil electrodes.



Figure 3.6 Carbon cloth electrode

The dimension of the carbon cloths was 8.0 cm x 7.0 cm x 0.04 cm i.e. the approximate surface area of the carbon cloths was 8.0 cm x 7.0 cm which were positioned in the anaerobic anode compartment.

The carbon cloth was supplied by Science Village, Mahir International Scientific Equipment Supplier, Dhaka, Bangladesh.

3.1.3 Salt Bridge of MFC

Saturated NaCl salt bridge connected the chambers. The salt bridge has a length of 36.5 cm. The sockets on chamber wall were on 4 cm above from the base. The outer diameter of the salt bridge was 0.8 inch and the inner diameter was 0.5 inch.



Figure 3.7: Salt bridge of double chambered microbial fuel cell

The salt bridge is used to maintain charge balance between the two chambers, prevent the cell from rapidly running its reaction to equilibrium for continuing the power generation, and eliminate the LJP (liquid junction potential) to obtain the accurate measurement in removing chromium.

Surgical adsorbent cotton was used to maintain regular diffusion of salt solution from the salt bridge to the electrolytes of both chambers. In case of necessity, araldite (adhesive) was applied to the respective experiments.

There were openings immediately after the valves, which were used to pour the salt solution in the bridge so that the solution could pass through the path and reach the electrolytes of the double-chambered microbial fuel cell (DC-MFC).

The pipe fittings of salt bridge were made of stainless steel (SS).

3.1.4 Electrical System

Multimeter

A digital multimeter, CD800a, Sanwa was utilized to measure the current and voltage generated in the cell. The device had sharp contrast LCD with character 1.75 mm height. The test pins were gold plated for accurate measurement.



Figure 3.8: Multi-meter

Air Pump

Aeration is important for the cathode compartment. The chamber was kept open and an air pump (bubbler), sebo SB-248A was set to take part in cell operation. Air pulled through the pump creates bubbles and oxygenates the water. This is important because the interaction provides an opportunity for the absorption of oxygen into the water. External pumps move the air via a hose that is dropped into the water.



Figure 3.9: Air Pump

3.2 Operation Principles

3.2.1 Operating Conditions

All the experiments were operated at room temperature at around 25⁰C and atmospheric pressure. The double chambered microbial fuel cell was operated in batch mode. The most efficient operation had a duration of 10 days i.e. 240 hrs.

3.2.2 Operations in Cell Chambers

Anode Chamber of MFC

In the anaerobic ambiance of anode chamber the metabolic activity of the microorganisms produces electron and proton which had advantages over the aerobic media. So, the electron can be utilized for the generation of electricity and removal of chromium while protons migrate through the salt bridge and produce water by combining with available oxygen at aerobic chamber of cathode.

Alternatively, aeration produces carbon di-oxide and water in anode chamber instead of electrons, protons, and carbon di-oxide. Besides, the aeration would decrease the thickness of biofilms around anode.

So, this is essential for the chamber of anode to be anaerobic to get feasible results. Glucose was used as nutrients in anode chamber for the stable growth of microbes [105].

Cathode Chamber of MFC

In aerobic ambiance of cathode chamber, the oxidizing agent O₂ produces water by combining with hydrogen ions migrated through salt bridge. The oxidizing agent was reduced by receiving the electrons.

The bio-electrochemical process was harnessed by the aerobic environment of cathode. The environment maintained the concentration of dissolved oxygen to trigger the redox reaction. Eventually, the pH of the electrolytes was maintained properly.

3.2.3 Series of Experimental Steps

The double- chambered MFC was operated in batch mode for nine experiments. The internal volume of each chamber was 1.5 L. The working volume was 1.2 L. Experimental steps for evaluating the performance of MFCs are given below:

1. The anode chamber was filled with waste water sample.
2. The opening of the anode compartment was tightly closed by polythene sheets to prevent air from entering in order to create an anaerobic atmosphere inside the chamber.
3. Cathode compartment was filled with potable water and kept open for proper aeration. Aeration pump was set to produce air bubble in the cathode chamber.
4. The multi-meter connected the electrodes externally by insulated copper wire and log the current and voltage during batch operations.



Figure 3.10: Complete experimental setup of microbial fuel cell

5. The chemical oxygen demand (COD) and total chromium concentration of raw wastewater were determined by spectrophotometric measurement.
6. In the final experiments nutrient was added to the wastewater for the stable growth of microorganisms. The experiments were observed both for the solution with and without nutrients.
7. The chemical oxygen demand (COD) and total chromium concentration of treated wastewater were determined by spectrophotometric measurement.
8. The raw and treated samples of carbon cloths were collected and preserved carefully for analytical analyses.
9. Carbon cloths were cut into specific pieces to observe the surface morphology by scanning electron microscopy (SEM).
10. Energy Dispersive X-Ray (EDX) gave the mass percentage of chromium deposition at a specific amount of energy emission.
11. Finally, X-Ray Diffraction (XRD) provided the elemental identification of chromium removed from aqueous wastewater by microbial fuel cell (MFC).



Figure 3.11: Experimental setup after a complete batch operation

3.3 Parameters of Cell Performance

Power Density: Cell Performance of MFC

The temporal trend of MFCs' electrical behavior was observed for each batch cycle relying on voltage and current measurement across the external circuit. The batch time for the first seven experiments was 12 hours and the batch time for experiment no. 8 and 9 was 240 hours (10 days). The current and voltage was logged periodically for calculating the power density of MFC.

The maximum power density obtained in any experiment represents the cell performance of microbial fuel cell (MFC). The power density is the power obtained per working volume.

$$\text{Fuel Cell Performance (max. power density)} = \frac{(\text{Power})_{\text{sww}}}{(\text{Volume})_{\text{cell}}} = \frac{(\text{Voltage} \times \text{Current})_{\text{sww}}}{(\text{Volume})_{\text{cell}}}$$

The energy recovered ($E_{\text{recovered}}$, in kJ/m^3) in each experiment can also be calculated from the fuel cell performance. The maximum energy recovered per working volume was determined at maximum current and voltage for each of nine experiment.

$$E_{\text{recovered}} = \text{Maximum Power Density} \times \text{Time}$$

Coulombic Efficiency: Global Efficiency of MFC

In order to estimate the global efficiency of the bio-electrochemical process, the MFC's coulombic efficiency was calculated.

It is defined as the ratio between electron moles extracted as current and the total electron moles made available for substrate oxidation [106]. Therefore,

$$C_E = \frac{\text{electron moles extracted as current}}{\text{total electron moles made available for substrate oxidation}}$$

The calculation was based on change in COD concentration of wastewater. Integrating measured power over time to reach the maximum, the coulombic efficiencies were calculated which is defined as the ratio of total coulombs actually transferred to the

anode from the substrate, to maximum possible coulombs if all substrate removal produced current. The formula utilized for calculating the efficacy is given below [106]:

$$C_E = \frac{M \int_0^t I dt}{F b V \Delta COD} = \frac{32 \int_0^t I dt}{F 4 V \Delta COD} = \frac{8 \int_0^t I dt}{F V \Delta COD}$$

$$\text{i.e. } C_E = \frac{8 \int_0^t I dt}{F V \Delta COD},$$

where, $M = 32$ g/mol, is the molecular weight of oxygen,

$b = 4$, is the number of electrons exchanged per mole of oxygen,

$F =$ Faraday's Constant = 96500 C/mol,

$V =$ Volume of the liquid in anode compartment = 1.2 L

Here, current flow I is in A, t is in second, volume is in L, and ΔCOD is in g/L

Chemical Oxygen Demand (COD)

In environmental chemistry, the chemical oxygen demand (COD) test is commonly used to indirectly measure the amount of organic compounds in water. Most applications of COD determine the amount of organic pollutants found in surface water or wastewater, making COD a useful measure of water quality. It is expressed in milligrams per liter (mg/L), which indicates the mass of oxygen consumed per liter of solution.

Measurement Procedures of COD

1. 2 mL potable water was collected in a blank COD vial then 3 mL H₂SO₄ and 4 mL digestion solution were added to the tube.
2. Then 2 mL of raw sample with 3 mL H₂SO₄ and 4 mL digestion solution were collected in another COD vial.
3. In another vial of COD experiment, 2 mL of treated wastewater with 3 mL H₂SO₄ and 4 mL digestion solution were collected eventually.
4. The three tubes were then heated up to 150°C for 120 minutes in HACH reactor.

5. Finally, the tube was kept to gain the normal temperature and then HACH spectrophotometer (automatic determination, 2720) was utilized to read the value of COD of each sample with respect to the blank sample (calibrated as 0 mg/L).



Figure 3.12: Experimental arrangements for COD measurements



Figure 3.13: Digestion and H₂SO₄ solution



Figure 3.14: HACH COD vials of raw and treated samples



Figure 3.15: HACH reactor and spectrophotometer (DR 6000)

Total chromium

Chromium presents in the environment in different forms under various chemical, physical, and morphological conditions. Concentration of total chromium was measured both for the raw and treated wastewater by DR 6000 HACH machine. Here,

$$\text{Chromium (Cr) removal efficiency of MFC} = \frac{(\text{Cr})_{\text{initial}} - (\text{Cr})_{\text{final}}}{(\text{Cr})_{\text{initial}}} \times 100\%$$

Measurement Procedures of Total Chromium

1. Firstly, 10 mL potable water was collected in a blank vial which is considered as the blank solution for being calibrated to the concentration of 0 mg/L.
2. Then, 1 mL raw sample of wastewater and 1 mL sample of treated wastewater were collected in two different blank vials where 9 mL of distilled water was added individually to both of them.
3. HACH PERMACHEM (Cat. 1271099 pk/100) ChromaVer 3, chromium reagent was added to the experimental vials 10 mL.
4. The three tubes were then heated up to 100°C for 60 minutes in HACH reactor.
5. Finally, the tube was kept to gain the normal temperature and then HACH machine spectrophotometer utilized to read the concentration (mg/L) of total chromium of each sample with respect to the blank sample (calibrated as 0 mg/L).



Figure 3.16: HACH vials and PERMACHEM (ChromaVer 3) for measurements of total chromium

3.4 Analytical Methodologies

3.4.1 Scanning Electron Microscopy (SEM) – Energy Dispersive X-Ray (EDX)

SEM (Scanning Electron Microscope) & EDS (Energy Dispersive Spectroscopy) were conducted by the Department of Glass and Ceramic Engineering (GCE), BUET in where both the raw and treated carbon cloth were analyzed. While, the untreated raw cloth showed the absence of chromium, the treated carbon cloth (please see Figure 3.17) has confirmed the removal of trace metal comparing the raw and treated sample of the electrode (carbon cloth as anode).

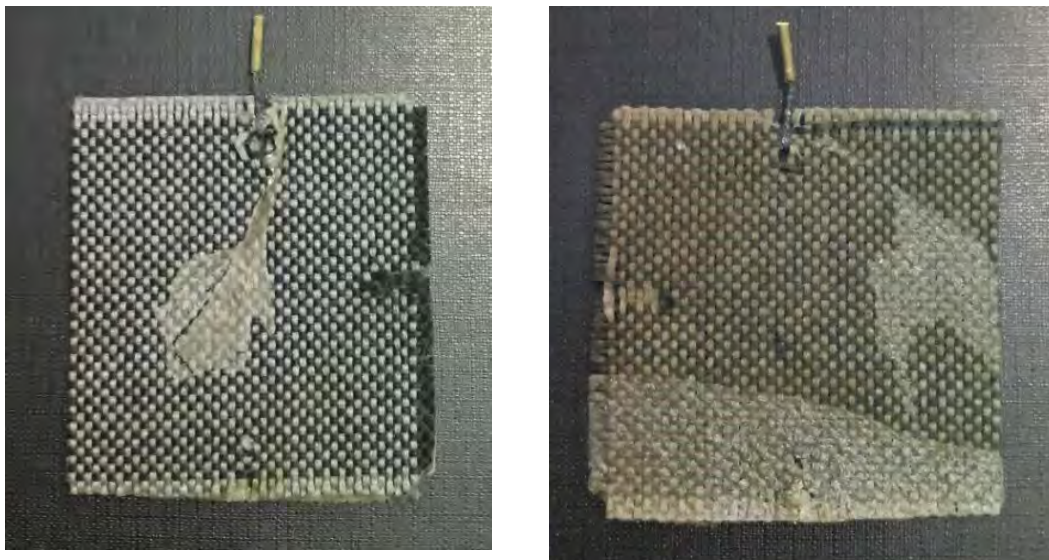


Figure 3.17: Treated carbon cloths (10 days of batch operation in anodic chamber of wastewater)



Figure 3.18: Raw and treated carbon cloths in SEM-EDX laboratory

Experimental Procedures of SEM – EDX analysis

1. Specific area was selected and localized on the basis of material deposition on the carbon cloths.
2. Then, the selected area was cut and collected for the perpetual experiments.
3. Specimen holders of SEM setup is utilized to hold and test the cut off cloths.



Figure 3.19: Laboratory setup for SEM – EDX analyses

4. Figure 3.18 illustrates that the device of analyses was switched on and electron gun emitted a narrow stream of electrons towards the condenser lens.

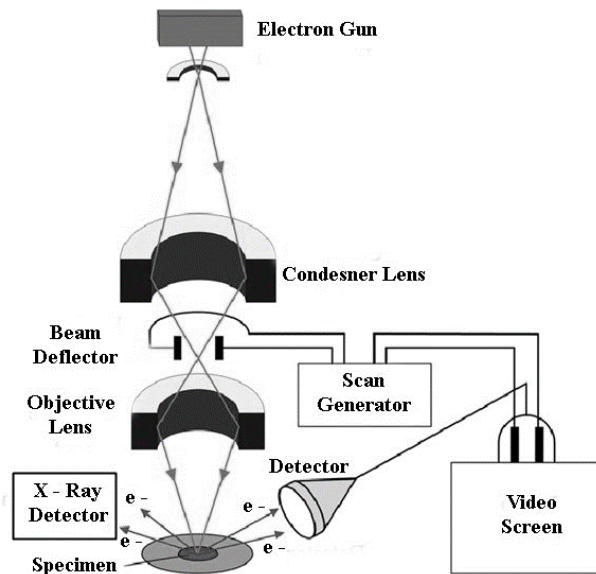


Figure: 3.20: Schematic diagram of SEM (Scanning Electron Microscopy) Analyses [107]

5. Then the condenser lens condensed and sent the processed stream towards beam deflector from where the stream went to the scan generator which was

connected to the video screen of computer (Figure 3.21) and to the objective lens simultaneously.

6. The path followed the way to reach the specimen (e.g. selected area of carbon cloths) from where high – energy electrons were emitted to generate a variety of signals at the surface of solid specimens which reached the detector and manifested themselves on the video screen. The data was collected over the selected area of the surface of the sample and a two – dimensional image was generated that displayed the spatial variations in properties including texture, chemical characterization, and elemental orientation of materials.

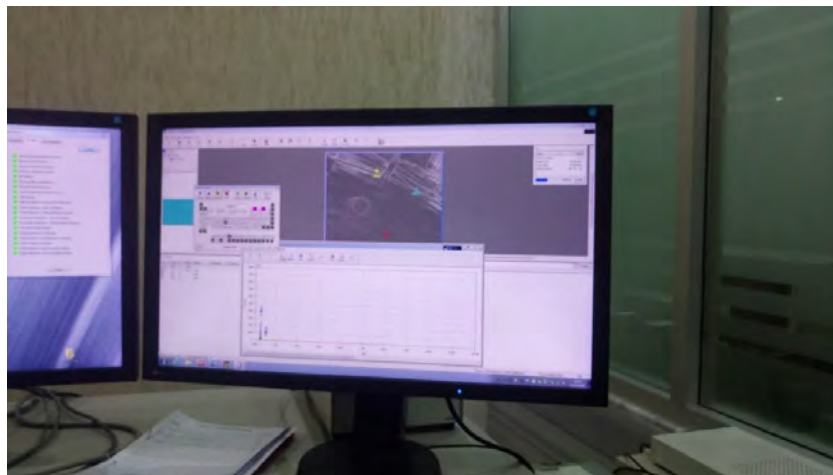


Figure 3.21: 2D images generation (SEM) and elemental analyses (EDX) of sample carbon cloth

7. The analyses of selected point locations on the sample was also performed following EDX analyses of specific metals concerning the presence of chromium on carbon cloth by dint of X – Ray detector.
8. The chemical composition (mass percentage) was determined qualitatively from the data received from computational analyses of SEM – EDX experiments.
9. EDX spectroscopy and system software of Jeol JSM – 7600F was used to analyze the energy spectrum in order to determine the compositional information of specific elements (e.g. Chromium).

3.4.2 X – Ray Diffraction (XRD) analyses

X – Ray Diffraction (XRD) experiments were conducted by the Department of Glass and Ceramic Engineering (GCE), BUET in where both the raw and treated carbon cloth were analyzed for Textile and Synthetic wastewater. Figure 3.22 shows the sample of treated cloths for XRD analyses and Figure 3.23 shows the laboratory setup of X-Ray Diffraction.



Figure 3.22: Samples of treated carbon cloths for XRD analyses



Figure 3.23: Laboratory setup of X – Ray Diffraction

Experimental Procedures of XRD analysis

1. Specific area was selected and cut from the sample carbon cloths.
2. Sample stage of goniometer was utilized to hold the cut off sample.
3. The device for XRD analysis was switched on and X – ray tube emitted the electromagnetic rays using the soller slit, divergence slit, and mask to reach the sample stage. Figure 3.24 shows the schematic diagram of XRD

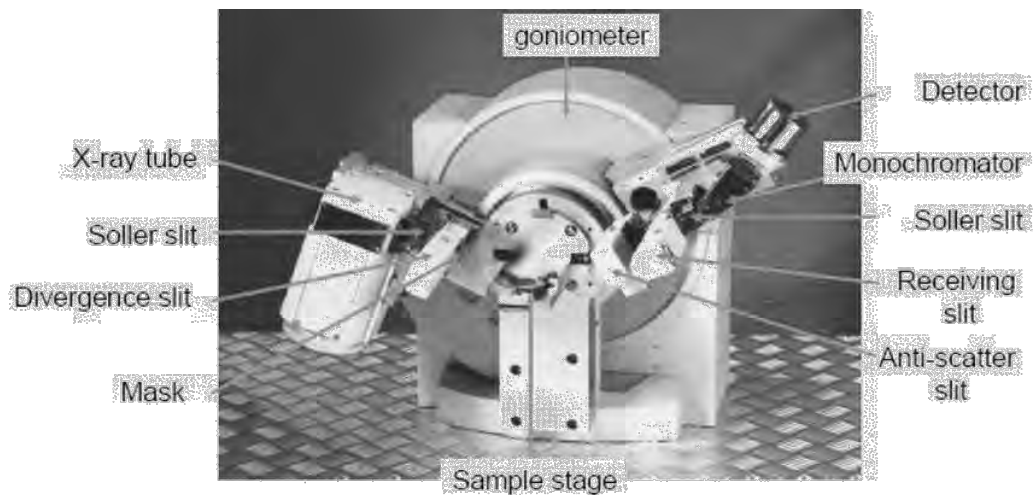


Figure 3.24: Schematic diagram of XRD (X-Ray Diffraction) Analyses [108]

4. The receiving slit received the reflection given by the sample due to X – ray irradiation.
5. The sample with a specific interplanar spacing was thus irradiated by X – ray beam with a comparable wavelength and monochromator.
6. The diffraction angle of the device was varied to satisfy the spacing of the component of concern (polycrystalline materials).
7. The angular positions and intensities of the resultant diffraction peaks were received in the computer through the detector.
8. The angular positions and diffraction peaks were plotted that produced a pattern with a view to characterizing the samples.

CHAPTER 4

RESULTS AND DISCUSSIONS

CHAPTER 4

RESULTS AND DISCUSSIONS

In this chapter the results of different experimental setups for microbial fuel cell (MFC) are presented to evaluate the performance comparatively. The evaluations help to compare different operational cases for different combinations of cell components in developing an efficient microbial fuel cell to remove chromium from textile wastewater. Logging the data for nine batches, the experimental investigations are discussed through graphical representations. The discussions provide logical explanations in evaluating the electrical performance and waste removal performances for COD and total chromium. This chapter presents the analytical assessments considering the surface morphology of electrodes applying SEM – EDX and XRD analyses. Finally, the optimum condition for cell environment and mechanism of microbial presence in removing chromium are also discussed.

4.1 Experimental Cases for Cell Operation

The experimental setup of microbial fuel cell (MFC) was ready for stable cell operations and data analyses after adjusting the cell components according to the design. The voltage and current output were logged by batch operation for 12 hours for Industry 1 and 240 hours (10 days) for synthetic wastewater (SWW) and textile wastewater (TWW) system. According to the availability of wastewater, initially seven experiments were conducted utilizing the wastewater of Industry 1. These seven experiments (Experiment no. 1 – 7) helped in developing an efficient setup for cell operation to remove chromium from textile wastewater (TWW, Industry 2). The finalized setup was then applied to Experiment no. 8 and Experiment no. 9 for treating SWW and TWW respectively considering the higher toxicity of Chromium (Cr).

Table 4.1 shows the relative results of cell operations. Table 4.2 presents the different combinations of cell components for different operational cases from Experiment no. 1 to Experiment no. 9.

Table 4.1: Relative results of cell operations

Exp. No.	Source of waste water	Batch Time (hours)	Max. Current (μA)	Max. Voltage (mV)	Max. Power Density $\times 10^3$ (Wm^{-3})	Removal of COD (%)	Removal of Total Cr (%)
1	Industry 1	12	81.2	358.2	24.73	19.21	-
2			139.2	438.5	50.86	21.68	-
3			151.9	483.0	63.55	31.26	-
4			194.7	736.0	114.41	30.07	-
5			239.4	866.6	172.89	34.51	-
6			256.9	930.5	174.29	45.42	-
7			332.8	1205.4	334.3	43.50	-
8	SWW	240	397.1	659.3	218.17	46.67	33.33
9	Industry 2		733.4	1100.1	672.34	52.20	53.75

Table 4.2: Combinations of cell components for different operational cases

Exp. No.	Source of wastewater	Batch Time (hours)	Anode (in anaerobic chamber of wastewater)	Cathode (in chamber of potable water)	Aeration in Cathode Chamber	Nutrient (Glucose) in Anode Chamber		
1	Industry 1	12	Graphite	Graphite	x	x		
2					✓	x		
3					✓	✓		
4			Industry 1	12	Al – Foil	Graphite	✓	✓
5					Al – Foil	Al – Foil		
6					Carbon Cloth	Graphite		
7					Carbon Cloth	Al – Foil		
8	SWW	240	Carbon Cloth	Graphite				
9	Industry 2		Carbon Cloth	Al – Foil over Graphite				

4.2 Evaluation of Electrical Parameters

The cell current and voltage were measured using a digital multi-meter (CD800a, Sanwa).

Table 4.3 shows the current generated for 12 hours of batch operation from Experiment no. 1 to Experiment no. 7. The values of current output aid to compare the performance of MFCs electrically for the first seven experiments and the bold values denote the maximum value of current generated for respective experiment.

The experimental data of Table 4.3 presents that Experiment no. 7 on wastewater of Industry 1 provides the maximum current output after 5 hours of batch operation. Besides, the table indicates that the value of current output decreases eventually for the 12 hours of batch operations after obtaining the maximum value.

Table 4.3: Current generation for 12 hours of batch operations from Experiment no. 1 to Experiment no. 7

Exp. No. Time (hours)	Exp. 1	Exp. 2	Exp. 3	Exp. 4	Exp. 5	Exp. 6	Exp. 7
	Current (μA)						
0	10.2	25.3	29.8	35.4	33.2	28.3	41.6
1	19.6	39.9	64.7	75.6	81.1	55.6	78.9
2	28.8	61.3	87.4	99.3	113.9	130.7	159.9
3	40.7	99.8	107.8	130.8	145.2	201.4	220.1
4	81.2	125.9	137.9	165.9	175.6	256.9	290.5
5	79.6	139.2	143.5	194.7	189.7	240.3	332.8
6	54.5	127.1	157.9	189.5	239.4	197.1	305.2
7	31.3	98.5	149.7	168.2	171.6	169.5	277.4
8	29.5	81.2	135.4	127.9	127.9	129.7	223.1
9	18.0	62.5	103.3	98.6	98.6	111.3	187.6
10	13.6	43.3	79.8	81.9	81.9	87.8	136.5
11	12.6	29.8	51.7	62.3	62.3	61.2	91.4
12	9.8	19.2	39.2	43.2	43.2	39.4	53.8

Table 4.4 shows the voltage output for 12 hours of batch operation from Experiment no. 1 to Experiment no. 7. They help to compare the electrical performances of first seven experiments and the bold values indicate the maximum value of voltage output at each experiment.

It is very clear from the experimental data of Table 4.4 that Experiment no. 7 on wastewater of Industry 1 provides the maximum voltage output after 5 hours of batch operation. Moreover, the table shows that the value of voltage output decreases eventually for the 12 hours of batch operations after obtaining the maximum value.

Table 4.4: Voltage output for 12 hours of batch operations from Experiment no. 1 to Experiment no. 7

Exp.No. Time (hours)	Exp. 1	Exp. 2	Exp. 3	Exp. 4	Exp. 5	Exp. 6	Exp. 7
	Voltage (mV)						
0	45.9	79.7	91.2	133.8	120.2	102.5	150.7
1	88.2	125.6	197.0	285.8	293.6	201.4	285.8
2	129.6	193.1	267.4	375.4	412.3	473.4	579.2
3	183.2	314.4	329.9	494.4	525.6	729.5	797.2
4	365.4	396.6	421.0	627.1	635.7	930.5	1052.2
5	358.2	438.5	439.1	736.0	686.7	870.4	1205.4
6	245.3	400.4	483.0	716.3	866.6	713.9	1105.4
7	140.9	310.1	458.1	635.8	621.2	613.9	1004.7
8	132.8	255.9	414.3	483.5	463.0	469.8	808.1
9	80.9	196.9	316.1	372.7	356.9	403.1	679.5
10	61.2	136.4	244.2	309.6	296.5	318.0	494.4
11	56.5	93.7	158.1	235.5	225.5	221.7	331.1
12	44.1	60.5	120.0	163.3	156.4	142.7	194.9

Bolding the maximum voltage and current outcome, Table 4.5 presents the voltage and current generation for 10 days (240 hours) of batch operations for the treatment of synthetic wastewater (Experiment 8) and textile wastewater (Experiment 9, Industry 2).

Table 4.5 that Experiment no. 8 on synthetic wastewater (SWW) provides the maximum voltage and current output after 72 hours of batch operation and Experiment no. 9 on textile wastewater of Industry 2 provides the maximum value of electricity after 120 hours of batch operation. According to the table, the values of electrical output decreases eventually for the 240 hours (10 days) of batch operations after obtaining the maximum value.

Table 4.5: Current and voltage outcome for 10 days of batch operations for the treatment of synthetic wastewater and textile wastewater

Time (hours)	Synthetic wastewater (SWW, Exp. no. 8)		Textile wastewater (TWW, Exp. no. 9, Industry 2)	
	Current (μA)	Voltage (mV)	Current (μA)	Voltage (mV)
0	3.9	9.6	8.7	13.1
12	62.3	105.8	76.6	114.9
24	128.1	214.4	169.7	254.6
36	184.1	310.2	260.5	390.8
48	239.0	408.6	273.4	410.1
60	309.2	497.8	347.1	520.6
72	397.1	659.3	403.8	605.7
84	348.3	605.6	468.6	703.2
96	295.4	591.2	580.7	870.9
108	254.1	576.6	670.3	1005.4
120	239.7	496.2	733.4	1100.1
132	201.2	432.0	663.7	995.6
144	187.6	401.8	564.5	846.7
156	169.2	379.2	464.3	696.5
168	113.7	287.7	361.3	541.9
180	93.3	153.9	266.7	400.2
192	79.8	143.7	240.1	359.7
204	58.2	96.1	157.2	235.8
216	49.6	82.8	96.4	144.6
228	31.3	51.6	38.1	56.9
240	4.1	6.8	6.9	10.5

4.2.1 Graphical Representations for Generation of Current

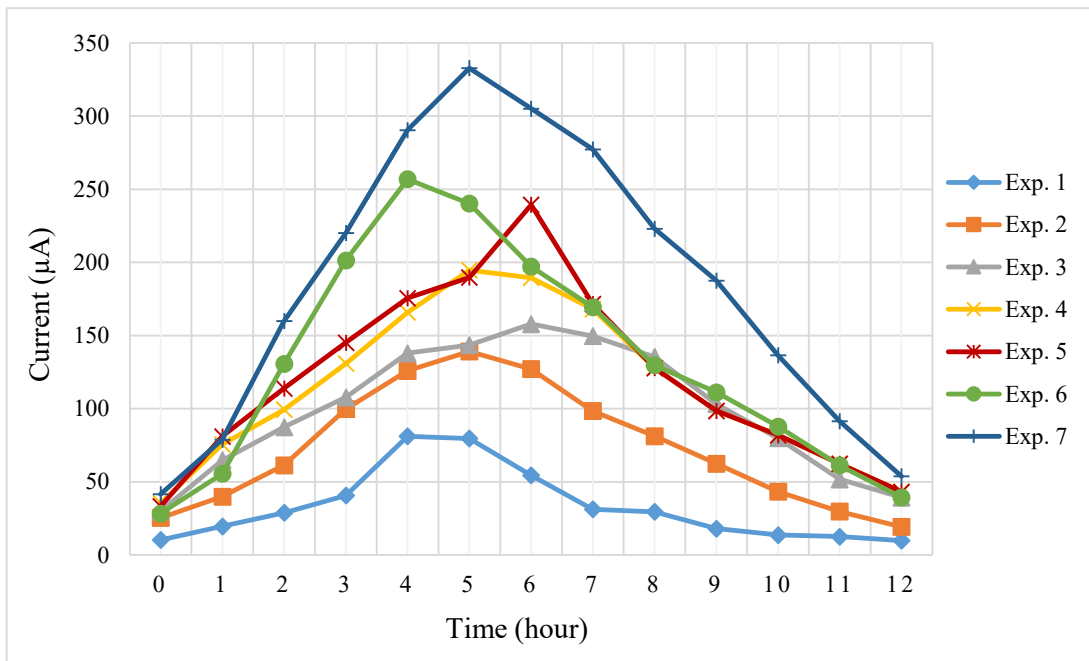


Figure 4.1: Current generation for 12 hours of batch operation for Industry 1 from Experiment no. 1 to Experiment no. 7

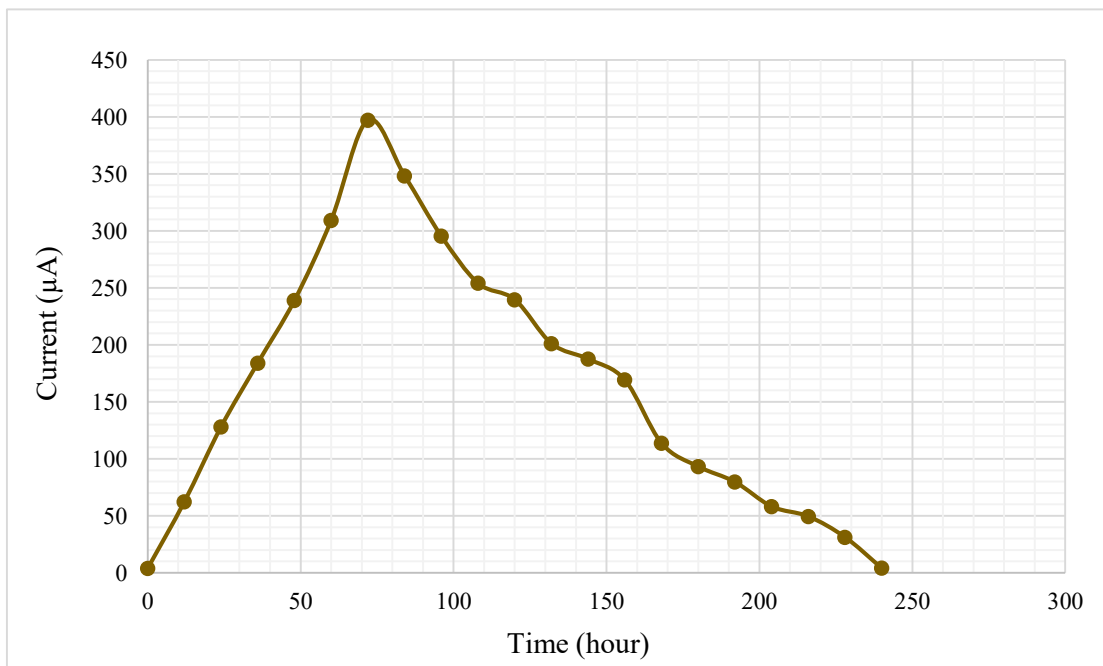


Figure 4.2: Current generation for 10 days (240 hours) of batch operation for synthetic wastewater (SWW, Experiment no. 8)

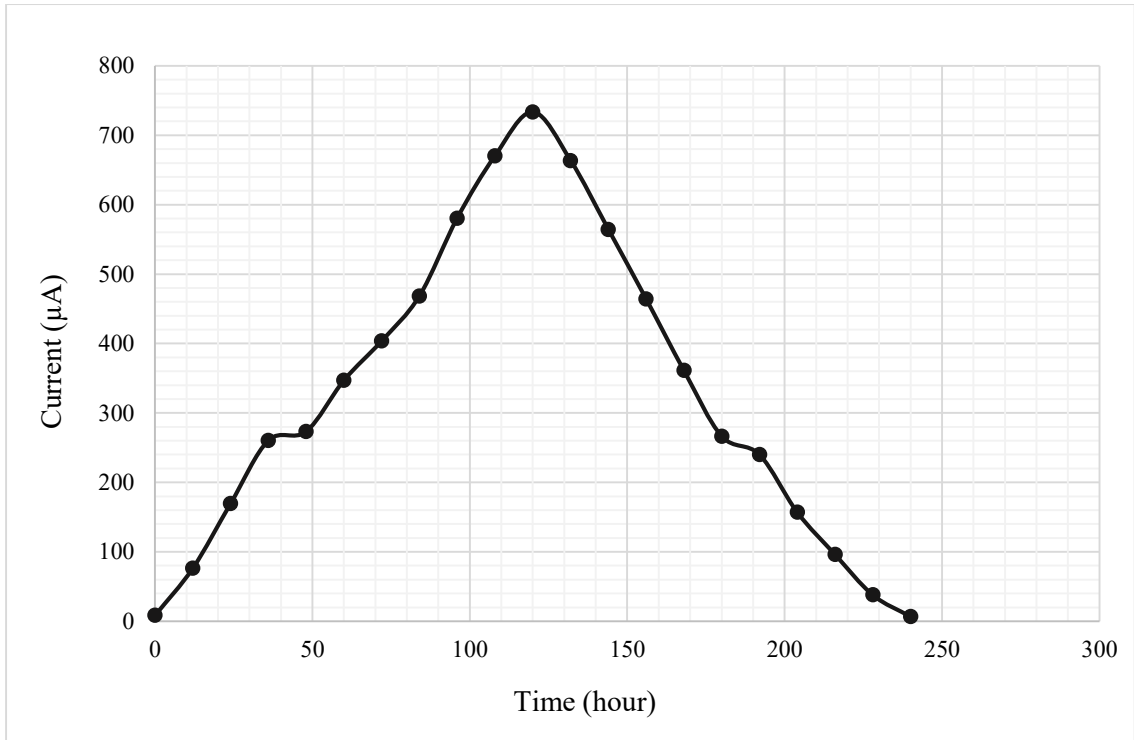


Figure 4.3: Current generation for 10 days (240 hours) of batch operation for wastewater of Industry 2 (TWW, Experiment no. 9)

4.2.2 Graphical Representations of Voltage Outcome

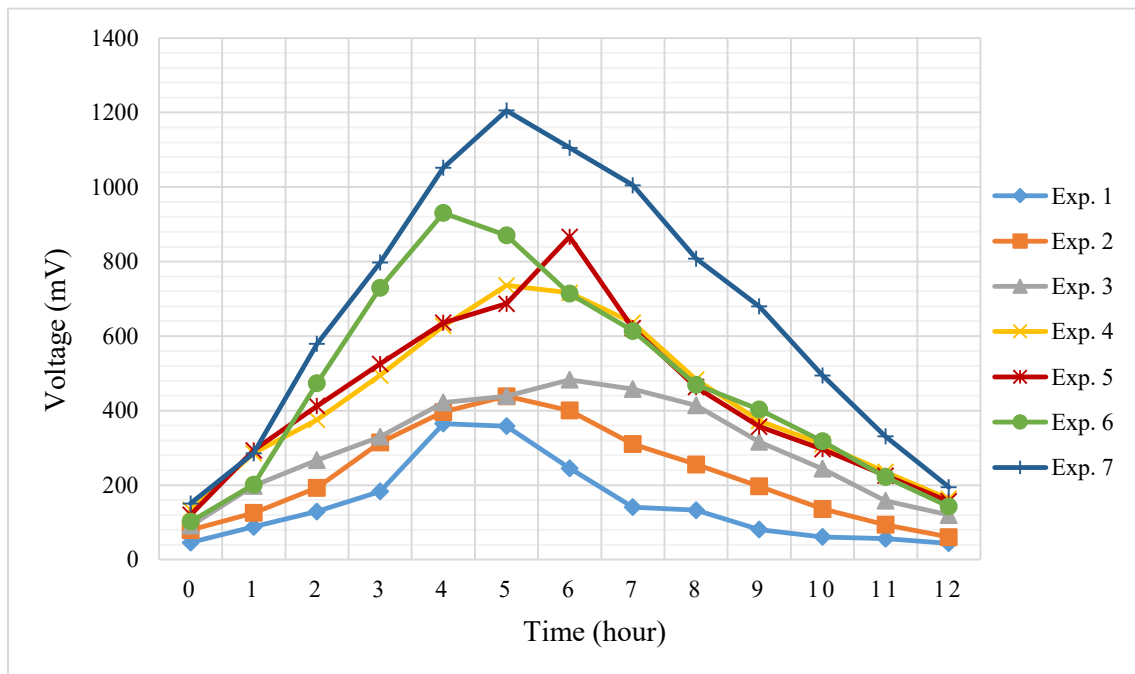


Figure 4.4: Voltage output for 12 hours of batch operation for Industry 1 from Experiment no. 1 to Experiment no. 7

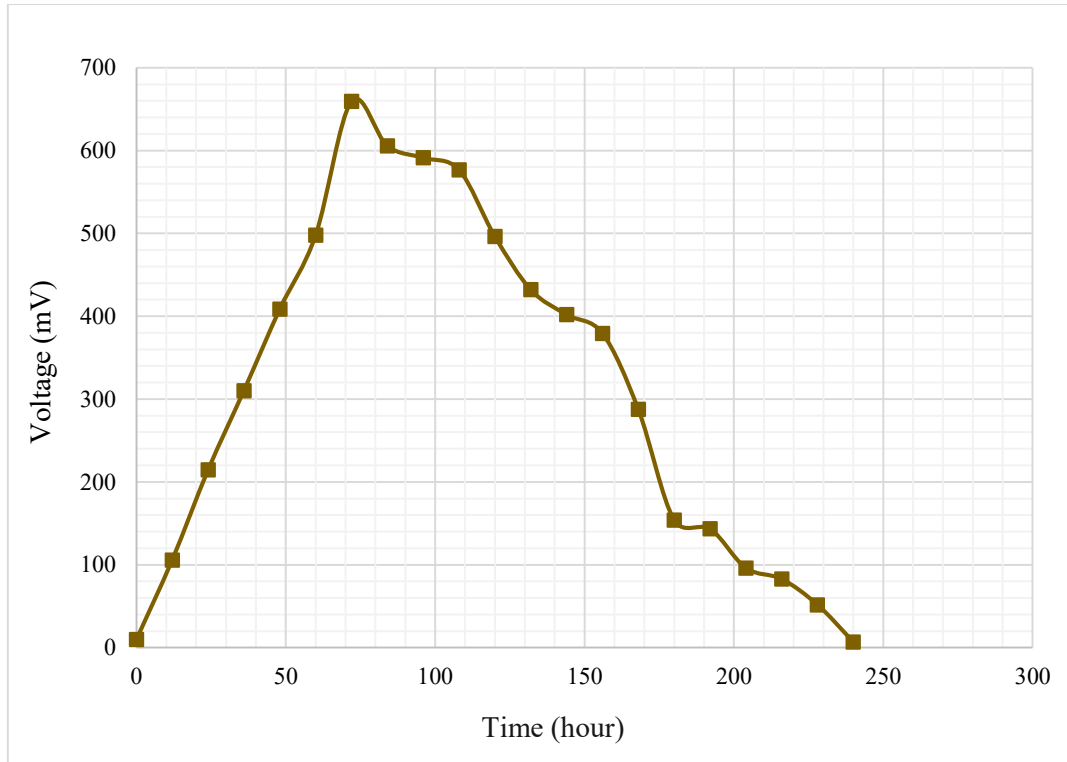


Figure 4.5: Voltage output for 10 days (240 hours) of batch operation for synthetic wastewater (SWW, Experiment no. 8)

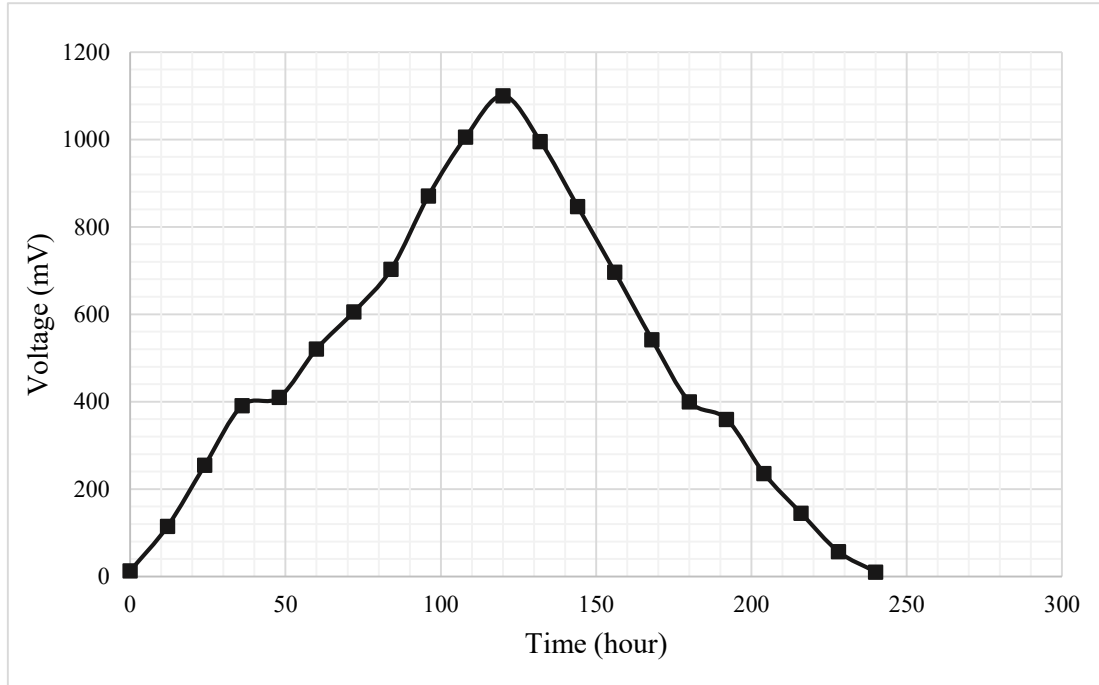


Figure 4.6: Voltage output for 10 days (240 hours) of batch operation for wastewater of Industry 2 (TWW, Experiment no. 9)

4.2.3 Graphical Relationship between Current and Voltage

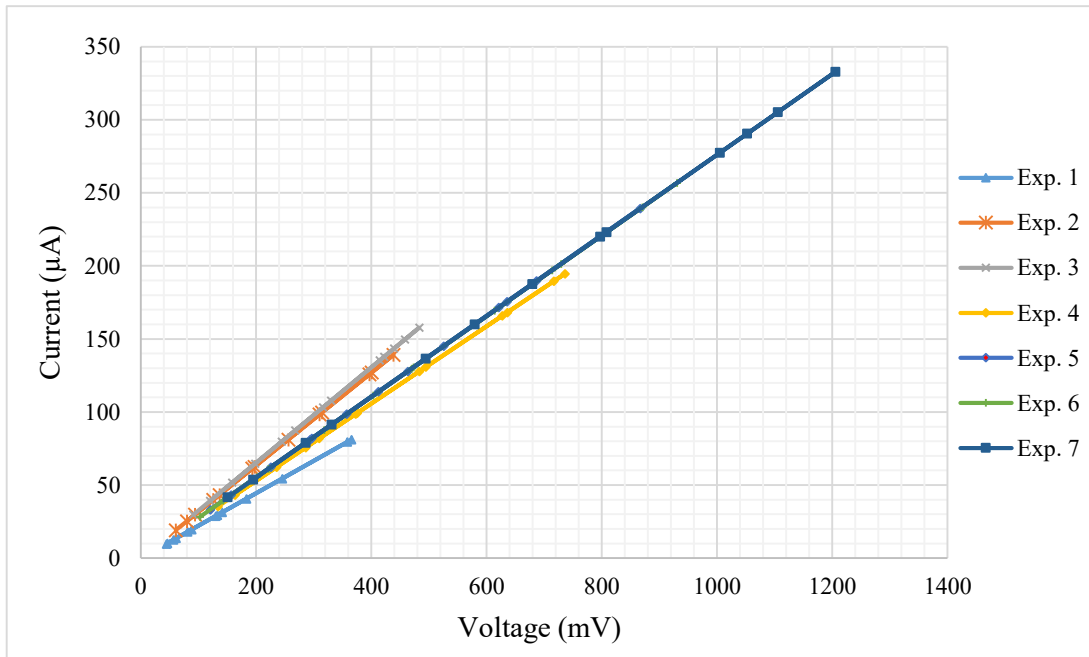


Figure 4.7: Relationship between current and voltage output for 12 hours of batch operation for Industry 1 from Experiment no. 1 to Experiment no. 7

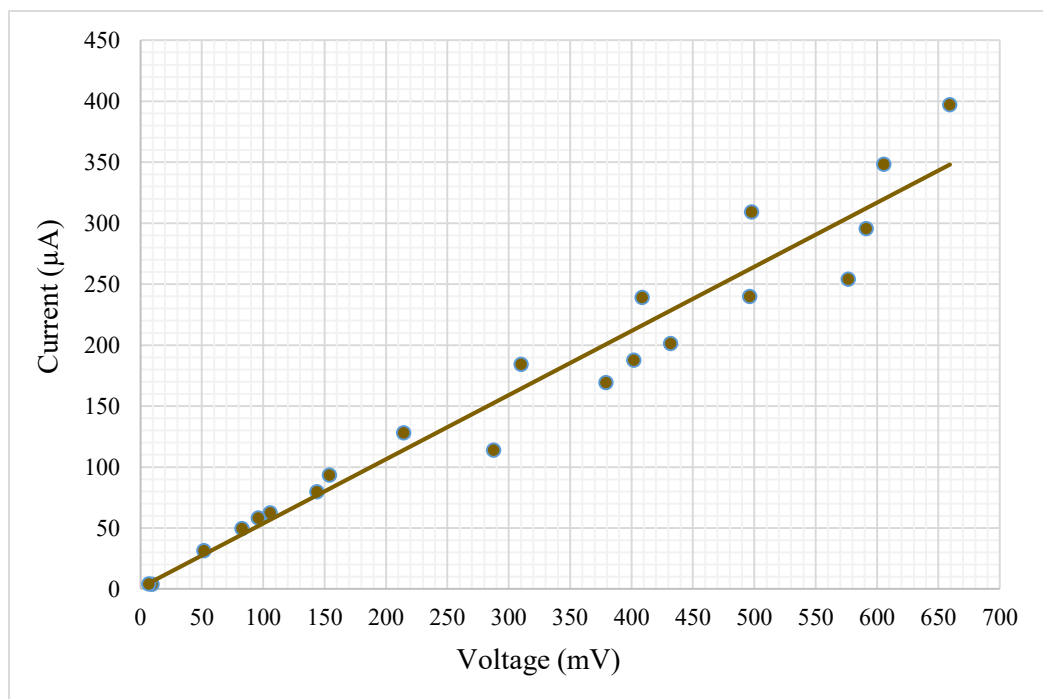


Figure 4.8: Relationship between current and voltage output for 240 hours (10 days) of batch operation for synthetic wastewater (SWW, Experiment no. 8)

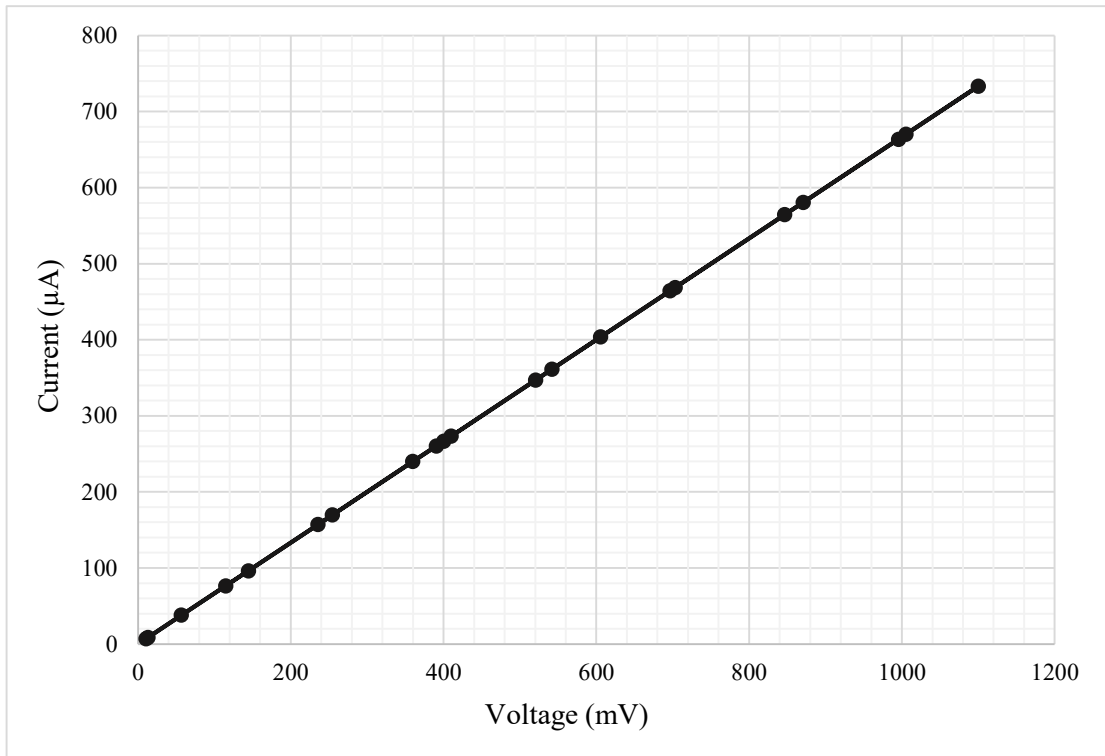


Figure 4.9: Relationship between current and voltage output for 240 hours (10 days) of batch operation for wastewater of Industry 2 (TWW, Experiment no. 9)

When a potential (voltage) difference is applied across the two ends of a wire current starts to run over through the path with respect to the resistance the material offers to the flow of charges to that material. The resistance is independent of current or voltage and so remains constant. Ohm's law states that the current is directly proportional to the voltage and inversely proportional to the resistance. This means that increasing the voltage will cause the current to increase. Figure 4.7, 4.8, and 4.9 represent graphs for current vs. voltage. The three graphs resulted in straight lines and thus verified the validity of Ohm's law for a DC circuit. The biggest advantage of DC electricity is that it is easier to store than AC, especially in such small scale.

4.2.4 Graphical Representations for Power Density

Table 4.6: Power density from 12 hours of batch operations for Experiment no. 1 to Experiment no. 7

Exp. No. Time (hours)	Exp. 1	Exp. 2	Exp. 3	Exp. 4	Exp. 5	Exp. 6	Exp. 7
	Power density $\times 10^3 \text{ (Wm}^{-3}\text{)}$						
0	0.39	1.68	2.26	3.95	3.33	2.42	5.22
1	1.44	4.17	10.67	18.00	19.84	9.33	18.79
2	3.11	9.86	19.48	31.06	39.14	51.56	77.17
3	6.21	26.15	29.63	53.89	63.60	122.43	146.22
4	24.73	41.60	48.49	86.698	93.02	199.20	254.72
5	23.76	50.86	52.51	119.41	108.56	174.29	334.30
6	11.14	42.41	63.55	113.13	172.89	117.26	281.15
7	3.67	25.44	57.15	89.12	88.83	86.72	232.26
8	3.26	17.32	46.75	51.53	49.35	50.77	150.23
9	1.21	10.25	27.21	30.62	29.33	37.39	106.23
10	0.69	4.92	16.24	21.13	20.23	23.27	56.24
11	0.59	2.32	6.81	12.23	11.71	11.30	25.22
12	0.36	0.97	3.92	5.88	5.63	4.69	8.74

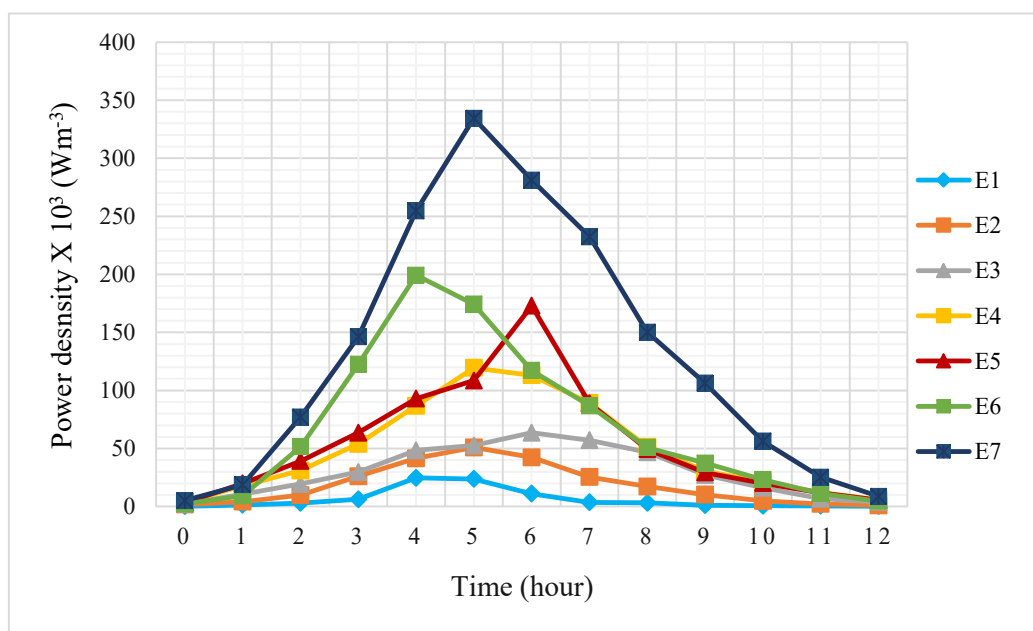


Figure 4.10: Power density for 12 hours of batch operation for Industry 1 from Experiment no. 1 to Experiment no. 7

Table 4.6 shows the calculated power density for 12 hours of batch operation from Experiment no. 1 – 7 by utilizing the voltage and current from Table 4.3 and 4.4. Besides, Table 4.7 shows the same by utilizing Table 4.5 for 10 days of batch operation

for SWW and TWW. Figure 4.10 to Figure 4.12 present the graphical representation to compare the different sets of experiment. Comparing the electrical performance, the bold values in the tables indicate the maximum value of power density generated at each experiment.

Table 4.7: Power density from 10 days (240 hours) batch operations of synthetic wastewater (SWW) and textile wastewater (TWW)

Time (hours)	Synthetic wastewater (SWW, Exp. no. 8)	Textile wastewater (TWW, Exp. no. 9, Industry 2)
	Power density x 10 ³ (Wm ⁻³)	Power density x 10 ³ (Wm ⁻³)
0	0.03	0.09
12	5.49	7.33
24	22.88	36.00
36	47.58	84.84
48	81.37	93.43
60	128.27	150.58
72	218.17	203.82
84	175.78	274.60
96	145.53	421.44
108	122.10	561.60
120	99.12	672.34
132	72.43	550.65
144	62.82	398.30
156	53.48	269.49
168	27.26	163.16
180	11.96	88.94
192	9.55	71.97
204	4.66	30.89
216	3.42	11.62
228	1.35	1.81
240	0.02	0.06

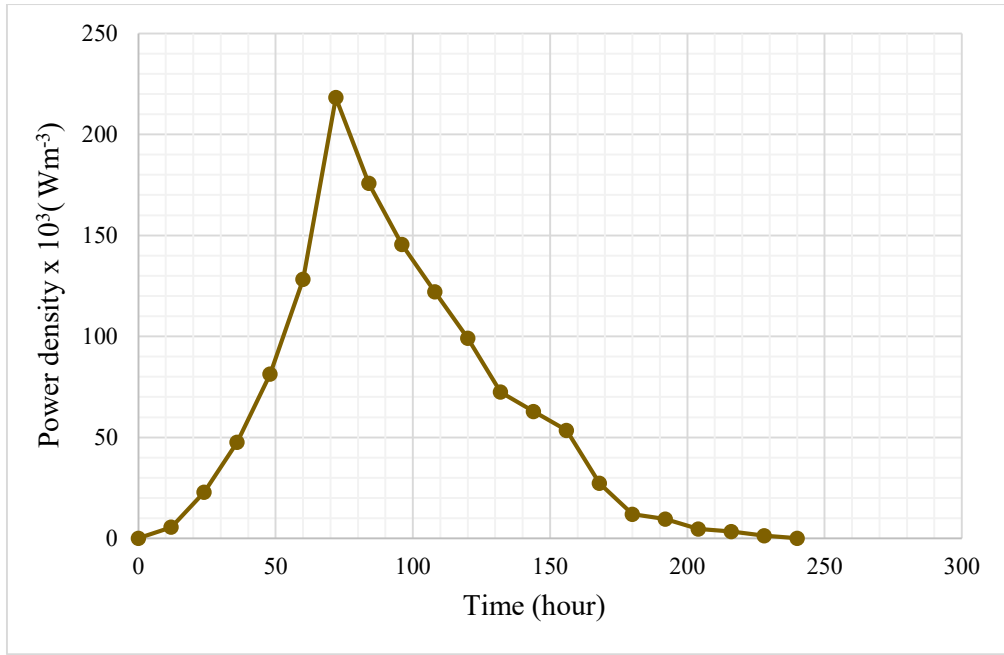


Figure 4.11: Power density for 10 days (240 hours) of batch operation for synthetic wastewater (SWW, Experiment no. 8)

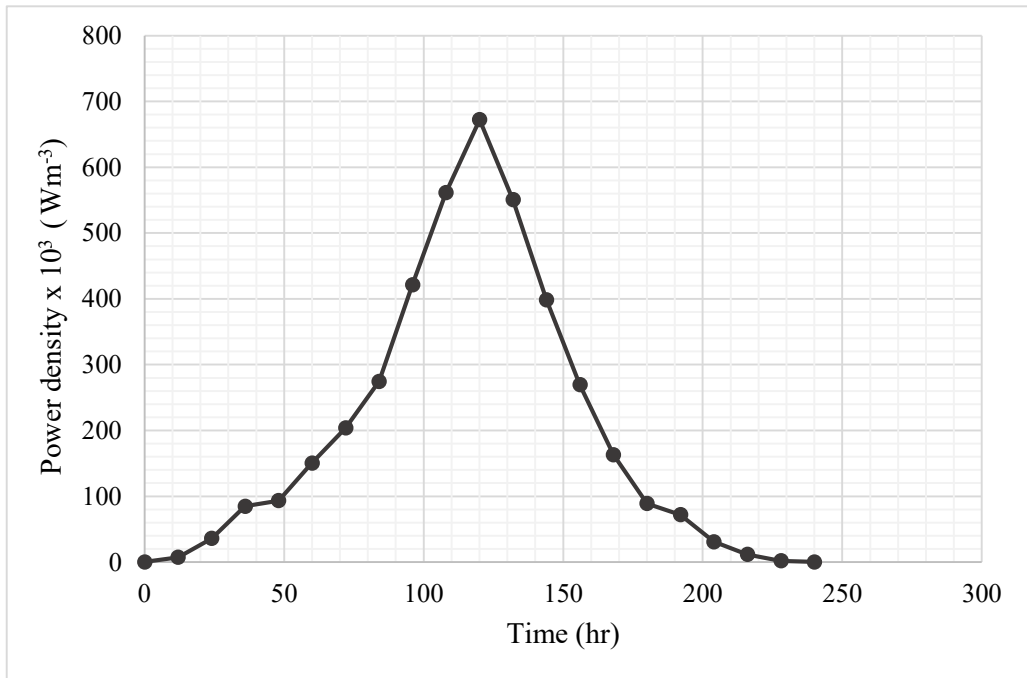


Figure 4.12: Power density for 10 days (240 hours) of batch operation for wastewater of Industry 2 (TWW, Experiment no. 9)

4.2.5 Graphical Representations of Recovered Energy

Table 4.8: Recovered energy from 12 hours of batch operations for Experiment no. 1 to Experiment no. 7

Exp. No. Time (hours)	Exp. 1	Exp. 2	Exp. 3	Exp. 4	Exp. 5	Exp. 6	Exp. 7
	Energy x 10 ³ (kJm ⁻³)						
0	0	0	0	0	0	0	0
1	5.19	15.02	38.43	64.81	71.43	33.59	67.64
2	22.39	71.02	140.25	223.64	281.78	371.24	555.64
3	67.08	282.37	320.04	582.04	686.89	1322.24	1579.18
4	356.05	599.07	698.28	1248.43	1339.489	2868.52	3667.94
5	427.69	915.55	945.18	2149.39	1954.04	3137.24	6017.36
6	240.59	915.96	1372.76	2443.33	3734.47	2532.76	6072.81
7	92.58	641.15	1440.07	2245.76	2238.53	2185.28	5853.03
8	93.99	498.83	1346.39	1484.03	1421.22	1462.31	4326.72
9	39.28	332.23	881.63	992.22	950.22	1211.44	3441.74
10	24.97	177.18	584.59	760.64	728.45	837.64	2024.58
11	23.43	92.002	269.595	484.15	463.66	447.68	998.52
12	15.56	41.80	169.28	253.96	243.21	202.42	377.41

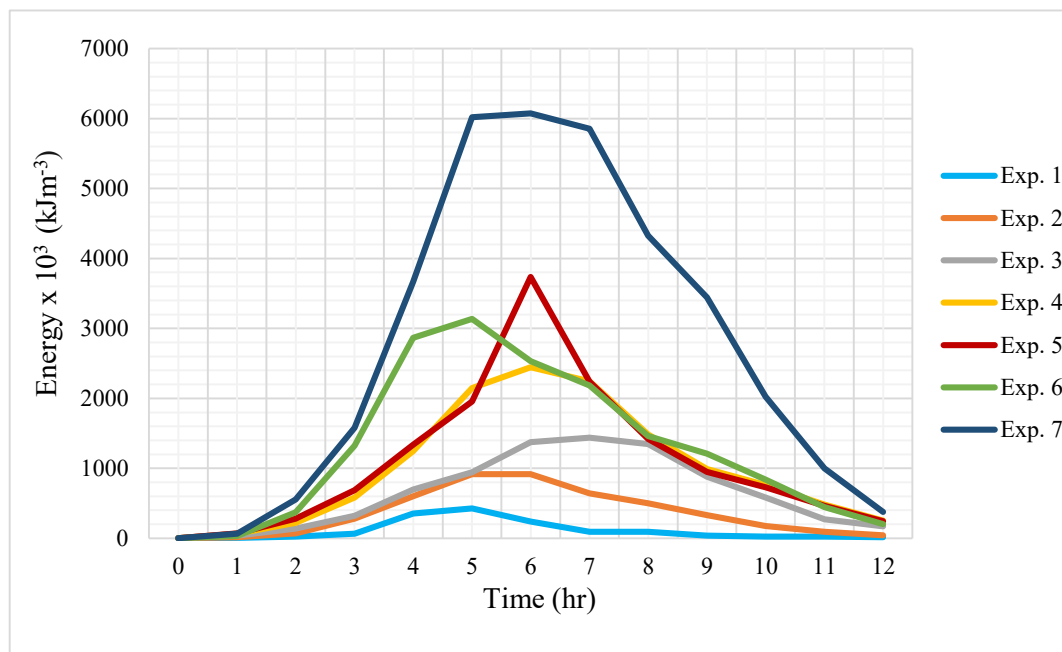


Figure 4.13: Recovered energy for 12 hours of batch operation for Industry 1 from Experiment no. 1 to Experiment no. 7

Table 4.8 and figure 4.13 show the recovered energy for 12 hours of batch operation from Experiment no. 1 – 7 and Table 4.9 shows the same for 10 days of batch operation

for SWW and TWW. Figure 4.13 to Figure 4.15 present the graphical representation to compare the different sets of experiment with respect to the recovered energy. Comparing the electrical performance, the bold faced values in the tables indicate the maximum value of energy recovered at each experiment.

Table 4.9: Recovered energy from 10 days (240 hours) batch operations of synthetic wastewater (SWW) and textile wastewater (TWW).

Time (hours)	Synthetic Wastewater (SWW, Exp. no. 8)	Textile Wastewater (TWW, Exp. no. 9, Industry 2)
	Energy x 10 ³ (kJm ⁻³)	Energy x 10 ³ (kJm ⁻³)
0	0	0
12	237.25	316.85
24	1976.99	3110.80
36	6166.64	10994.77
48	14061.20	16145.47
60	27705.56	32526.05
72	56550.53	52829.64
84	53154.48	83038.92
96	50296.46	145650.71
108	47470.56	218349.96
120	42820.68	290452.80
132	34418.09	261668.77
144	32566.40	206479.65
156	30034.88	151344.16
168	16484.30	98677.39
180	7749.41	57636.00
192	6601.19	49745.65
204	3423.98	22685.47
216	2657.29	9032.76
228	1104.87	1482.84
240	20.07	52.16

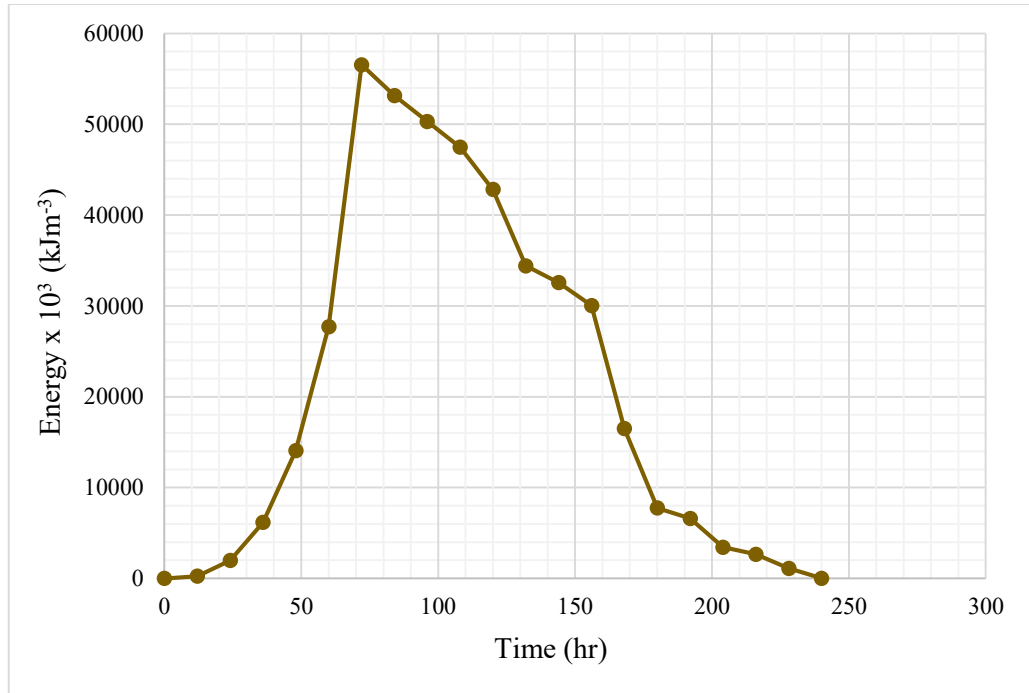


Figure 4.14: Recovered energy for 10 days (240 hours) of batch operation for synthetic wastewater (SWW, Experiment no. 8)

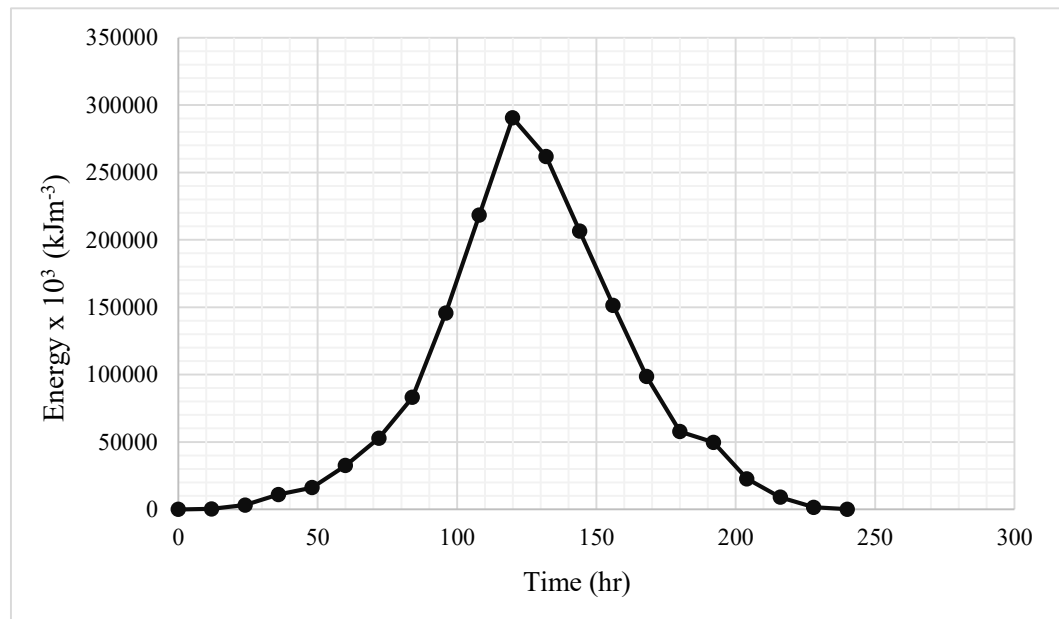


Figure 4.15: Recovered energy for 10 days (240 hours) of batch operation for wastewater of Industry 2 (TWW, Experiment no. 9)

4.2.6 Coulombic Efficiency of MFC

Table 4.10 calculates the coulombic efficiency utilizing the electrical parameters of microbial fuel cell (MFC) and change of chemical oxygen demand (COD) in wastewater.

Table 4.10: Coulombic efficiency of microbial fuel cell in treating wastewater

Experiment No.	8	9
Source of wastewater	Synthetic wastewater	Textile wastewater
Working volume, V (L)	1.2	
Time to generate maximum current, t (s)	72×3600	120×3600
Maximum current, I (μA)	397.1	733.4
Initial COD concentration, $\text{COD}_{\text{initial}}$ (mgL^{-1})	512	1544
COD concentration at maximum current generation, COD_t (mgL^{-1})	409	1310
Coulombic Efficiency, C_E (%)	6.90	9.35

4.3 Removal Percentages of COD and Total Chromium

Table 4.11 and 4.12 show the experimental data for removal percentage of total chromium and COD presented in the wastewater. Figure 4.16 represents the comparative removal percentage for the 9 experiments to evaluate the cell performance in removing chromium from textile wastewater (TWW).

Table 4.11: Experimental data for percentage removal of total chromium (Cr)

Exp. No.	Source of Wastewater	Initial Concentration of Total Cr (mgL^{-1})	Final Concentration of Total Cr (mgL^{-1})	Total Cr Removal (%)
1 – 7	Industry 1	0	0	-
8	Synthetic Wastewater	0.030	0.020	33.33
9	Industry 2 (TWW)	0.080	0.037	53.75

Table 4.12: Experimental data for percentage of COD removal

Exp. No.	Source of Wastewater	Initial Concentration of COD (mgL ⁻¹)	Final Concentration of COD (mgL ⁻¹)	COD Removal (%)
1	Industry 1	984	795	19.21
2		987	773	21.68
3		891	613	31.26
4		765	535	30.07
5		739	484	34.51
6		698	381	45.42
7		701	396	43.50
8	Synthetic Wastewater	512	273	46.67
9	Industry 2 (TWW)	1544	738	52.20

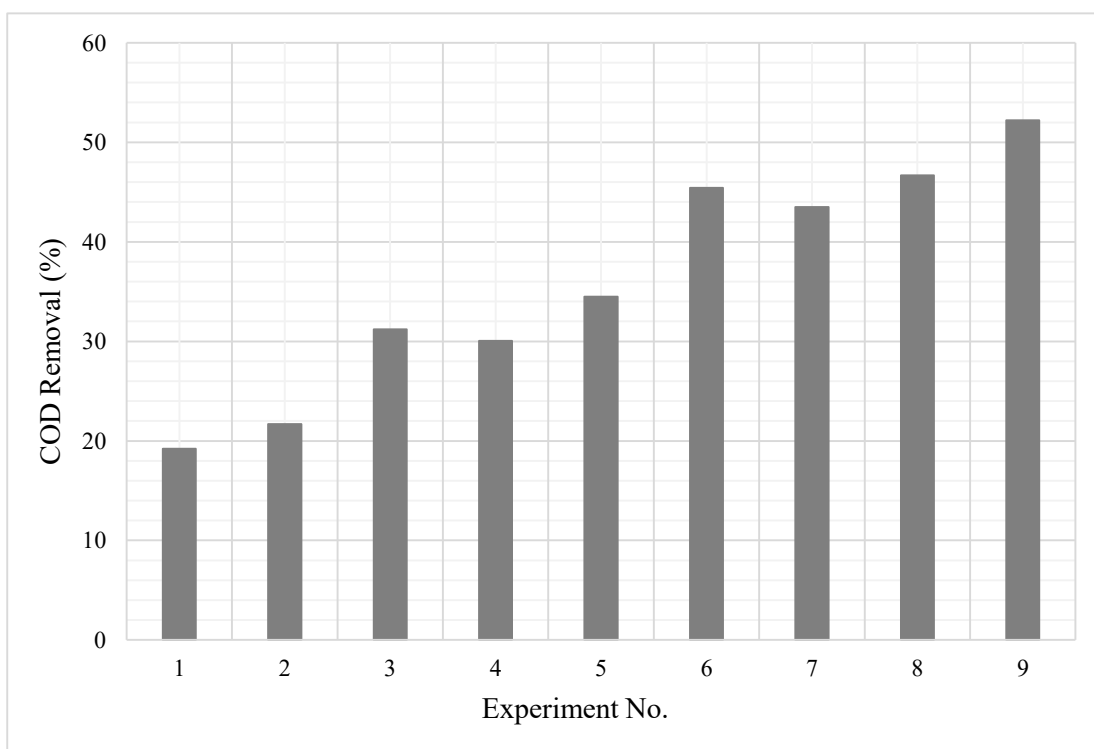


Figure 4.16: Removal percentage of COD from Experiment no. 1 to Experiment no. 9

4.4 Discussions

4.4.1 Advantage of Aeration in Cathode Chamber

Figure 4.1 and 4.4 present the current and voltage for industry 1 from Experiment no. 1 to Experiment no. 7. Each of the seven experiments were conducted for a batch operation of 12 hours. Apart from Experiment 1 the cathode compartment was aerated from Experiment no. 2 to Experiment no. 9. Figure 4.1, Figure 4.4, and Figure 4.16 have showed that the presence of aeration in cathode chamber gives increase amount of electricity generation and percentage of COD removal than the absence of aeration. Experiment no. 1 and Experiment no. 2 had same arrangement of cell operation with anode and cathode of graphite except the presence of aeration process in Experiment no. 2. Aeration in cathode harnessed the reduction reaction by increasing the dissolved oxygen in electrolyte [109].

Air pump of MFC creates bubble and oxygenates the water for providing oxygen as available electron acceptor. The oxygen combines with hydrogen ions and maintains the pH of microbial fuel cell (MFC). In this way, MFC provides a better system than other treatment methods where external and advanced unit operations are required to provide aeration and chemical reagents are required to maintain pH which are expensive. Therefore, MFC is cost-effective because it requires neither external unit operations nor chemical reagents.

Reasonably, Experiment no. 2 generated more electricity than Experiment no. 1. When Experiment no. 1 gave a maximum of 81.2 μA current with 358.2 mV voltage and 19.21% COD removal in absence of aeration and nutrient. Experiment no. 2 generated a maximum of 139.2 μA current and 438.48 mV voltage with 21.68% COD removal in presence of aeration but no nutrient was added to the anaerobic chamber of anode. Figure 4.10 and Figure 4.13 show that the maximum power density of Experiment no. 1 is 24.73 mWm^{-3} when the maximum power density for Experiment no. 2 is 50.86 mWm^{-3} . From the figures it is evident that aeration in cathode increases the production of bio-electricity as Experiment no. 1 recovered a maximum of 0.428 kJm^{-3} energy and Experiment no. 2 recovered a maximum of 0.916 kJm^{-3} energy. Therefore, aeration in cathode is an important parameter to enhance cell performance. In this regard, it is important to mention that aeration in anode stops the production of electrons because the organics react with available oxygen to produce carbon di-oxide and water instead

of carbon di-oxide, protons, and electrons. Moreover, the aeration creates a shear disturbance around the anode. The disturbance hinders the microbial community to transfer electrons that eventually decreases the thickness of biofilms.

4.4.2 Impact of Nutrients in Anode Chamber

Nutrients are added in microbial fuel cell (MFC) as the substrate for organic wastes [105] so that the microbes can receive available organics to degrade for generating their survival energy (ATP). The active presence of microbes is important to get uninterrupted electron transfer between the half-cells.

Nutrient was added to the anode compartment of all other experiments except Experiment no. 1 and Experiment no. 2. Nutrient provides excess substrates for the microbes. Therefore, the microbes can receive necessary organics to degrade and produce more electrons for continuing the treatment process.

Figure 4.1 and Figure 4.4 show five experiments from Experiment no. 3 to Experiment no. 7 generated more electricity in presence of nutrient than Experiment no. 1 and Experiment no. 2 where no nutrient was applied. In case of Experiment no. 2, 139.2 μA current and 438.48 mV voltage were generated with 21.68% COD removal. On the other hand, Experiment no. 3 (anode and cathode of graphite) generated 157.87 μA current for a voltage drop of 483.08 mV with 31.26% COD removal in presence of nutrient.

Therefore, the nutrient can increase the production of electrons and the percentage of waste removal which contribute directly to the removal of chromium from wastewater. In this work, glucose was added as a nutrient (the source of carbon) from Experiment no. 3 to Experiment no. 9. The required concentration of carbon source was maintained at a concentration that was greater than 10^{-2} mol/L for the stable growth of microbes [105].

4.4.3 Effect of Electrode Materials on Cell Performance

Graphite electrode was used for both anode and cathode from Experiment no. 1 to Experiment no. 3. Al – Foil anode and graphite cathode was used in Experiment no. 4. Al – Foil electrode was used for both anode and cathode in Experiment no. 5. Figure

4.1, Figure 4.4, and Figure 4.16 show that Experiment no. 4 generated more electricity than Experiment no. 3 as anode was replaced by an Al – Foil electrode because the conductivity of Al – Foil electrode is more than graphite electrode [110]. Experiment no. 4 resulted in maximum 194.7 μA current and 735.966 mV voltage with 30.07% COD removal. Figure 4.10 and Figure 4.13 show that the maximum recovered energy was increased by 55.47% from 1.44 kJm^{-3} (Experiment no. 3) to 2.245 kJm^{-3} (Experiment no. 4) for a maximum power density of 63.55 mWm^{-3} (Experiment no. 3) and 119.410 mWm^{-3} (Experiment no. 4) respectively.

Experiment no. 5 used Al – Foil for both anode and cathode. In this consideration, Figure 4.1, 4.4, and Figure 4.16 show that Experiment no. 5 generated maximum 239.4 μA current with 866.628 mV voltage and 34.51% COD removal. Considering the maximum current and voltage for Experiment no. 5 Figure 4.10 and Figure 4.13 show that the maximum recovered energy was increased by 66.3% from 2.25 kJm^{-3} (Experiment no. 4) to 3.73 kJm^{-3} (Experiment no. 5) for a maximum power density of 119.41 mWm^{-3} and 172.89 mWm^{-3} respectively. For developing an efficient setup of MFC, Experiment no. 5 provided better results than Experiment no. 4. Here, Al-Foil electrodes can provide better conductivity and surface area so that the chemical oxygen demand (COD) can be removed more efficiently.

Figure 4.1, Figure 4.4, and Figure 4.16 showed that the change in anode from Experiment no. 5 (Al-Foil anode) to Experiment no. 6 (carbon cloth anode) brought about 7.3% rise in the result when a maximum of 256.9 μA current and 930.492 mV voltage were generated with 45.42% COD removal. Figure 4.10 and 4.13 show that Experiment no. 6 recovered a maximum of 3.14 kJm^{-3} energy for a maximum power density of 174.29 mWm^{-3} .

The change of cathode from Experiment no. 6 (Graphite cathode) to Experiment no. 7 (Al – Foil cathode) supported the earlier finding where Al – Foil electrode generated more electrons than graphite electrode. Figure 4.1, Figure 4.4, and Figure 4.16 shows that Experiment no. 7 generated maximum 332.8 μA current and 1205.406 mV voltage with 43.50% COD removal. In this regard, Figure 4.10 and 4.13 show that Experiment no. 7 recovered a maximum energy of 6.07 kJm^{-3} for a maximum power density of 334.298 mWm^{-3} .

Therefore, it is observed that, MFC provided better results with carbon cloth electrodes than graphite or Al – Foil electrodes because carbon cloth has high electrical conductivity, lower resistance and chemical stability [112-113]. Moreover, nanostructures – impregnated anodes of carbon cloth provide higher porosity and surface area than graphite electrodes and aluminum foil. Therefore, it can provide more suitable positions specifically for the adsorption of contaminants (e.g. chromium) through microbial metabolism [63]. Thus carbon cloth was the most efficient electrode among the available electrodes of the cell. It is because the growth of microbes and electron transport system required considerable surface areas to make the flow continuous

The significance of comparing different types of electrodes is that it helps to find the workable, electrically efficient for removing chromium by microbial metabolism, easily available, and cost-effective electrode.

4.4.4 Comparative Analyses for Removing Chromium

Wastewater from Industry 1 was used in Experiment no. 1 – 7. The experimental setups of these seven experiments provide significant comparison for developing an efficient MFC configuration. Carbon cloth anode, Al-Foil/graphite cathode, NaCl salt bridge, nutrient, and aeration made the most efficient combination for cell operation considering all experimental results.

The electrolyte of anode chamber was synthetic wastewater (SWW) for Experiment no. 8 with carbon cloth anode and graphite cathode). Figure 4.2, Figure 4.5, and Figure 4.16 show that this combination of cell components generated a maximum 397.1 μA current and 659.3 mV voltage with 46.67% COD removal for Experiment no. 8.

Besides, Figure 4.11 and Figure 4.14 show that Experiment no. 8 recovered a maximum of 56.55 kJm^{-3} energy at 72 hours during the batch operation of 10 days (240 hours). The maximum power density obtained at 72 hours was 218.17 mWm^{-3} .

In Experiment no. 8, the initial concentration of total chromium was maintained at 0.03 mgL^{-1} . The 10 days (240 hours) of batch operation provided the final concentration (0.02 mgL^{-1}) of total chromium (Cr) at anode which resulted in 33.33% removal of total chromium. The coulombic efficiency for the MFC of Exp. no. 8 was 6.90%.

The electrolyte of anode chamber was textile wastewater (TWW, industry 2) for Experiment no. 9. In this case, the anaerobic chamber of carbon cloth anode was connected by the salt bridge of NaCl with the aerobic chamber of Al – Foil over Graphite cathode. The cathodic reaction can be improved by the use of catalytic-coated electrodes [114]. In order to improve the performance of the cell the available electrodes were taken and Al – Foil was wrapped over graphite electrode (carbon rod). Aluminum foil gives not only a better performance than graphite due to higher conductivity [110] but also provides higher surface area according to the experimental analyses. Thus the artificial coating aids to increase the sustenance of the current towards a maximum value for providing electricity generation for a longer time.

Figure 4.3 and Figure 4.6 show in Experiment no. 9 that the efficient combination of cell for textile wastewater generated maximum 733.4 μA current and 1101.1 mV voltage with 52.20% COD removal.

Figure 4.12 and Figure 4.15 show that Experiment no. 9 recovered a maximum of 290.453 kJm^{-3} energy at 120 hours during the batch operation of 240 hours when MFC generated a maximum power density of 672.34 mWm^{-3} . Thus, the time to reach a maximum was increased to 120 hours. Besides, the cell performance was also enhanced.

The nine experiments eventually helped to develop and design an efficient cell which ultimately resulted in a feasible decision to select carbon cloth as anode. Consequently, the sustenance time of electron supply and power generation to reach the maximum value was increased. The increase in the sustenance time to reach a maximum eventually increases the removal percentage of COD and total chromium due to the treatment for a longer period.

Table 4.11 shows that Experiment no. 9 removes 53.75% of total chromium during 10 days of batch operation. The initial and final concentration of total chromium were maintained at 0.08 mgL^{-1} and 0.037 mgL^{-1} respectively. The MFC of Experiment no. 9 attained a coulombic efficiency of 9.35%.

4.5 Analyses of SEM (Scanning Electron Microscopy) – EDX (Energy Dispersive X – ray Spectroscopy)

SEM reports on different positions of raw carbon cloth

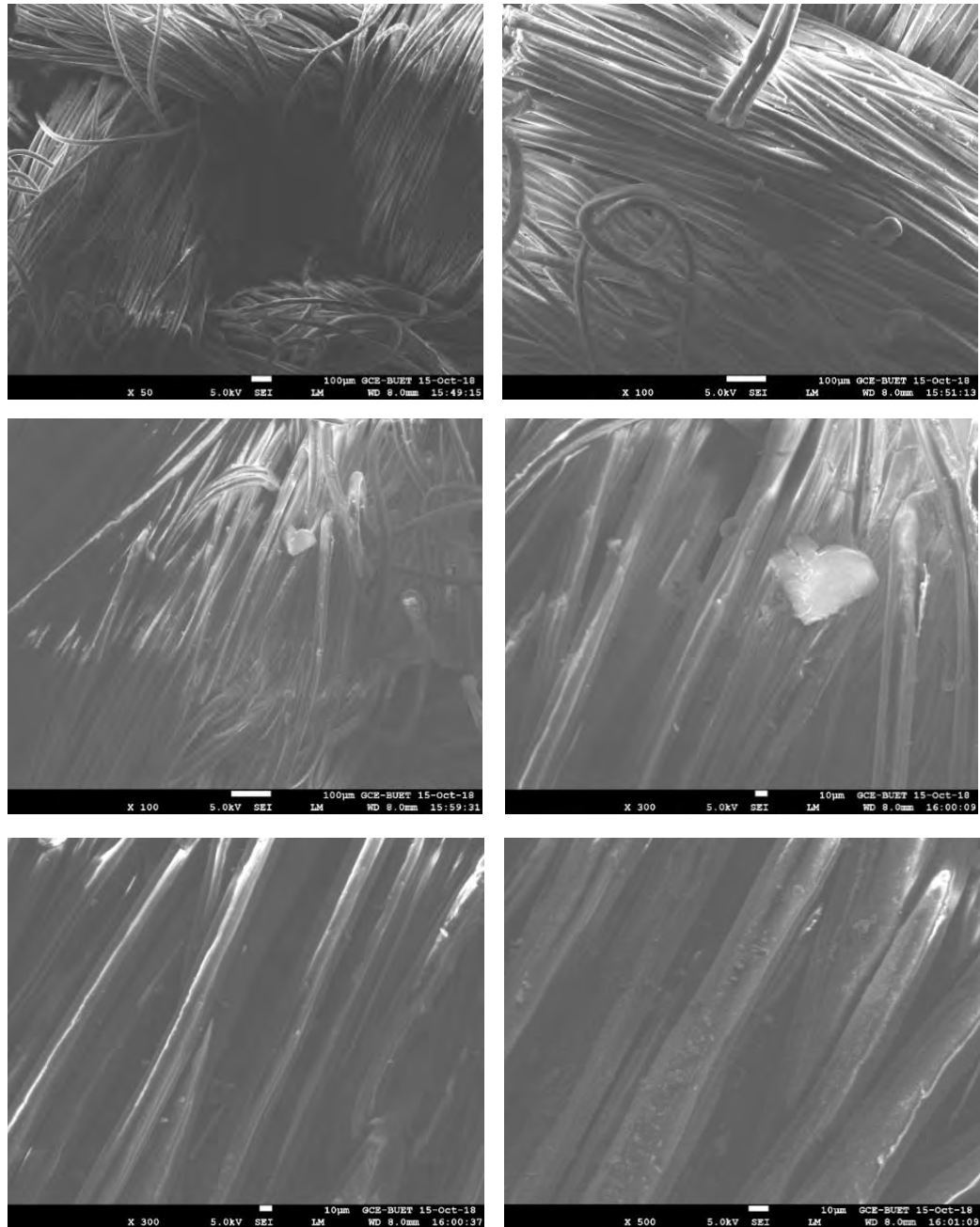


Figure 4.17: SEM analyses of raw carbon cloth

SEM reports on different positions of carbon cloth treated by SWW

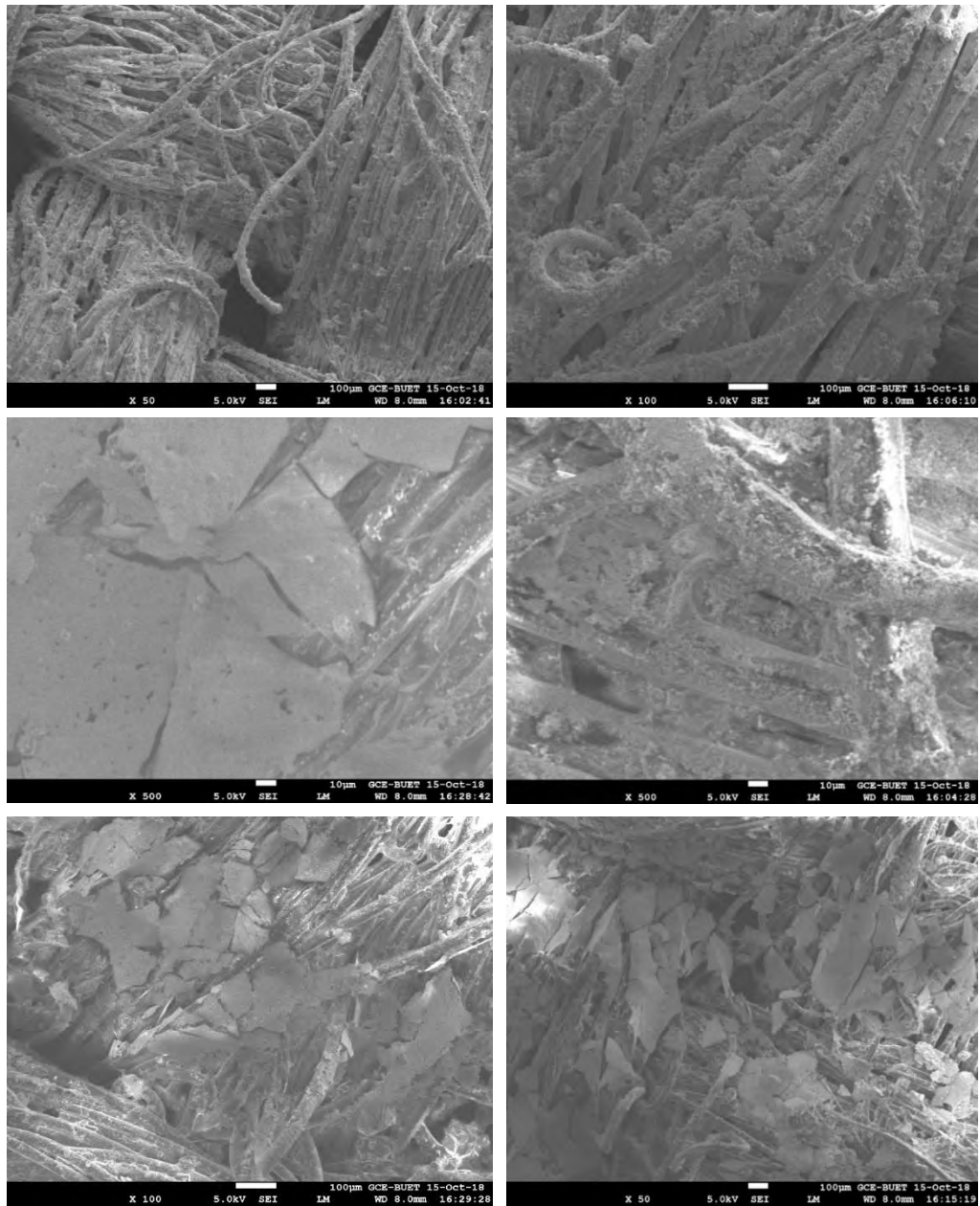


Figure 4.18: SEM analyses of treated carbon cloth for synthetic wastewater (SWW)

SEM Reports on different positions of carbon cloth treated by TWW

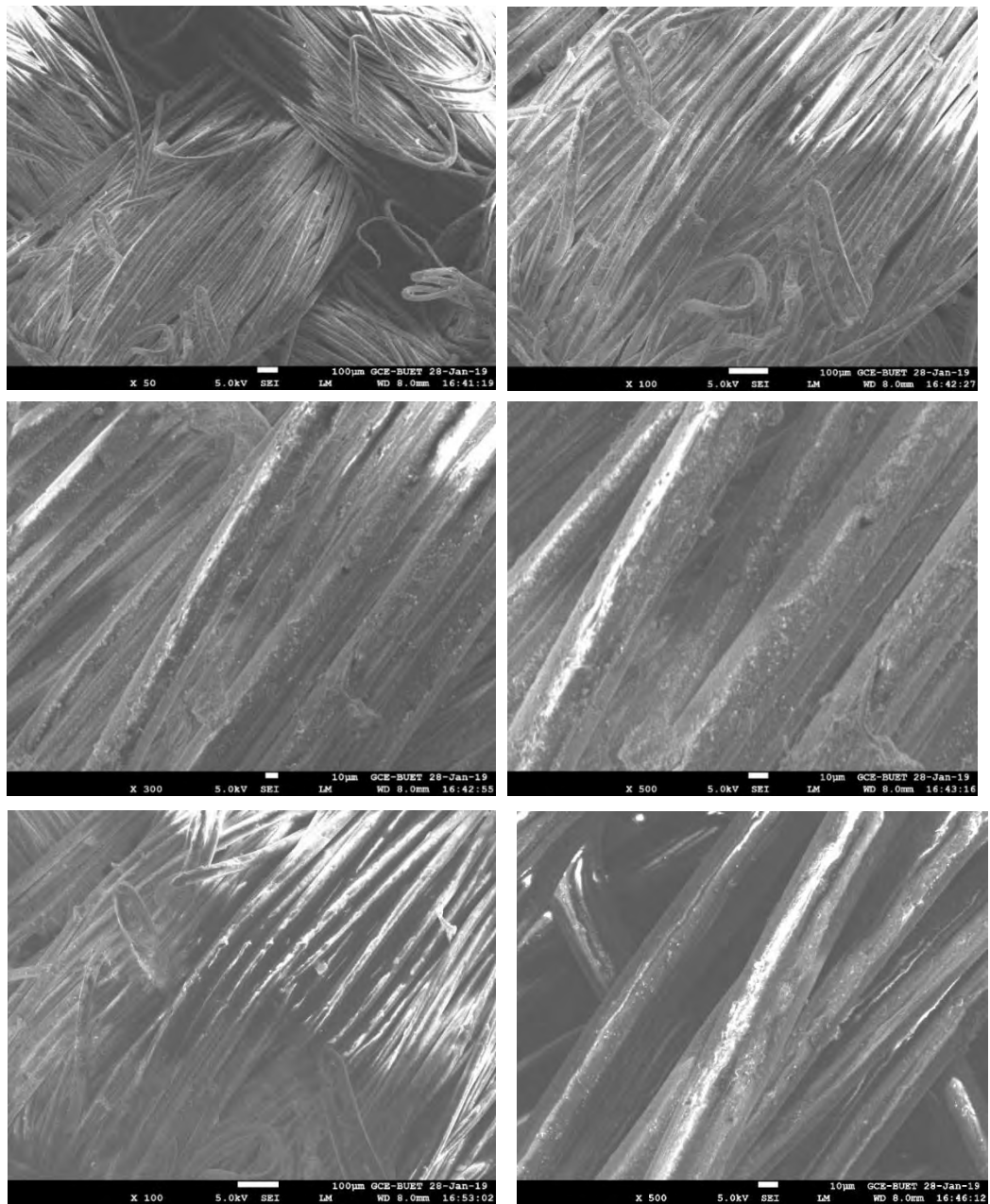
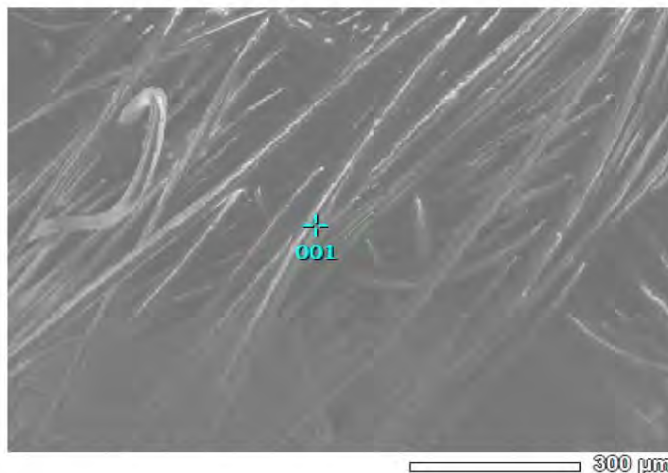


Figure 4.19: SEM analyses of treated carbon cloth for textile wastewater (TWW)

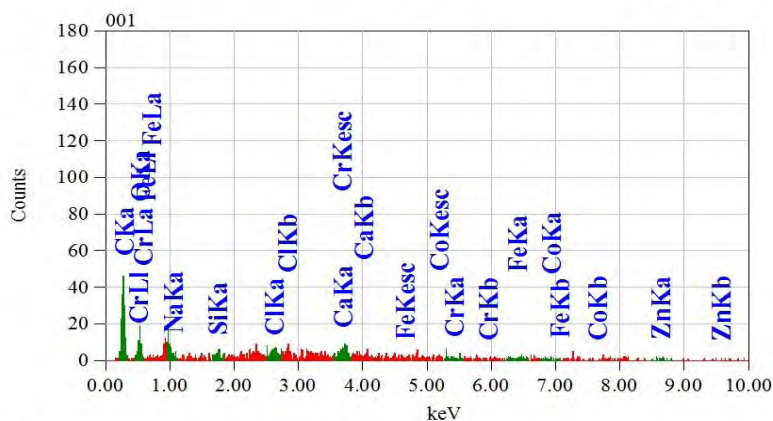
SEM – EDX reports of raw carbon cloth

View000



JEOLUSER 1/1

Title : IMG1
 Instrument : 7600F
 Volt : 5.00 kV
 Mag. : x 100
 Date : 2019/01/28
 Pixel : 512 x 384



Acquisition Parameter
 Instrument : 7600F
 Acc. Voltage : 15.0 kV
 Probe Current : 1.00000 nA
 PHA mode : T3
 Real Time : 30.03 sec
 Live Time : 30.00 sec
 Dead Time : 0 %
 Counting Rate : 66 cps
 Energy Range : 0 - 20 keV

ZAF Method Standardless Quantitative Analysis
 Fitting Coefficient : 0.5151

Element	(keV)	Mass%	Sigma	Atom%	Compound	Mass%	Cation	K
C	0.277	75.61	2.37	86.96				67.8277
O	0.525	10.23	1.05	8.83				6.5566
Na								
Si	1.739	1.23	0.36	0.60				2.1069
Cl	2.621	1.48	0.42	0.58				3.0407
Ca	3.690	4.34	0.83	1.50				9.1694
Cr								
Fe	6.398	0.62	0.85	0.15				1.0631
Co								
Zn	8.630	6.49	2.78	1.37				10.2356
Total		100.00		100.00				

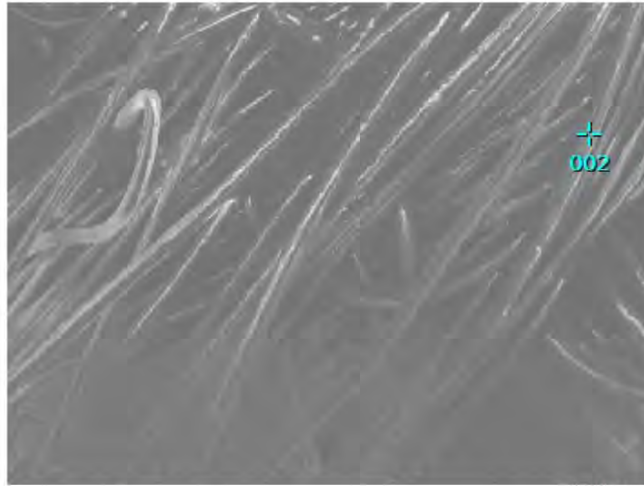
JED-2300 AnalysisStation

JEOL

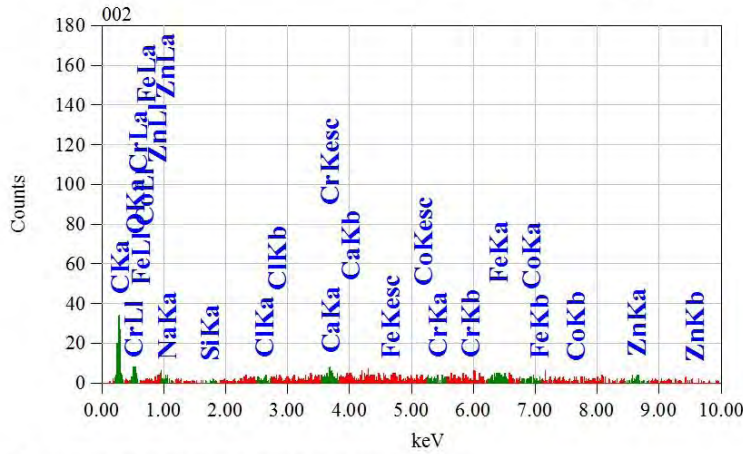
Figure 4.20 a: EDX report of raw carbon cloth

View000

JEOLUSER 1/1



Title : IMG1
 Instrument : 7600F
 Volt : 5.00 kV
 Mag. : x 100
 Date : 2019/01/28
 Pixel : 512 x 384



Acquisition Parameter
 Instrument : 7600F
 Acc. Voltage : 15.0 kV
 Probe Current: 1.00000 nA
 PHA mode : T3
 Real Time : 30.06 sec
 Live Time : 30.00 sec
 Dead Time : 0 %
 Counting Rate: 66 cps
 Energy Range : 0 - 20 keV

ZAF Method Standardless Quantitative Analysis
 Fitting Coefficient : 0.5637

Element	(keV)	Mass%	Sigma	Atom%	Compound	Mass%	Cation	K
C	0.277	67.28	0.50	88.43				45.5967
O	0.525	3.79	0.21	3.74				3.0230
Na	1.041	0.47	0.24	0.32				0.5371
Si								
Cl	2.621	0.86	0.18	0.38				1.7821
Ca	3.690	1.56	0.45	0.61				3.4715
Cr								
Fe	6.398	4.49	1.05	1.27				8.4682
Co	6.924	1.38	0.91	0.37				2.5996
Zn	8.630	20.17	2.40	4.87				34.5219
Total		100.00		100.00				

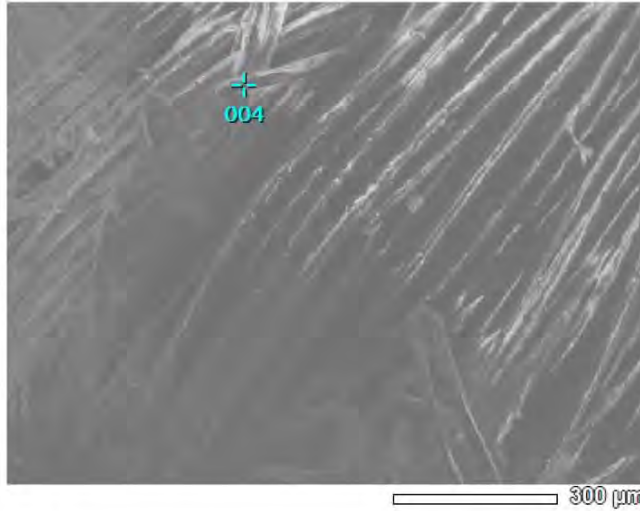
JED-2300 AnalysisStation

JEOL

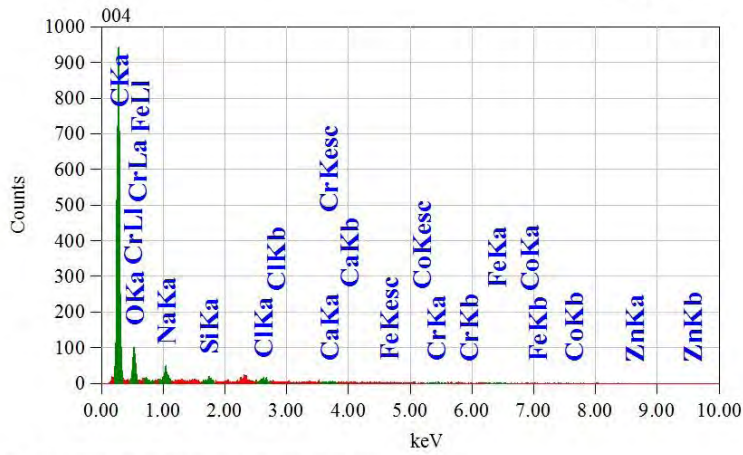
Figure 4.20 b: EDX report of raw carbon cloth

View001

JBOLUSER 1/1



Title : IMG1
 Instrument : 7600F
 Volt : 10.00 kV
 Mag. : x 100
 Date : 2019/01/28
 Pixel : 512 x 384



Acquisition Parameter
 Instrument : 7600F
 Acc. Voltage : 10.0 kV
 Probe Current: 1.00000 nA
 PHA mode : T3
 Real Time : 30.10 sec
 Live Time : 30.00 sec
 Dead Time : 0 %
 Counting Rate: 279 cps
 Energy Range : 0 - 20 keV

ZAF Method Standardless Quantitative Analysis
 Fitting Coefficient : 0.1028

Element	(keV)	Mass%	Sigma	Atom%	Compound	Mass%	Cation	K
C	0.277	80.47	0.11	85.93				84.7515
O	0.525	15.67	0.22	12.56				10.5249
Na	1.041	1.21	0.07	0.67				1.4167
Si	1.739	0.42	0.06	0.19				0.5771
Cl	2.621	0.77	0.07	0.28				1.1042
Ca	3.690	0.39	0.11	0.12				0.5254
Cr	5.411	0.16	0.20	0.04				0.1826
Fe	6.398	0.67	0.29	0.15				0.7610
Co	0.776	0.24	0.37	0.05				0.1566
Zn								
Total		100.00		100.00				

JED-2300 AnalysisStation

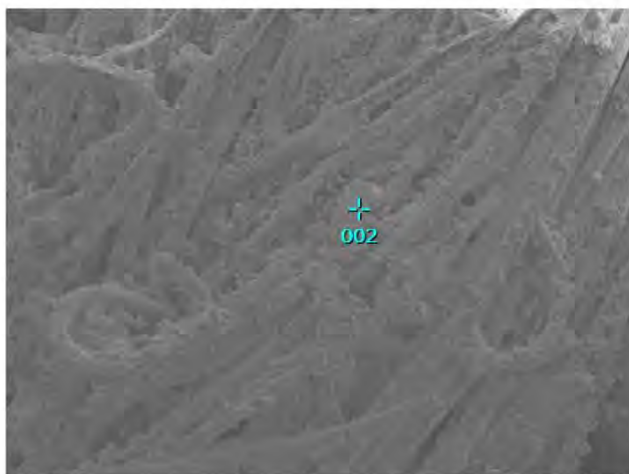
JEOL

Figure 4.20 c: EDX report of raw carbon cloth

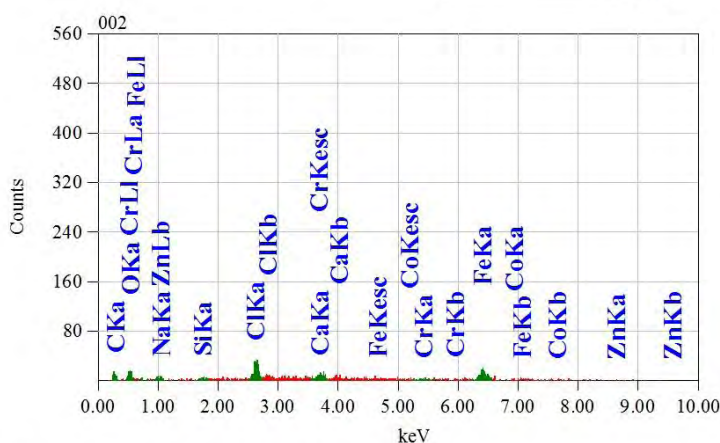
SEM – EDX Report –1 of treated carbon cloth for synthetic wastewater

View000

JEOLUSER 1/1



Title : IMG1
 Instrument : 7600F
 Volt : 5.00 kV
 Mag. : x 100
 Date : 2018/10/15
 Pixel : 512 x 384



Acquisition Parameter
 Instrument : 7600F
 Acc. Voltage : 10.0 kV
 Probe Current : 1.00000 nA
 PHA mode : T3
 Real Time : 30.05 sec
 Live Time : 30.00 sec
 Dead Time : 0 %
 Counting Rate : 101 cps
 Energy Range : 0 - 20 keV

ZAF Method Standardless Quantitative Analysis

Fitting Coefficient : 0.3899

Element	(keV)	Mass%	Sigma	Atom%	Compound	Mass%	Cation	K
C K*	0.277	12.16	0.72	33.62				3.9132
O K	0.525	5.51	0.51	11.43				5.6444
Na K*	1.041	1.17	0.28	1.68				0.7695
Si K*	1.739	0.69	0.23	0.82				0.7095
Cl K	2.621	10.39	0.74	9.74				12.8100
Ca K*	3.690	3.99	0.79	3.30				4.8336
Cr K*	5.411	2.89	1.22	1.85				3.3796
Fe K*	6.398	62.67	6.14	37.28				67.6765
Co L*								
Zn L	1.012	0.55	0.46	0.28				0.2636
Total		100.00		100.00				

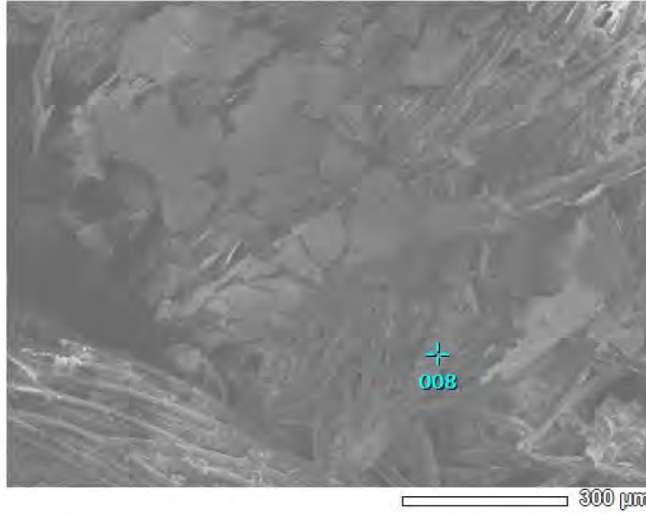
JED-2300 AnalysisStation

JEOL

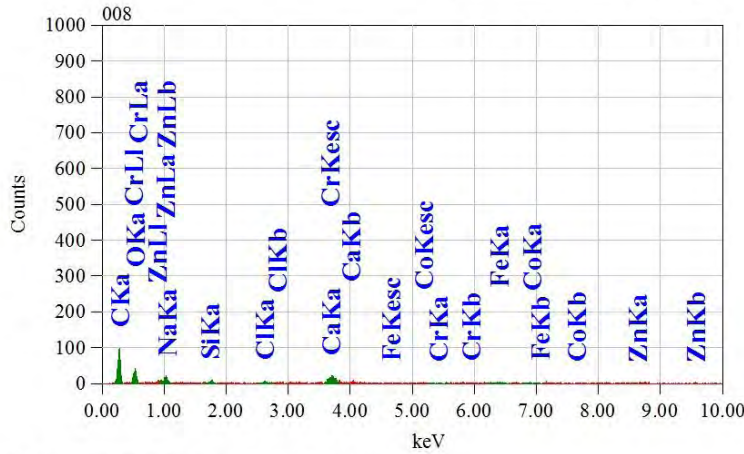
Figure 4.21 a: EDX report 1 of treated carbon cloth for synthetic wastewater

View002

JEOLUSER 1/1



Title : IMG1
 Instrument : 7600F
 Volt : 5.00 kV
 Mag. : x 100
 Date : 2018/10/15
 Pixel : 512 x 384



Acquisition Parameter
 Instrument : 7600F
 Acc. Voltage : 15.0 kV
 Probe Current: 1.00000 nA
 PHA mode : T3
 Real Time : 30.03 sec
 Live Time : 30.00 sec
 Dead Time : 0 %
 Counting Rate: 92 cps
 Energy Range : 0 - 20 keV

ZAF Method Standardless Quantitative Analysis

Fitting Coefficient : 0.3133

Element	(keV)	Mass%	Sigma	Atom%	Compound	Mass%	Cation	K
C K	0.277	67.77	1.53	81.54				60.8520
O K	0.525	13.58	0.81	12.26				8.8083
Na K	1.041	1.25	0.35	0.78				1.5381
Si K	1.739	0.86	0.20	0.44				1.4051
Cl K	2.621	0.65	0.18	0.26				1.2827
Ca K	3.690	7.68	0.71	2.77				15.7752
Cr K	5.411	0.13	0.29	0.04				0.2182
Fe K	6.398	2.10	0.66	0.54				3.5411
Co K*	6.924	1.12	0.61	0.27				1.8871
Zn L	1.012	4.87	0.81	1.08				4.6922
Total		100.00		100.00				

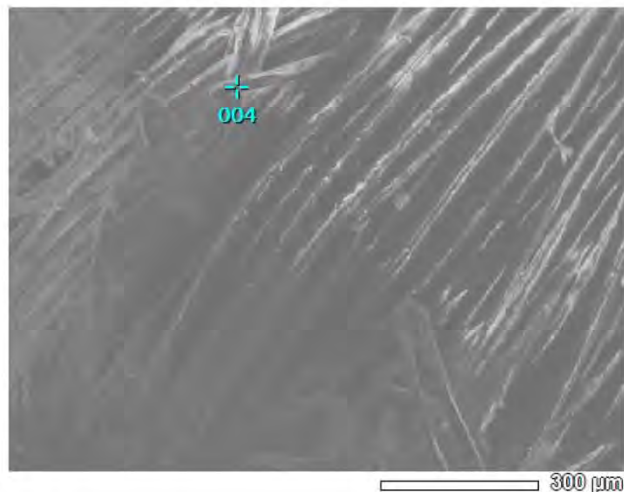
JED-2300 AnalysisStation

JEOL

Figure 4.21 b: EDX report 1 of treated carbon cloth for synthetic wastewater

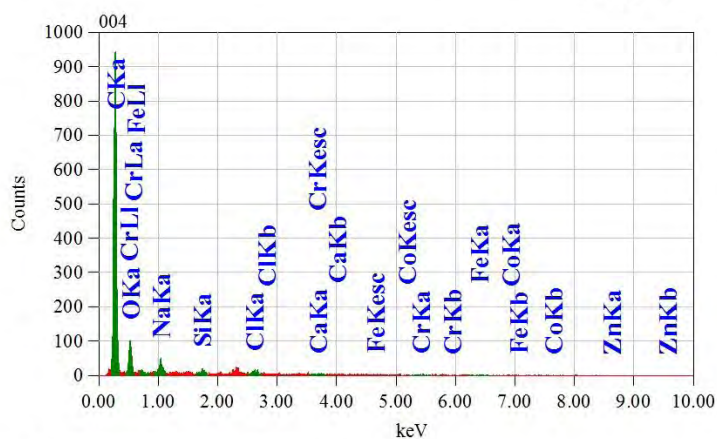
SEM – EDX Report –1 of treated carbon cloth for textile wastewater

View001



JEOLUSER 1/1

Title : IMG1
 Instrument : 7600F
 Volt : 10.00 kV
 Mag. : x 100
 Date : 2019/01/28
 Pixel : 512 x 384



Acquisition Parameter
 Instrument : 7600F
 Acc. Voltage : 10.0 kV
 Probe Current : 1.00000 nA
 PHA mode : T3
 Real Time : 30.10 sec
 Live Time : 30.00 sec
 Dead Time : 0 %
 Counting Rate : 279 cps
 Energy Range : 0 - 20 keV

ZAF Method Standardless Quantitative Analysis

Fitting Coefficient : 0.1028

Element	(keV)	Mass%	Sigma	Atom%	Compound	Mass%	Cation	K
C K	0.277	80.47	0.11	85.93				84.7515
O K	0.525	15.67	0.22	12.56				10.5249
Na K*	1.041	1.21	0.07	0.67				1.4167
Si K*	1.739	0.42	0.06	0.19				0.5771
Cl K*	2.621	0.77	0.07	0.28				1.1042
Ca K	3.690	0.39	0.11	0.12				0.5254
Cr K*	5.411	0.16	0.20	0.04				0.1826
Fe K*	6.398	0.67	0.29	0.15				0.7610
Co L*	0.776	0.24	0.37	0.05				0.1566
Zn L*								
Total		100.00		100.00				

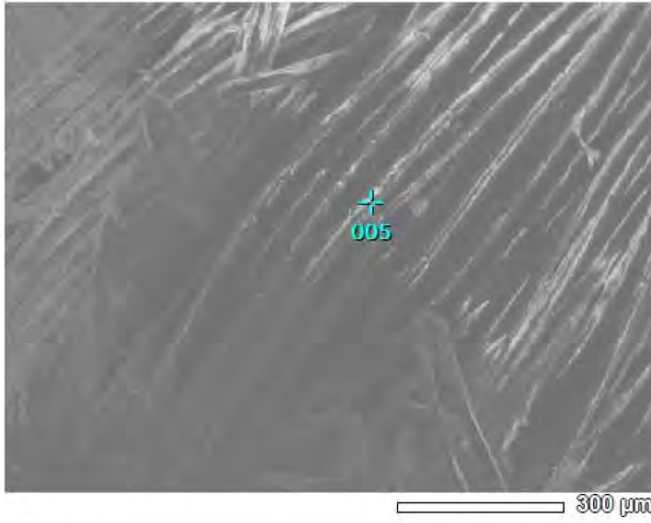
JED-2300 AnalysisStation

JEOL

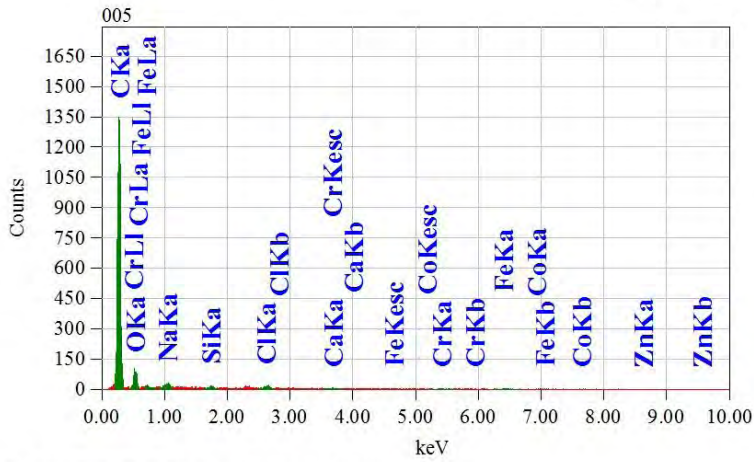
Figure 4.22 a: EDX report 1 of treated carbon cloth for textile wastewater

View001

JEOLUSER 1/1



Title : IMG1
 Instrument : 7600F
 Volt : 10.00 kV
 Mag. : x 100
 Date : 2019/01/28
 Pixel : 512 x 384



Acquisition Parameter
 Instrument : 7600F
 Acc. Voltage : 10.0 kV
 Probe Current: 1.00000 nA
 PHA mode : T3
 Real Time : 30.09 sec
 Live Time : 30.00 sec
 Dead Time : 0 %
 Counting Rate: 363 cps
 Energy Range : 0 - 20 keV

ZAF Method Standardless Quantitative Analysis

Fitting Coefficient : 0.1037

Element	(keV)	Mass%	Sigma	Atom%	Compound	Mass%	Cation	K
C	0.277	85.16	0.48	89.70				88.8733
O	0.525	11.52	0.44	9.11				7.0957
Na	1.041	0.68	0.07	0.37				0.7726
Si	1.739	0.45	0.07	0.20				0.5966
Cl	2.621	0.81	0.10	0.29				1.1184
Ca	3.690	0.08	0.08	0.02				0.0974
Cr	5.411	0.46	0.19	0.11				0.5225
Fe	6.398	0.85	0.36	0.19				0.9234
Co								
Zn								
Total		100.00		100.00				

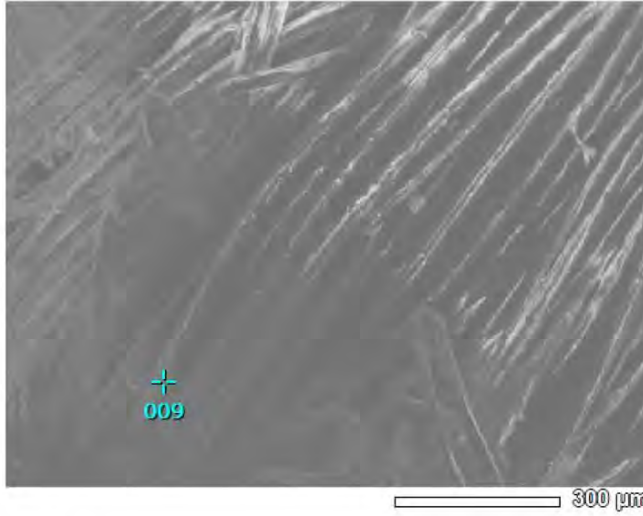
JED-2300 AnalysisStation

JEOL

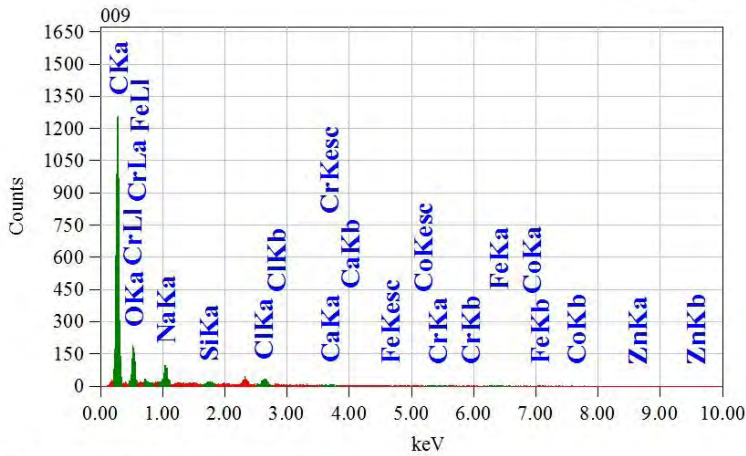
Figure 4.22 b: EDX report 1 of treated carbon cloth for textile wastewater

View001

JEOLUSER 1/1



Title : IMG1
 Instrument : 7600F
 Volt : 10.00 kV
 Mag. : x 100
 Date : 2019/01/28
 Pixel : 512 x 384



Acquisition Parameter
 Instrument : 7600F
 Acc. Voltage : 10.0 kV
 Probe Current: 1.00000 nA
 PHA mode : T3
 Real Time : 30.11 sec
 Live Time : 30.00 sec
 Dead Time : 0 %
 Counting Rate: 407 cps
 Energy Range : 0 - 20 keV

ZAF Method Standardless Quantitative Analysis

Fitting Coefficient : 0.1015

Element	(keV)	Mass%	Sigma	Atom%	Compound	Mass%	Cation	K
C	0.277	76.42	0.45	83.25				78.6678
O	0.525	17.44	0.48	14.26				13.2148
Na	1.041	2.22	0.11	1.26				2.8069
Si	1.739	0.30	0.06	0.14				0.4453
Cl	2.621	1.59	0.12	0.59				2.4857
Ca	3.690	0.26	0.09	0.09				0.3838
Cr	5.411	0.04	0.15	0.01				0.0568
Fe	6.398	1.39	0.39	0.32				1.7082
Co	0.776	0.34	0.35	0.07				0.2307
Zn								
Total		100.00		100.00				

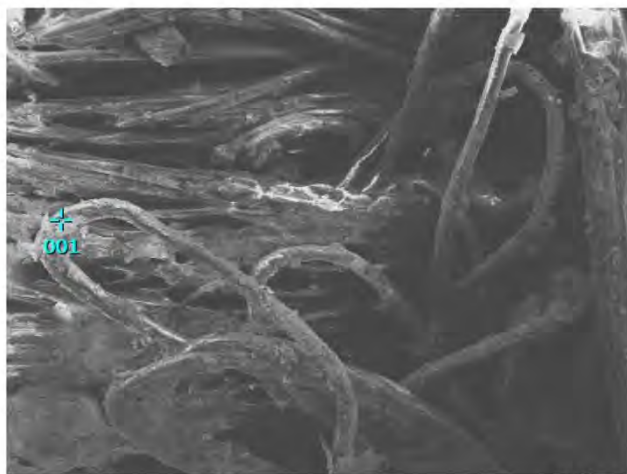
JED-2300 AnalysisStation

JEOL

Figure 4.22 c: EDX report 1 of treated carbon cloth for textile wastewater

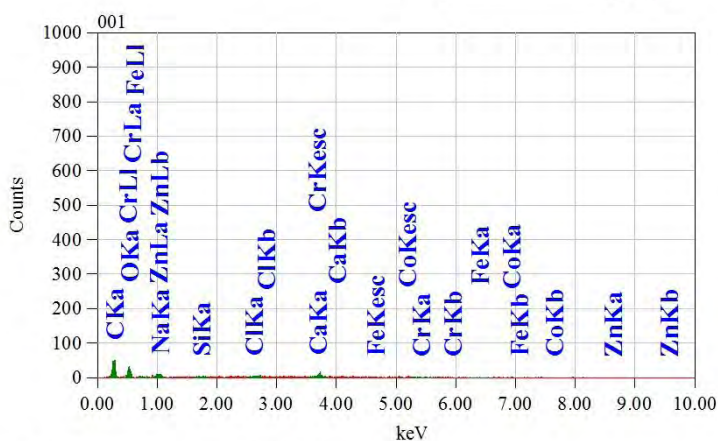
SEM – EDX Report –2 of treated carbon cloth for synthetic wastewater

View000



JEOLUSER 1/1

Title : IMG1
 Instrument : 7600F
 Volt : 5.00 kV
 Mag. : x 100
 Date : 2018/11/02
 Pixel : 512 x 384



Acquisition Parameter
 Instrument : 7600F
 Acc. Voltage : 10.0 kV
 Probe Current: 1.00000 nA
 PHA mode : T3
 Real Time : 30.03 sec
 Live Time : 30.00 sec
 Dead Time : 0 %
 Counting Rate: 53 cps
 Energy Range : 0 - 20 keV

ZAF Method Standardless Quantitative Analysis

Fitting Coefficient : 0.3457

Element	(keV)	Mass%	Sigma	Atom%	Compound	Mass%	Cation	K
C	0.277	48.79	0.29	61.03				47.5444
O	0.525	35.08	0.83	32.94				30.9040
Na	1.041	1.78	0.36	1.17				2.0257
Si								
Cl	2.621	0.26	0.38	0.11				0.4113
Ca	3.690	9.58	1.10	3.59				14.2648
Cr								
Fe	6.398	2.80	1.09	0.75				3.5264
Co	0.776	0.51	1.52	0.13				0.3070
Zn	1.012	1.20	0.77	0.28				1.0164
Total		100.00		100.00				

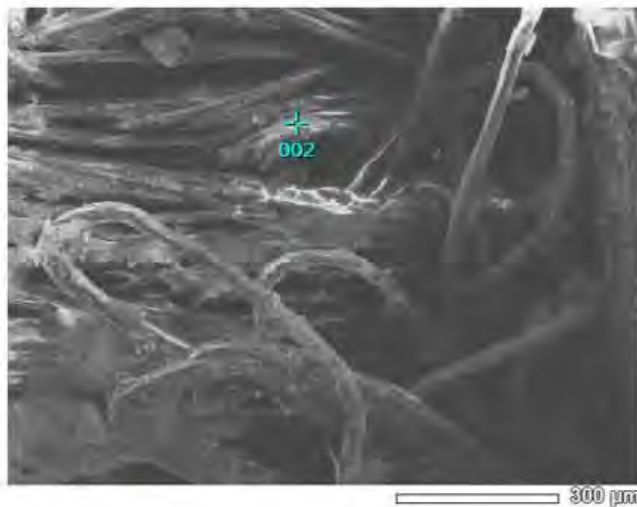
JED-2300 AnalysisStation

JEOL

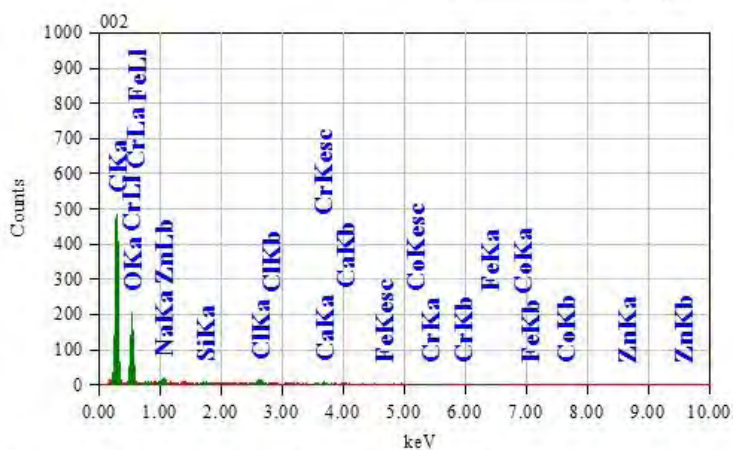
Figure 4.23 a: EDX report 2 of treated carbon cloth for synthetic wastewater

View000

JEOLUSER 1/1



Title : IMG1
 Instrument : 7600F
 Volt : 5.00 kV
 Mag. : x 100



Acquisition Parameter
 Instrument : 7600F
 Acc. Voltage : 10.0 kV
 Probe Current: 1.00000
 PHA mode : T3
 Real Time : 30.06 s
 Live Time : 30.00 s
 Dead Time : 0 %
 Counting Rate: 203 cps

ZAF Method Standardless Quantitative Analysis

Fitting Coefficient : 0.0996

Element	(keV)	Mass%	Sigma	Atom%	Compound	Mass%	Cation
C K*	0.277	63.54	0.12	71.33			
O K	0.525	32.09	0.31	27.04			
Na K*	1.041	0.85	0.07	0.50			
Si K*							
Cl K*	2.621	1.22	0.09	0.46			
Ca K*	3.690	1.17	0.14	0.39			
Cr K*	5.411	0.25	0.21	0.06			
Fe K*	6.398	0.88	0.28	0.21			
Co L*							

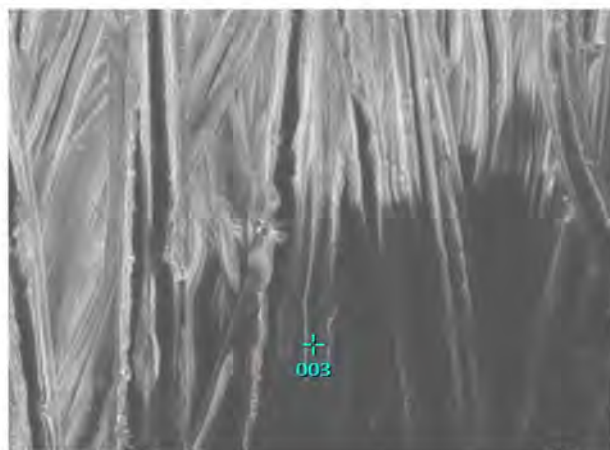
JED-2300 AnalysisStation

JEOL

Figure 4.23 b: EDX report 2 of treated carbon cloth for synthetic wastewater

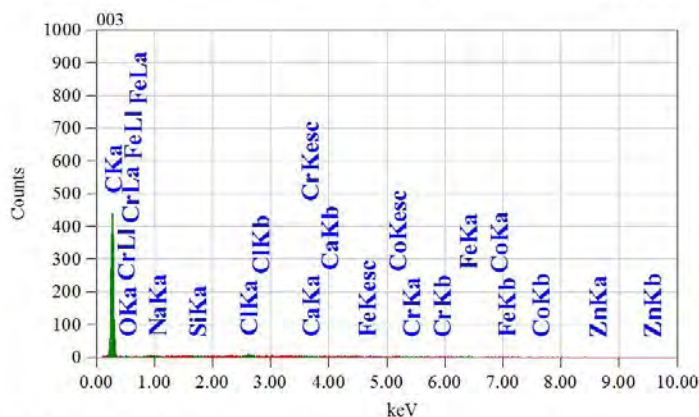
SEM – EDX Report –2 of treated carbon cloth for textile wastewater

View000



JEOLUSER 1/1

Title : IMG1
 Instrument : 7600F
 Volt : 10.00 kV
 Mag. : x 300
 Date : 2018/11/02
 Pixel : 512 x 384



Acquisition Parameter
 Instrument : 7600F
 Acc. Voltage : 10.0 kV
 Probe Current: 1.00000 nA
 PHA mode : T3
 Real Time : 30.05 sec
 Live Time : 30.00 sec
 Dead Time : 0 %
 Counting Rate: 132 cps
 Energy Range : 0 - 20 keV

ZAF Method Standardless Quantitative Analysis
 Fitting Coefficient : 0.1600

Element	(keV)	Mass%	Sigma	Atom%	Compound	Mass%	Cation	K
C	0.277	95.76	0.94	98.32				96.0193
O	0.525	1.02	0.27	0.79				0.5083
Na	1.041	0.13	0.08	0.07				0.1365
Si								
Cl	2.621	1.11	0.22	0.38				1.3895
Ca								
Cr	5.411	0.10	0.50	0.02				0.0997
Fe	6.398	1.88	1.04	0.42				1.8467
Co								
Zn								
Total		100.00		100.00				

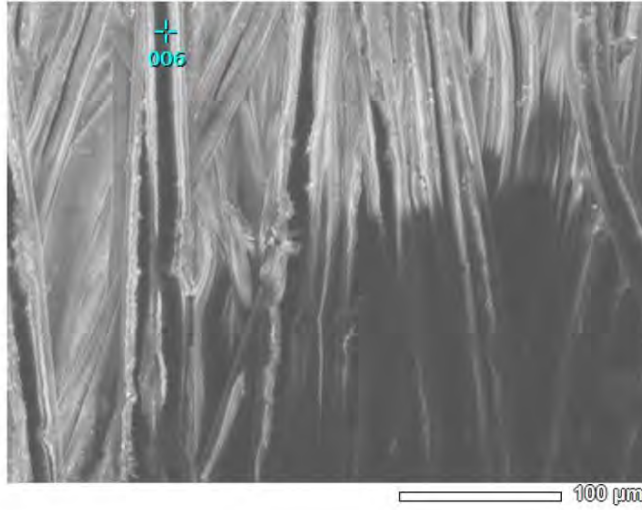
JED-2300 AnalysisStation

JEOL

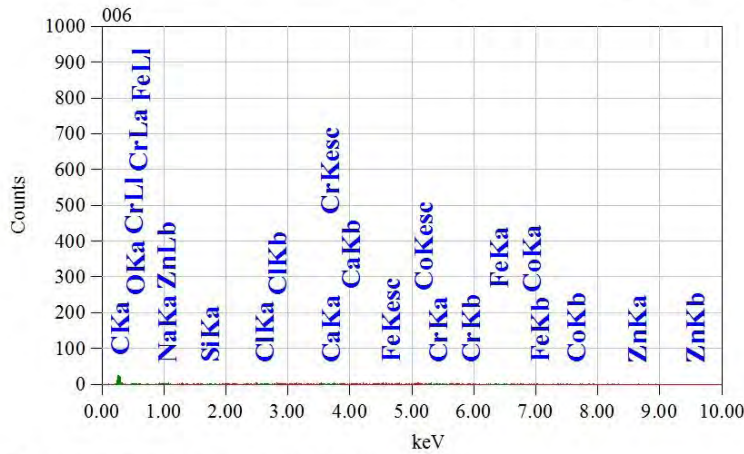
Figure 4.24 a: EDX report 2 of treated carbon cloth for textile wastewater

View000

JEOLUSER 1/1



Title : IMG1
 Instrument : 7600F
 Volt : 10.00 kV
 Mag. : x 300
 Date : 2018/11/02
 Pixel : 512 x 384



Acquisition Parameter
 Instrument : 7600F
 Acc. Voltage : 10.0 kV
 Probe Current: 1.00000 nA
 PHA mode : T3
 Real Time : 30.02 sec
 Live Time : 30.00 sec
 Dead Time : 0 %
 Counting Rate: 33 cps
 Energy Range : 0 - 20 keV

ZAF Method Standardless Quantitative Analysis

Fitting Coefficient : 0.6346

Element	(keV)	Mass%	Sigma	Atom%	Compound	Mass%	Cation	K
C	0.277	71.92	223.44	89.19				62.1766
O	0.525	3.39	153.92	3.16				2.8717
Na	1.041	0.76	57.88	0.49				0.9222
Si	1.739	1.39	80.95	0.74				2.1735
Cl	2.621	2.33	121.09	0.98				3.9351
Ca	3.690	0.28	58.76	0.10				0.4517
Cr	5.411	1.29	232.19	0.37				1.9116
Fe	6.398	18.64	1282.28	4.97				25.5575
Co								
Zn								
Total		100.00		100.00				

JED-2300 AnalysisStation

JEOL

Figure 4.24 b: EDX report 2 of treated carbon cloth for textile wastewater

4.5.1 Quantitative Analyses of SEM – EDX

SEM (scanning electron microscopy) characterizes the surface properties of electrodes. Figure 4.17 to Figure 4.19 present the SEM images of raw and treated carbon cloths. They show the electrodeposition of elements over the electrode. The images of SEM were obtained at micro and nano scale level for respective compositions show in the figures. Though the commonly investigated removal mechanism for heavy metals in MFCs is reduction at the cathode, this thesis work emphasized the work to confirm the presence of microbial metabolism to remove chromium from textile wastewater of anode chamber. Figure 4.17 shows that the raw carbon cloth provided a homogeneous surface of woven fiber. Figure 4.18 (SWW) and 4.19 (TWW) show addition and increase of mass percentage for different elements due to gradual addition of organics and metals from the wastewater. The surface of carbon cloth showed increase in roughness after 240 hours of batch operation for removing chromium from textile wastewater.

EDX (energy dispersive X-Ray) generates photon that emits specific energy for obtaining mass percentage of specific metals that deposit on the surface of carbon cloth [115]. EDX spectroscopy determines the elemental composition in a very small sample of material (e.g. a few cubic micrometers of carbon cloth) analyzing the composition of the surface. The energy of the X – ray photon is characteristic of the element which produces the energy. The EDS (energy dispersive spectroscopy) X-ray detector measures the number of emitted X-rays versus their energy (keV). The energy of the X-ray is characteristic of the chemical element from which the X-ray is emitted [116] e.g. the X-ray photon emits 5.411 keV energy for chromium (Cr). The micro – nano analyses are utilized to measure the amounts of elements present in the sample. present the mass percentage. The EDX analyses of raw and treated carbon cloths is conducted by selected certain positions on the SEM images. The investigations of the localized point are shown from Figure 4.17 to Figure 4.19. The mass percentage of chromium in raw carbon cloth (untreated) was found 0 at position 001 and 002 when position 004 gave 0.16% of chromium for the emission of 5.411 keV energy.

In the experiment of synthetic wastewater (SWW), SEM – EDX Report – 1 provided the experimental results after 10 days of batch operation. Figure 4.21 a – 4.21 c show the increase in mass percentage of chromium on different positions of treated carbon.

The figures show 2.89% Cr at position 002, 0.13% Cr at position 008, and 0.10% Cr at position 010 for the elemental emission of 5.411 keV energy.

In the experiment of textile wastewater (TWW), SEM – EDX Report – 1 provided the experimental results after 240 hours (10 days) of batch operation. Figure 4.22 a – 4.22 c show the increase in mass percentage of chromium on different positions of treated carbon. The figures show 0.16% Cr at position 004, 0.46% Cr at position 005, and 0.04% Cr at position 009 for the elemental emission of 5.411 keV energy.

Report – 2 of SEM – EDX presents the mass percentage of accumulated chromium on the surface of anode after few days of preservation. Figure 4.23 a – 4.23 b indicates that the mass percentage of chromium (Cr) for the treated carbon cloth of SWW. They show 0% Cr at position 001, 0.25% Cr at position 002 for elemental emission of 5.411 keV energy. Similarly, Figure 4.24 a – 4.24 b presented the results for textile wastewater (TWW) where the mass percentage of chromium (Cr) for the treated carbon cloth of TWW. The figures provide 0.10% Cr at position 003 and 1.29% Cr at position 006 for the elemental emission of 5.411 keV energy.

Table 4.13: Experimental Data for SEM – EDX Analyses

Characteristics of Carbon Cloth	Energy Emission of X – Ray Photon for Cr (keV)	Maximum Mass Percentage of Cr on a Certain Position (%)
Raw	5.411	0.16
Treated (SWW)		2.89
Treated (TWW)		1.29

The quantitative analyses of SEM – EDX confirmed the removal of chromium at anode (carbon cloth in the chamber of wastewater) which is possible only when the microbes actively participate to accumulate chromium from the wastewater by means of their metabolism and microbial electro-metallurgy.

4.6 Analyses of XRD (X – Ray Diffraction)

X-ray powder diffraction (XRD) is a rapid analytical technique which was utilized for elemental identification of chromium (as the deposit on carbon cloth anode). The experiments were based on constructive interference of monochromatic X-rays and specimens of carbon cloth. The specific wavelengths of X-rays are characteristic of the target materials. These X-rays were collimated and directed onto the sample. As the sample and detector were rotated, of the intensity of the reflected X-rays was recorded. A detector recorded and processed this X-ray signal and converted the signal to a count rate which was then output to a device such as computer monitor. By scanning the sample through a range of 2 Theta ($^{\circ}$), all possible diffraction directions of the target should be attained due to the random orientation of the material of concern [117]. Table 4.14 represents the experimental data for XRD analysis of the carbon cloth anode from Experiment no. 8 and Experiment no. 9.

Table 4.14: Experimental Data for XRD Analyses

Characteristics of Carbon Cloth	Maximum 2θ for Diffraction to Peak ($^{\circ}$)	Intensity (X – Ray Signal or Count Rate)
Raw	44.4	3600
Report 1: Treated (SWW)	44.8	4600
Report 1: Treated (TWW)	45	3600
Report 2: Treated (SWW)	44.5	1400
Report 2: Treated (TWW)	43.2	2600

The XRD patterns of carbon cloth are shown in Figure 4.25 a – e. According to International Centre for Diffraction Data, the diffraction pattern for every phase or individual material is as unique as fingerprint [117]. The specimen of raw carbon cloth (untreated) shows in Figure 4.25 a. The figure utilizes the diffraction pattern obtained from the surface of raw cloth corresponds to the pattern of chromium (Cr). The intensity i.e. count rate was 3600 for the peak of raw carbon cloth.

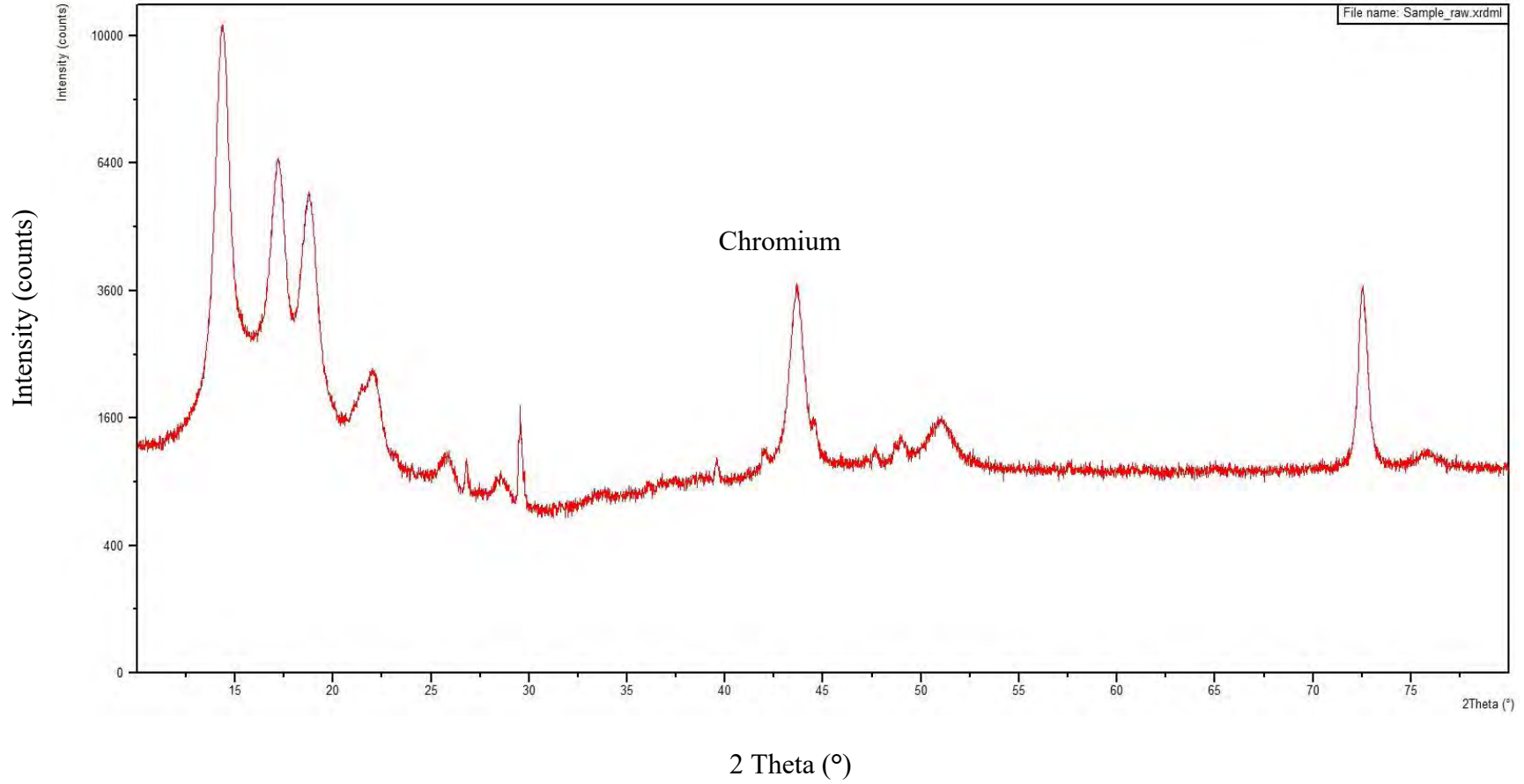


Figure 4.25 a: XRD report 1 of raw carbon cloth

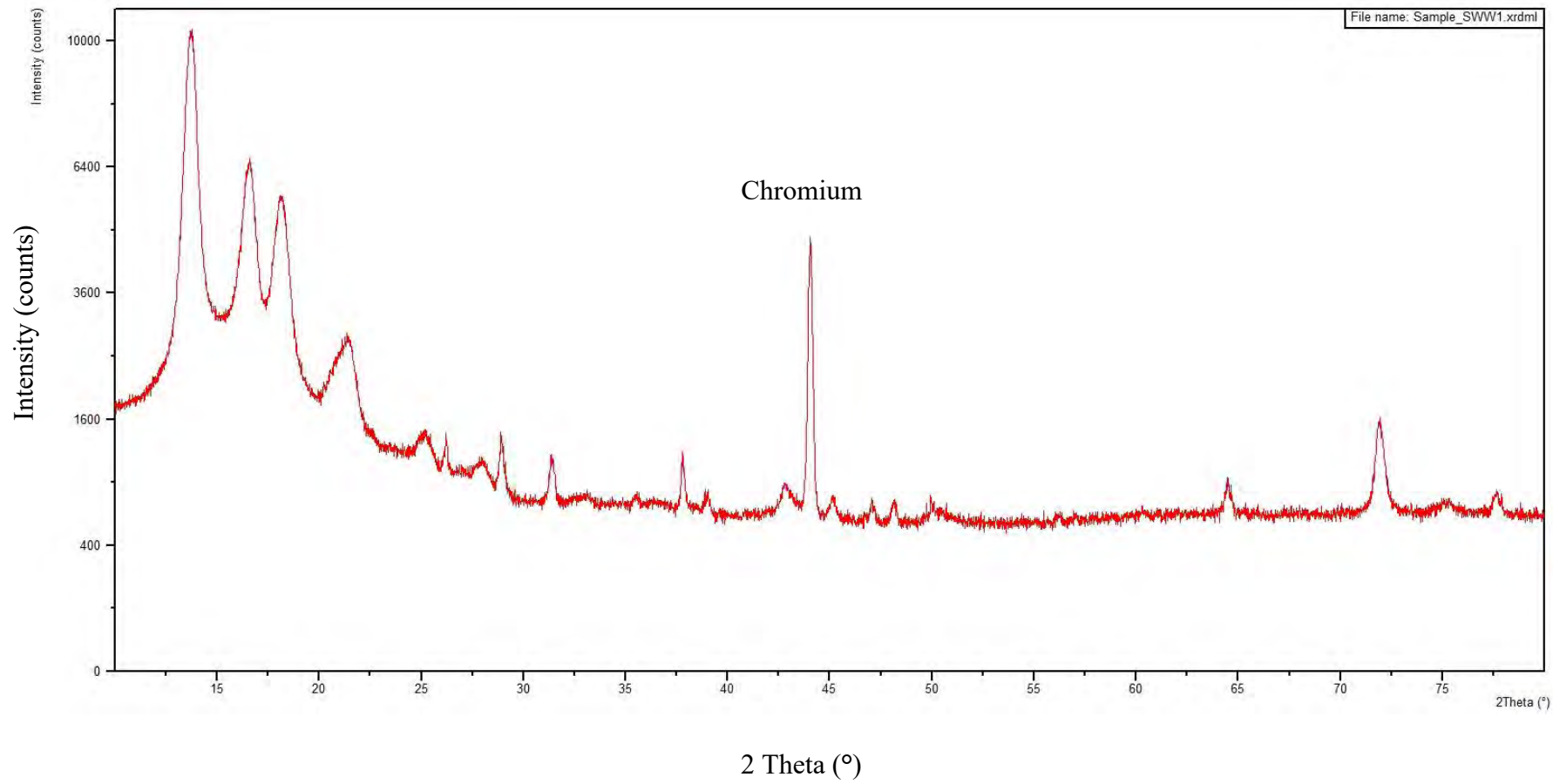


Figure 4.25 b: XRD report 1 of treated carbon cloth for synthetic wastewater

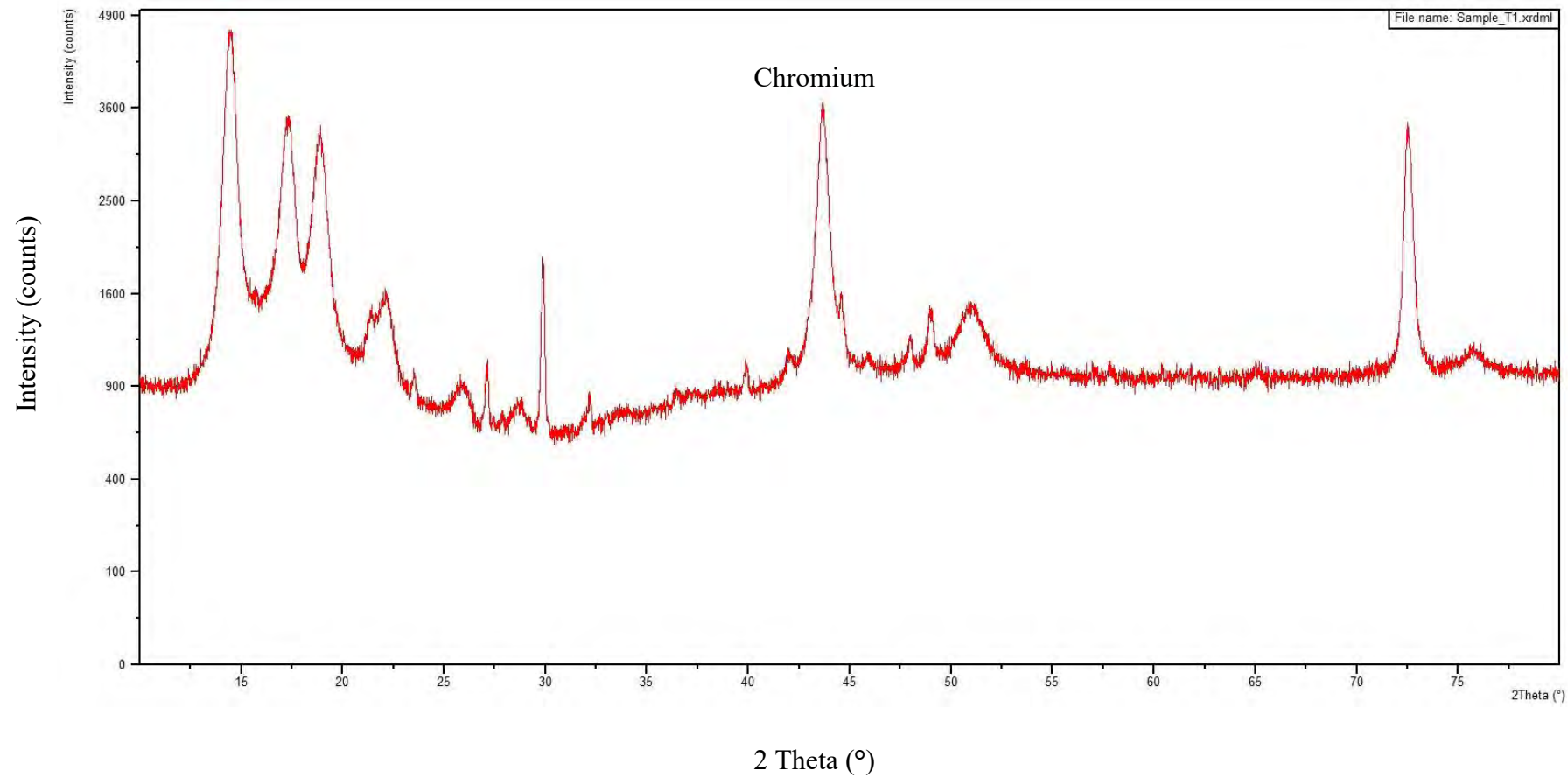


Figure 4.25 c: XRD report 1 of treated carbon cloth for textile wastewater

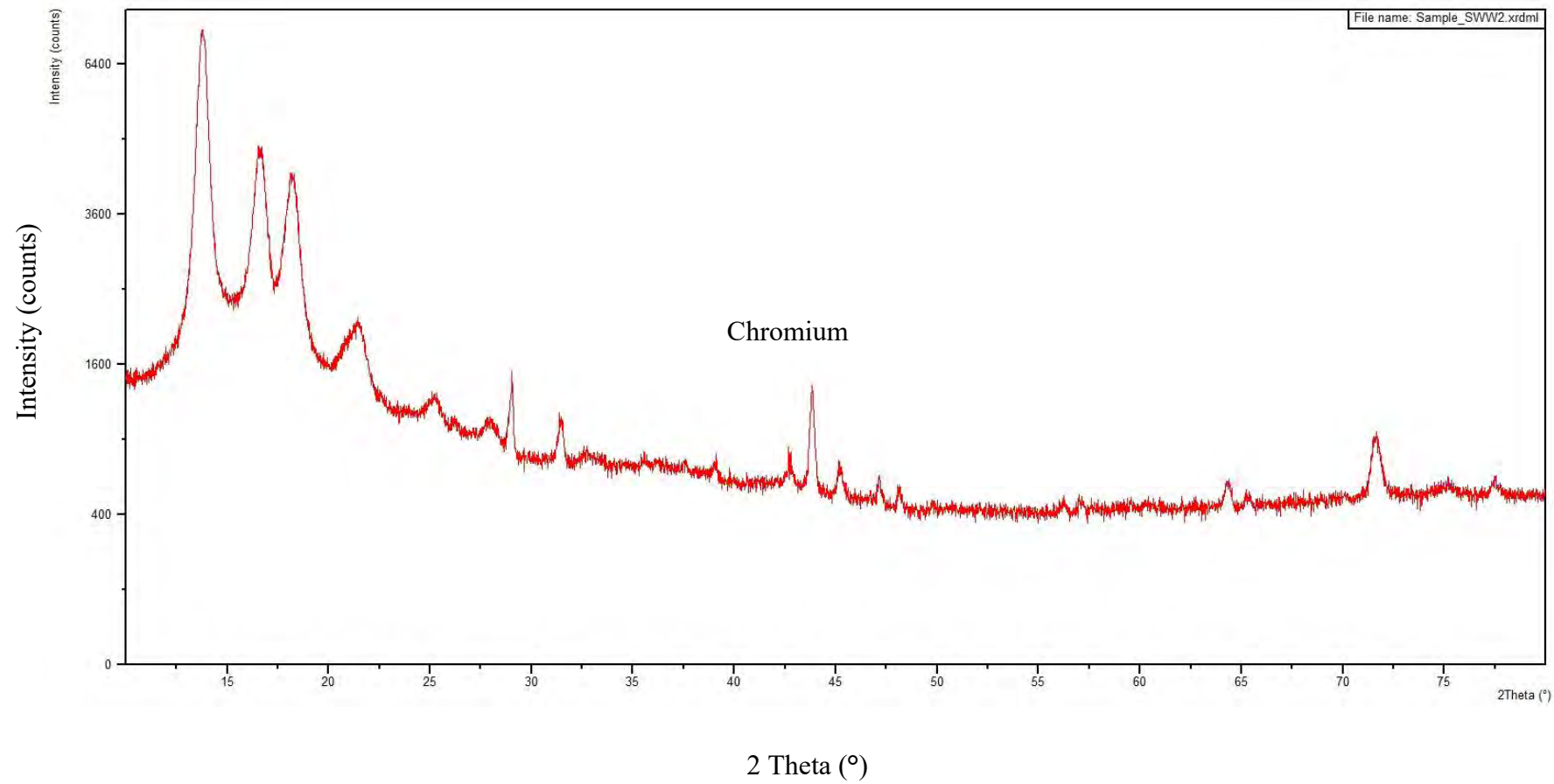


Figure 4.25 d: XRD report 2 of treated carbon cloth for synthetic wastewater

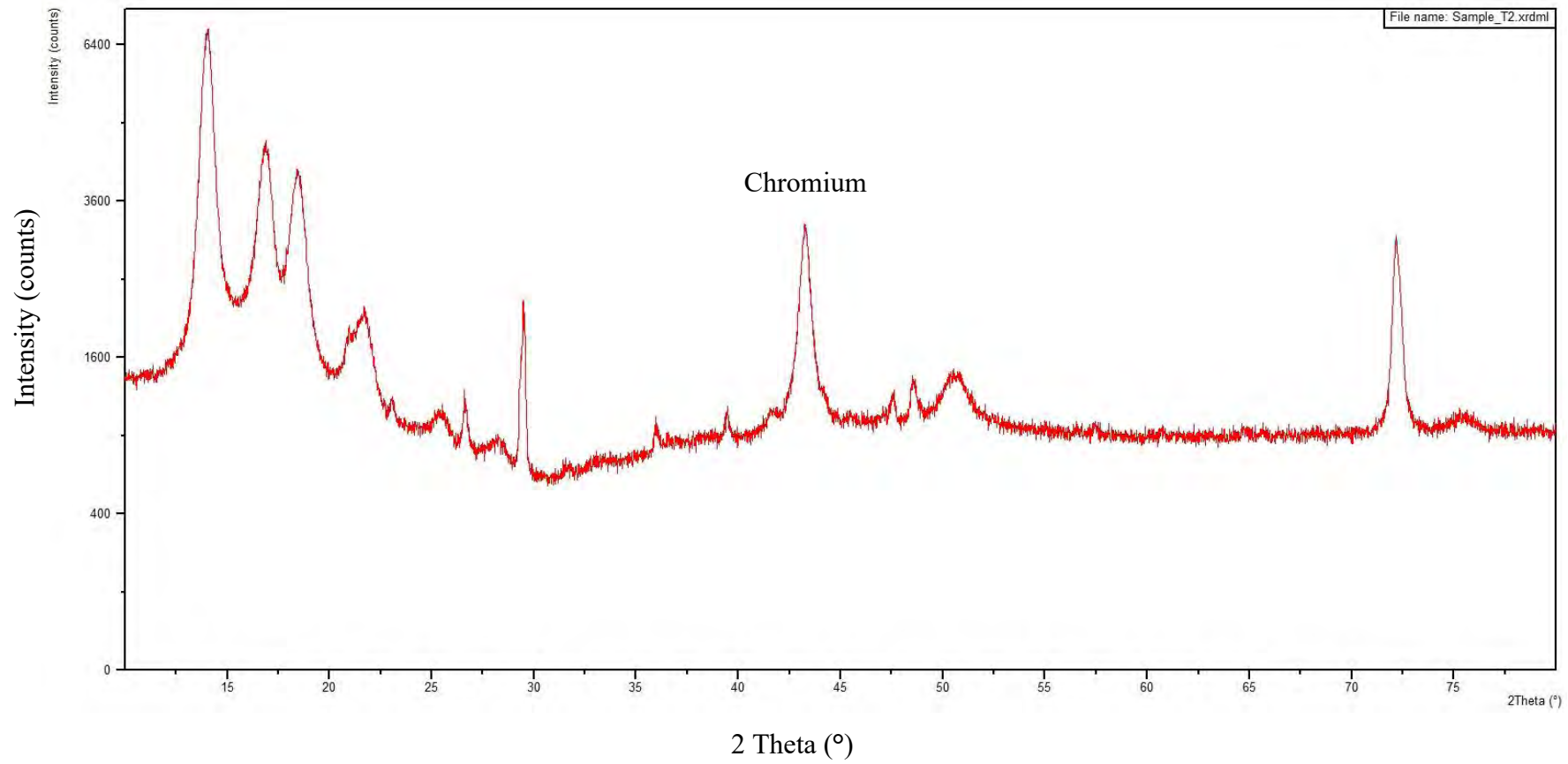


Figure 4.25 e: XRD report 2 of treated carbon cloth for textile wastewater

The diffraction peaks at approximately $2\theta = 66.6^\circ$ or 44.4° corresponding to chromium (Cr) according to the international database for diffraction [117]. Databases such as the Powder Diffraction File (PDF) contains the lists for thousands of crystalline phases. Report 1 of treated carbon cloth shows in Figure 4.25 b and 4.25 c that a count rate of 4600 for synthetic wastewater (SWW, report 1) and 3600 for textile wastewater (TWW) are obtained that peak at approximately $2\theta = 44.8^\circ$ and $2\theta = 45^\circ$ respectively.

Higher intensity or sharp peak is an indication of more order [118], crystallization and arrangement. The treated specimens were equally or highly intense and sharper than the raw specimen due to the deposit of chromium on the anode. Table 4.14 and Figure 4.25 b gives a higher count rate and an increasing value of 2θ at where diffraction peaks for chromium deposition from synthetic wastewater.

On the other hand, Figure 4.25 c shows an equal amount of count rate but the value of 2θ is increased. It indicates the more ordered accumulation and crystallization of chromium (Cr) because the diffraction peaks at approximately $2\theta = 45^\circ$ corresponding to metallic nanocrystal of Cr. Thus the performance of microbial fuel cell is supported by microbial metabolism for removing of chromium from the textile wastewater (TWW, report 1).

Figure 4.25 d and 4.25 e presents a count rate of 1400 for synthetic wastewater (SWW, report 2) and 2600 for textile wastewater (TWW, report 2) that peak at $2\theta = 44.5^\circ$ and $2\theta = 43.2^\circ$ respectively. Report – 2 of XRD presents the elemental identification of chromium on the surface of anode after few days of preservation. It can be assumed that the decrease happened over time due to a decrease in mass percentage and order of crystallization [118].

CHAPTER 5

CONCLUSIONS AND RECOMMENDATIONS

CHAPTER 5

CONCLUSIONS AND RECOMMENDATIONS

5.1 Conclusions

The thesis mainly focused on the improvement of power generation, metal (i.e. chromium) removal efficiency, and overall performance of microbial fuel cell (MFC). The major contributions of this thesis work are summarized as follows:

- A comparatively new textile wastewater treatment approach to remove heavy metals (e.g. chromium) was developed based on the integration of biochemical reactions of microbial metabolism and electrochemical reactions of waste contaminants.
- This research work evidently presented the interactive effect and mechanism of microbial presence in removing chromium from textile wastewater.
- This thesis contributed not only to cathodic removal of chromium (metal) ions as electron acceptors in cathode but also to anodic removal of chromium (metal) ions at low concentrations which eventually confirmed the active metabolism (anaerobic) of microbes during cell operations.
- The performance of the laboratory scale double chambered Microbial Fuel Cell (MFC) was perpetually enhanced by comparative study and research on construction materials of electrodes. Consequently, the carbon cloth anode contributed to the cell performance efficiently which resulted in 53.75% removal of total chromium, 52.20% removal of COD, 9.35% coulombic efficiency, and 672.34 mWm^{-3} power density in the batch operation of 10 days.
- The cell had an advantage of working at ambient temperature and pressure that excluded the consideration of cost for employing external unit operations.
- Compared to conventional treatments, energy consumption is significantly reduced and this novel work recovered a maximum of 290.45 kJm^{-3} energy from the cell operation.

5.2 Prospects and Recommendations

Evaluating the performance of microbial fuel cell (MFC) for removing chromium (Cr) from textile wastewater, even in very low concentration, this thesis work signifies the bio – electrochemical mechanism of MFC which takes MFC one step ahead of conventional waste treatment technologies. Thus many other metal complexes are eligible to be studied for removal and recovery by utilizing the same process of the cell operation. Along with wastewater treatment and power generation, scientists, engineers, and researchers can work on the several other applications of MFCs such as production of hydrogen (H₂) and methane (CH₄), production of solar energy by photosynthesis (plant MFC), synthesis of necessary chemicals, invention of sensors and biosensors, etc.

Yet, there are difficulties to solve for enhancing the cell performance. Therefore, extensive research is required to optimize the cell operation considering scale up for large scale wastewater treatment, low power density, current instability, low rate of microbial growth, membrane or salt bridge fouling or choking, and cost of material fabrication. As the metal removal concept of MFCs is still in nascent state, it requires detailed studies. Studies on microbial reaction kinetics, mass transfer in biofilm, research on microbial population and genetic modification can provide necessary information for improving cell performance.

It is recommended to determine and compare different reaction parameters such as temperature, pressure, time, and pH to optimize MFCs efficiently. Besides, experiments should be conducted not only on mediator free double-chambered microbial fuel cells (DC-MFC) but also on other types of MFCs e.g. single-chambered microbial fuel cells (SC-MFC), mediated MFCs, microbial electrolysis cell (MEC), soil based MFCs, phototropic biofilm MFCs, or membrane based MFCs.

Clean water-body is an oasis in the premises of pollution. So prevention of water contamination and treatment of wastewater are the keys for conserving a sustainable future. Hope, that this thesis will encourage to attempt the removal of heavy metals of interest (e.g. Chromium) from wastewater (e.g. textile wastewater) by employing the MFC technology within the industrial effluent treatment plant (ETP), maintaining engineering ethics for constructing ETP, and developing environmental safety to a sustainable extent.

REFERENCES

REFERENCES

- [1] Santoro, C., Abad, F. B., Serov, A., Kodlai, M., Howe, K. J., Soavi, F., and Atanassov, P. (2017). Supercapacitive microbial desalination cells: New class of power generating devices for reduction of salinity content. *Applied Energy*, 208, pp. 25-26. doi: 10.1016/j.apenergy.2017.10.056
- [2] Wu, M. S., Xu, X., Zhao, Q., and Wang, Z. Y. (2017). Simultaneous removal of heavy metals and biodegradation of organic matter with sedimentation microbial fuel cells. *Royal Society of Chemistry Advances*, 7(84), pp. 53433-53438. doi: 10.1039/C7RA11103G
- [3] Mathuriya, A. S., and Yakhmi, J.V. (2014). Microbial fuel cell to recover heavy metals. *Environmental Chemistry Letter*, 12(4), pp. 483-494. doi: 10.1007/s10311-014-0474-2
- [4] Abdel-Raouf, M.S., and Abdul-Raheim, A.R.M. (2017). Removal of heavy metals from industrial wastewater by biomass – based material: A review. *Journal of Pollution Effects and Control*, 5(1), pp. 1-13. doi: 10.4172/2375-4397.1000180
- [5] Nancharaiah, Y. V., Mohan, S., and Lens, P. N. L. (2015). Metals removal and recovery in bioelectrochemical systems: A review. *Bioresource Technology*, 195, pp. 102-114. doi: 10.1016/j.biortech.2015.06.058
- [6] Bangladesh Bureau of Statistics, Statistics and Informatics Division, Ministry of Planning, Bangladesh. (2018). *National Accounts Statistics*. Retrieved from <http://bbs.portal.gov.bd>
- [7] Nahid, A., Sarkar, P., Anjum, A., and Khan, E. A. (2017). Overview of major industries in Bangladesh. *Journal of Chemical Engineering, Institute of Engineers, Bangladesh*, 30(1), pp. 51-58. doi: 10.3329/jce.v30i1.34798
- [8] United Nations Environmental Programme (UNEP). (1994). The Textile Industry and the Environment. *UNEP Technical Report*, 16, p. 39. Retrieved from <https://wedocs.unep.org/handle/20.500.11822/30281>
- [9] Colantonio, N. (2016). *Heavy metal removal from wastewater using microbial electrolysis cell*, M.Sc.Engg. Thesis, McMaster University, Canada. Retrieved from https://macsphere.mcmaster.ca/bitstream/11375/19325/2/colantonio_natalie_finalsubmission2016may_MASC.pdf

- [10] Kurniawan, T., Chan, G., Lo, W. H., and Babel, S. (2006). Physico–chemical treatment techniques for wastewater laden with heavy metals. *Chemical Engineering Journal*, 118 (1-2), pp. 83–98. doi: 10.1016/j.cej.2006.01.015
- [11] Pozo, G., Pongy, S., Keller, J., Ledezma, P., and Freguia, S. (2017). A novel bioelectrochemical system for chemical-free permanent treatment of acid mine drainage. *Water Research*, 126, pp. 411-420. doi: 10.1016/j.watres.2017.09.058
- [12] Dominguez-Benetton, X., Varia, J. C., Pozo, G., Modin, O., Heijne, A. T., Fransaeer, J., and Rabaey, K. (2018). Metal recovery by microbial electro-metallurgy. *Progress in Material Science*, 94, pp. 435-461. doi: 10.1016/j.pmatsci.2018.01.007
- [13] Moinee, A. Al., Islam, T., and Sanzida, N. (2017). Effect of electrodes, aeration, salt bridges and source of microbes in a mediator-free double chambered microbial fuel cell. In proceedings of *Fifth International Conference on Chemical Engineering (ICChE), Bangladesh*, pp. 339-348.
- [14] Prakash, J. (2016). Microbial Fuel Cells: A source of bioenergy. *Journal of Microbial and Biochemical Technology*, 8(3), pp. 247-255. doi: 10.4172/1948-5948.1000293
- [15] Logan, B. E., Call, D., Cheng, S., Hamelers, H. V. M., Sletuels, T. H. J. A., Jeremiase, A. W., and Rozendal, R. A. (2008). Microbial electrolysis cells for high yield hydrogen gas production from organic matter. *Environmental Science and Technology*, 42, pp. 8630–8640, doi: 10.1021/es801553z
- [16] Sophia, A. C., and Saikant, S. (2016). Reduction of chromium (VI) with energy recovery using microbial fuel cell technology. *Journal of Water Process Engineering*, 11, pp. 39-45. doi: 10.1016/j.jwpe.2016.03.006
- [17] Pant, D., Singh, A., Van Bogaert, G., Olsen, S. I., Nigam, P. S., Deils, L., and Vanbroekhoven, K. (2012). Bioelectrochemical systems (BES) for sustainable energy production and product recovery from organic wastes and industrial wastewaters. *Royal Society of Chemistry Advances*, 2, pp. 1248–1263. doi: 10.1039/C1RA00839K
- [18] Das, D. (2018). Introduction. In Debabrara Das (Ed.), *Microbial Fuel Cell: A bioelectrochemical system that converts waste to watts* (pp. 1 – 20). New Delhi, India: Capital Publishing Company
- [19] Varanasi, J. L., Veerubhotla, R., and Das, D. (2018). Diagnostic tools for the assessment of MFC. In Debabrara Das (Ed.), *Microbial Fuel Cell: A bioelectrochemical system that converts waste to watts* (pp. 249 – 268). New Delhi, India: Capital Publishing Company

- [20] Singhvi, P., and Chhabra, M. (2013). Simultaneous chromium and power generation using algal biomass in a dual chambered salt bridge microbial fuel cell. *Journal of Bioremediation and Biodegradation*, 04 (05), pp. 1-4. doi: 10.4172/2155-6199.1000190
- [21] Michael, G. W., and Thomas, A. T. (2013). Review of microbial fuel cells for wastewater treatment: Large-scale applications, future needs and current research gaps. In proceedings of the *ASME 7th international conference on energy sustainability & 11th fuel cell science, Minneapolis, USA*, pp. 2-8. doi: 10.1115/FuelCell2013-18185
- [22] Rozendal, R. A., Hamelers, H. V. M., Rabaey, K., Keller, J., and Buisman, C. J. N. (2008). Towards practical implementation of bioelectrochemical wastewater treatment. *Trends in Biotechnology*, 26 (8), pp. 450-459. doi: 10.1016/j.tibtech.2008.04.008
- [23] Wang, B., and Han, J. I. (2009). A single chamber stackable microbial fuel cell with air cathode. *Biotechnology Letters*, 31 (3), pp. 387–393. doi: 10.1021/es0502876
- [24] United Nations Population Fund. (2009). Reproductive Health and Rights is Fundamental for Sound Economic Development and Poverty Alleviation. *UNFPA Report*. Retrieved from <https://www.unfpa.org>
- [25] Sakamoto, M., Ahmed, T., Begum, S., and Huq, H. (2019). Water pollution and the textile industry in Bangladesh: Flawed corporate practices or restrictive opportunities?. *Sustainability*, 11(7), 1951, pp. 1-14. doi: 10.3390/su11071951
- [26] Hossain, L., Sarker, S.K., and Khan, M.S. (2018). Evaluation of present and future wastewater impacts of textile dyeing industries in Bangladesh. *Environmental Development*, 26, pp. 23-33. doi: 10.1016/j.envdev.2018.03.005
- [27] Khan, M. S., Selim, S., Evans, A. E., and Chadwick, M. (2011). Characterizing and measuring textile effluent pollution using a material balance approach: Bangladesh case study. In proceedings of *19th International Conference on Mechanical Engineering (ICME), Bangladesh*, 11-RT-019-025, pp. 1-6.
- [28] Islam, M., Chowdhury, M., Billah, M., Tusher, T., and Sultana, N. (2012). Investigation of effluent quality discharged from the textile industry of Purbani group, Gazipur, Bangladesh and its management. *Bangladesh Journal of Environmental Science*, 23, pp. 123-130. doi: 0.12944/CWE.13.2.05
- [29] El-Gohary, F., Tawfik, A., and Mahmoud, U. (2010). Comparative study between chemical coagulation/precipitation (C/P) versus coagulation/dissolved air flotation

(C/DAF) for pre-treatment of personal care products (PCPs) wastewater. *Desalination*, 252, pp. 106-112. doi: 10.1016/j.desal.2009.10.016

[30] Rott, U., and Minke, R. (1999). Overview of wastewater treatment and recycling in the textile processing industry. *Water Science and Technology*, 40, pp. 137-144. doi: 10.1016/S0273-1223(99)00381-9

[31] Nergis, Y., Sharif, M., Akhtar, N., and Hussain, A. (2009). Quality characterization and magnitude of pollution implication in textile mills effluents. *Journal of Quality and Technology Management*, p. 5. Retrieved from <https://www.scribd.com/document/301628412>

[32] Dey, S., and Islam, A. (2015). A review on textile wastewater characterization in Bangladesh. *Resources and Environment*, 5, pp. 15-44. doi: 10.5923/j.re.20150501.03

[33] Patel, H., and Vashi, R. T. (2015). *Characterization and treatment of textile wastewater* (1st ed.). United Kingdom: Butterworth Heinemann

[34] Sultana, M. S., Islam, M. S., Saha, R., and Al-Mansur, M. (2009). Impact of the effluents of textile dyeing industries on the surface water quality inside DND embankment, Narayanganj. *Bangladesh Journal of Scientific and Industrial Research*, 44, pp. 65-80. doi: 10.3329/bjsir.v44i1.2715

[35] Ali, M., Ahmed, S., and Khan, M. (2010). Characteristics and treatment process of wastewater in a nylon fabric dyeing plant. *Journal of Chemical Engineering*, 23, pp. 1-6. doi: 10.3329/jce.v23i0.5566

[36] Mohiuddin, A.K. (2019). Chemical contaminants and pollutants in the measurable life of Dhaka city. *Journal of Environmental Science and Public Health*, 3(1), pp. 57-73. doi: 10.26502/jesph.96120047

[37] Rajeswari, R., and Silaja, N. (2014). Impact if heavy metals on environmental pollution. *National Seminar on Impact of Toxic Metals, Minerals and Solvents leading to Environmental Pollution-Journal of Chemical and pharmaceutical sciences*, 3, pp. 175-181. Retrieved from [https://www.jchps.com/specialissues/Special issue3/42 jchps si3 addn sailaja 175-181.pdf](https://www.jchps.com/specialissues/Special%20issue3/42%20jchps%20si3%20addn%20sailaja%20175-181.pdf)

[38] Vivekanandan, E., Hermes, R., and O'brien, C. (2016). Climate change effects in the Bay of Bengal large marine ecosystem. *Environmental development*, 17, pp. 46-56. doi: 10.1016/j.envdev.2015.09.005

[39] Nevill, J. C., Hancock, P. J., Murray, B. R., Ponder, W. F., Humphreys, W. F., Phillips, M. L., and Groom, P. K. (2010). Groundwater-dependent ecosystems and the

dangers of groundwater overdraft: A review and an Australian perspective. *Pacific Conservation Biology*, 16, pp. 187-208. doi: 10.1071/PC100187

[40] Moinee, A. Al. (2019). Engineering Ethics: The Essence of Engineering Excellence. In proceedings of 59th Convention of Institute of Engineers (IEB), Bangladesh, pp. 07-10.

[41] Hegazi, H. A. (2013). Removal of heavy metals from wastewater using agricultural and industrial wastes as adsorbents. *Housing and building national research center (HBRC) journal*, 9 (3), pp. 276-282. doi: 10.1016/j.hbrj.2013.08.004

[42] Chowdhury, R. M., Alam, K. S., and Hossain, A. B. M. I. (2019). Efficiency of powdered activated carbon for removing heavy metal from industrial wastewater. In proceedings of 59th Convention of Institute of Engineers (IEB), Bangladesh, pp. 20-24.

[43] Zhang, L., Ruizhe, G., Yiyang, L., Jie, L., Chi, Y., Yang, J., Lankun, C., and Lehua, Z. (2018). Behavior of Copper, Nickel, Cadmium, Mercury ions in anode chamber of microbial fuel cells. *International Journal of Electrochemical Science*, 13, pp. 3050-3062. doi: 10.20964/2018.03.69

[44] Ebrahimi, A., Najafpour, G. D., Yousefi, K., and Kebria, D. Y. (2018). Performance of microbial desalination cell for salt removal and energy generation using different catholyte solutions. *Desalination*, 432, pp. 1-9. doi: 10.1016/j.desal.2018.01.002

[45] Mathuriya A. S. and Sharma, V. N. (2009). Bioelectricity production from various wastewaters through microbial fuel cell technology. *Journal of Biochemical Technology*, 2, pp. 133–137. Retrieved from <https://www.researchgate.net/publication/44130487>

[46] Anthony, J., Slatea, B. C., Kathryn, A., Whiteheada, B., Dale A. C., Brownsona, C., Craig, E., and Banksa, C. (2019). Microbial fuel cells: An overview of current technology. *Renewable and Sustainable Energy Reviews*, 101, pp. 60-81. doi: 10.1016/j.rser.2018.09.044

[47] Ismail, I. M. I., Kim, T., and Oh, S.-E. (2019). Overview of recent advancements in the microbial fuel cell from fundamentals to applications: Design, major elements, and scalability. *Energies*, 12 (17), 3390, pp. 1-20. doi: 10.3390/en12173390

[48] Flimban, S. G. A., Hassan, S. H. A., Rahman, M. M., and Oh, S.-E. (2018). The effect of Nafion membrane fouling on the power generation of a microbial fuel cell. *International Journal of Hydrogen Energy*, pp. 1-9. doi: 10.1016/j.ijhydene.2018.02.0

- [49] Song, H. L., Zhu, Y., and Li, J. (2019). Electron transfer mechanisms, characteristics and applications of biological cathode microbial fuel cells – A mini review. *Arabian Journal of Chemistry*, pp. 1-8. doi: 10.1016/j.arabjc.2015.01.008
- [50] Kumar, R., Singh, L., and Zularisam, A. W. (2016). Exoelectrogens: Recent advances in molecular drivers involved in extracellular electron transfer and strategies used to improve it for microbial fuel cell applications. *Renewable and Sustainable Energy Reviews*, 56, pp. 1322-1336. doi: 10.1016/j.rser.2015.12.029
- [51] Bond, D. R., and Lovely, D. R. (2003). Electricity production by *Geobacter Sulfurreducens* attached to electrodes. *Applied and Environmental Microbiology*, 69(3), pp. 1548-1555. doi: 10.1128/AEM.69.3.1548-1555.2003
- [52] Shukla, A. K., Suresh, P., Berchmans, S., and Rajendran, A. (2004). Biological fuel cells and their applications. *Current Science*, 87(4), pp. 455-468. Retrieved from: <https://www.researchgate.net/publication/242092112>
- [53] Balat, M. (2016). Microbial fuel cells as an alternative energy option. *Energy Source, Part A: Recovery, Utilization, and Environmental Effect*, 32, pp. 26–35. doi: 10.1080/15567030802466045
- [54] Rittmann, B. E. (2008). Opportunities for renewable bioenergy using microorganisms. *Biotechnology and Bioengineering*, 100, pp. 203-212. doi: 10.1002/bit.21875
- [55] Watanabe, K. (2008). Recent developments in microbial fuel cell technologies for sustainable bioenergy. *Journal of Bioscience and Bioengineering*, 106, 528-536. doi: 10.1263/jbb.106.528
- [56] Rabaey, K., and Verstraete, W. (2005). Microbial fuel cells: Novel biotechnology for energy generation. *Trends in Biotechnology*, 23, pp. 291–298. doi: 10.1016/j.tibtech.2005.04.008
- [57] Du, Z., Li, H., and Gu, T. (2007). A state of the art review on microbial fuel cells: a promising technology for wastewater treatment and bioenergy. *Biotechnology Advances*, 25, pp. 464-482. doi: 10.1016/j.biotechadv.2007.05.004
- [58] Jang, J. K., Pham, T. H., Chang, I. S., Kang, K. H., Moon, H., Cho, K. S., and Kim, B. H. (2004). Construction and operation of a novel mediator and membraneless microbial fuel cell. *Process Biochemistry*, 39, pp. 1007-1012. doi: 10.1016/S0032-9592(03)00203-6
- [59] Abourached, C. (2014). *Microbial fuel cell for wastewater treatment: heavy metal removal, sewage sludge treatment, and its potential application in wastewater reuse in*

irrigation, Ph.D. Thesis, Biological and Ecological Engineering, Oregon State University, USA. Retrieved from: ir.library.oregonstate.edu

[60] Ucar, D., Zhang, Y., and Angelidaki, I. (2017). An overview of electron acceptors in microbial fuel cells. *Frontiers in Microbiology*, 8, p. 643. doi: 10.3389/fmicb.2017.00643

[61] Mathuriya, A. S. (2014). Eco-affectionate face of microbial fuel cells. *Critical Reviews in Environmental Science and Technology*, 44 (2), pp. 97-153. doi: 10.1080/10643389.2012710445

[62] Kumar, R., Singh, L., and Wahid, Z. Ab. (2015). Role of microorganisms in microbial fuel cells for bioelectricity production. In Vipin Chandra Kalia (Ed.), *Microbial Factories: Biofuels, Waste Treatment, Volume 1* (pp. 135-154). Germany: Springer

[63] Mustakeem. (2015). Electrode materials for microbial fuel cells: Nanomaterial approach. *Materials for Renewable and Sustainable Energy*, 4, p. 22. doi: 10.1007/s40243-015-0063-8

[64] Delaney, G. M., Bennetto, H. P., Mason, J. R., Roller, S. D., Stirling, J. L., and Thurston, C. F. (2008). Electron-transfer coupling in microbial fuel cells and performance of fuel cells containing selected microorganism-mediator-substrate combinations. *Journal of Chemical Technology and Biotechnology*, 34, pp. 13–27. doi: 10.1002/jctb.280340103

[65] Lithgow, A. M., Romero, L., Sanchez, I. C., Souto, F. A., and Vega, C. A. (1986). Interception of electron-transport chain in bacteria with hydrophilic redox mediators. *Journal of Chemical Research, Sage Journal*, pp. 178-179.

[66] Shi, L., Dong, H., Reguera, G., Beyenal, H., Lu, A., Liu, J., Yu, H. Q., and Fredrickson, J. K. (2016). Extracellular electron transfer mechanisms between microorganisms and minerals. *Nature Reviews Microbiology*, 14 (10), pp. 651-662. doi: 10.1038/nrmicro.2016.93

[67] Clark, D. P., and Pazdernik, N. J. (2016). Environmental Biotechnology. *Biotechnology: Applying the genetic revolution* (pp. 393-418). England: Academic Cell, Elsevier

[68] Ehrlich, H. L. (1997). Microbes and metals. *Applied Microbiology and Biotechnology*, 48 (6), pp. 687-692. doi: 10.1007/s002530051116

- [69] Speers, A. M., and Reguera, G. (2012). Electron donors supporting growth and electroactivity of *Geobacter sulfurreducens* anode biofilms. *Applied Environmental Microbiology*, 78 (2), pp. 437-444. doi: 10.1128/AEM.06782-11
- [70] Gil, G. C., Chang, I. S., Kim, B. H., Kim, M., Jang, J. K., Park, H. S., and Kim, H. J. (2003). Operational parameters affecting the performance of a mediator-less microbial fuel cell. *Biosensors & Bioelectronics*, 18, pp. 327-334. doi: 10.1016/S0956-5663(02)00110-0
- [71] Greenwood, N. N., and Earnshaw, A. (1984). *Chemistry of the Elements* (pp. 82–87). Oxford, England: Pergamon Press
- [72] Liu, L., Yuan, Y., Li, F. B., and Feng, C. H. (2011). In-situ Cr(VI) reduction with electrogenerated hydrogen peroxide driven by iron-reducing bacteria. *Bioresource Technology*, 102, pp. 2468-2473. doi: 10.1016/j.biortech.2010.11.013
- [73] Hussain, J., Hussain, I. A., and Arif, M. (2004). Characterization of textile wastewater. *Journal of Industrial Pollution Control*, 20 (1), pp. 137-144. Retrieved from <https://www.researchgate.net/publication/287641417>
- [74] Deepali, and Gangwar, K. K. (2009). Metals concentration in textile and tannery effluents, associated soils and ground water. *New York Science Journal*, 3 (4), pp. 82-89. Retrieved from <https://www.researchgate.net/publication/267785821>
- [75] Kotas, J., and Stasicka, Z. (2010). Chromium occurrence in the environment and methods of its speciation. *Environmental Pollution*, 107, pp. 263-283. doi: 10.1016/s0269-7491(99)00168-2
- [76] Oliveira, H. (2012). Chromium as an environmental pollutant: Insights on induced plant toxicity. *Journal of Botany*, 2012, pp. 1-8. doi: 10.1155/2012/375843
- [77] López-Luna, J., González-Chávez, M. C., Esparza-García, F. J., and Rodríguez-Vázquez, R. (2009). Toxicity assessment of soil amended with tannery sludge, trivalent chromium and hexavalent chromium, using wheat, oat and sorghum plants. *Journal of Hazardous Materials*, 163 (2-3), pp. 829-834. doi: 10.1016/j.jhazmat.2008.07.034
- [78] Fischer, G., and Jena, V. (1995). Damage mechanisms and protective measures. In Holger Brill (Ed.), *Microbial material protection and material destruction*. Germany: Stuttgart
- [79] Hogendoorn, Bob. (2011). *Heinemann Chemistry Enhanced 2* (p. 416). Melbourne, Australia: Pearson Education Australia
- [80] Puir, B. R., Sharma, L. R., Pathania, M. S., and Navjot, K. (2019). *A Textbook of Physical Chemistry II* (1st ed.). Punjab, India: Vishal Publishing Company

- [81] Beveridge T. J, and Doyle, R. (Eds.). (1989). *Metal ions and bacteria* (1st ed.). New York, USA: Wiley- Interscience
- [82] Gadd, G. M. (1993). Interactions of fungi with toxic metals. *New Phytologist*, 124, pp. 25-60. doi: 10.1111/j.1469-8137.1993.tb03796.x
- [83] Macaskie, L. E., Dean, A. C. R., Cheetham, A. K., Jakeman, R. J. B., and Skarnulis, A. J. (1987). Cadmium accumulation by a *Citrobacter* sp.: The chemical nature of the accumulated metal precipitate and its location on the bacterial cells. *The Journal of General Microbiology*, 133, pp. 53-544. doi: 10.1099/00221287-133-3-539
- [84] Macaskie, L. E., Empson, R. M., Cheetham, A. K., Grey, C. P., and Skarnulis, A. J. (1992). Uranium bioaccumulation by a *Citrobacter* sp. as a result of enzymically mediated growth of polycrystalline $\text{H}_2\text{UO}_2\text{PO}_4$. *Science*, 257, pp. 782-784. doi: 10.1126/science.1496397
- [85] Schultze-Lam, S., Fortin, D., Davis, B. S., and Beveridge, T. J. (1996). Mineralization of bacterial surfaces. *Chemical Geology*, 132, pp. 171-181. doi: 10.1016/S0009-2541(96)00053-8
- [86] Taherzadeh, D., Picioreanu, C., and Horn, H. (2012). Mass transfer enhancement in moving biofilms structures. *Biophysical Journal*, 102, 1483-1492. doi: 10.1016/j.bpj.2012.02.033
- [87] Wei, J. C., Liang, P., Cao, X. X., and Huang, X. (2010). A new insight into potential regulation on growth and power generation of *Geobacter sulfurreducens* in microbial fuel cells based on energy viewpoint. *Environmental Science Technology*, 44, pp. 3187-3191. doi: 10.1021/es903758m
- [88] Briandet, R., Herry, J., and Bellon-Fontaine, M. (2001). Determination of the van der Waals, electron donor and electron acceptor surface tension components of static Gram-positive microbial biofilms. *Colloids and Surface B: Biointerfaces*. 21 (4), pp. 299-310. doi: 10.1016/s0927-7765(00)00213-7
- [89] Deplanche, K., Murray, A., Mennan, C., Taylor, S., and Macaskie, L. (2011). Biorecycling of precious metals and rare earth elements. *Nanomaterials*, 2011, pp. 279-314. doi: 10.5772/25653
- [90] Abourached, C., Catal, T., and Liu, H. (2014). Efficacy of single-chamber microbial fuel cells for removal of cadmium and zinc with simultaneous electricity production. *Water Research*, 51, pp. 228-233. doi: 10.1016/j.watres.2013.10.062

- [91] Klaus-Joerger, T., Joerger, R., Olsson, E., and Granqvist, C-G. (2001). Bacteria as workers in the living factory: metal-accumulating bacteria and their potential for materials science. *Trends in Biotechnology*, 19, pp. 15–20. doi: 10.1016/S0167-7799(00)01514-6
- [92] Macaskie, L., Mikheenko, I., Yong, P., Deplanche, K., Murray, A., and Paterson-Beedle, M. (2009). Today's wastes, tomorrow's materials for environmental protection. *Hydrometallurgy*, 104, pp. 483–477. doi: 10.4028/www.scientific.net/AMR.71-73.541
- [93] Islam, M. A., Woon, C. W., Ethiraj, B., Cheng, C. K., Yousuf, A., and Khan, M. M. R. (2016). Ultrasound driven biofilm removal for stable power generation in microbial fuel cell. *Energy Fuel*, 31, pp. 968-976. doi: 10.1021/acs.energyfuels.6b022994
- [94] Thrash, J, C, and Coates, J, D. (2008). Review: direct and indirect electrical stimulation of microbial metabolism. *Environmental Science and Technology*, 42, pp. 3921–3. doi: 10.1021/es702668w
- [95] Daniels, J. A., Krishnamurthi, R., and Rizvi, S. S. H. (1984). A review of effects of carbon dioxide on microbial growth and food quality institute of food science. *Journal of Food Protection*, 48 (6), pp. 532-537. doi: 10.4315/0362-028X-48.6.532
- [96] Logan, B. E. (2010). Scaling up microbial fuel cells and other bioelectrochemical systems. *Applied Microbiology and Biotechnology*, 85 (6), p. 1665. doi: 10.1007/s00253-009-2378-9
- [97] Natarajan, D., and Van Nguyen, T. (2004). Effect of electrode configuration and electronic conductivity on current density distribution measurements in PEM fuel cells. *Journal of Power Sources*, 135 (1), p. 95. doi: 10.1016/j.jpowsour.2004.03.063
- [98] Rismani-Yazdi, H., Carver, S. M., Christy, A. D., and Tuovinen, O. H. (2008). Cathodic limitations in microbial fuel cells: an overview. *Journal of Power Sources*, 180 (2). doi: 10.1016/j.jpowsour.2008.02.074
- [99] Pandit, S., Khilari, S., Roy, S., Ghangrekar, M. M., Pradhan, D., and Das, D. (2015). Reduction of start-up time through bioaugmentation process in microbial fuel cells using an isolate from dark fermentative spent media fed anode. *Water Science and Technology*, 72, pp. 106-115. doi: 10.2166/wst.2015.174
- [100] Chandrasekhar, K., and Venkata, M. S. (2012). Bio-electrochemical remediation of real field petroleum sludge as an electron donor with simultaneous power generation facilitates biotransformation of PAH: Effect of substrate concentration. *Bioresource Technology*, 110, 517-525. doi: 10.1016/j.biortech.2012.01.128

- [101] Pant, D., Van Bogaert, G., Diels, L., and Vanbroekhoven, K. (2010). A review of the substrates used in microbial fuel cells (MFCs) for sustainable energy production. *Bioresource Technology*, 101, 1533–1543. doi: 10.1016/j.biortech.2009.10.017
- [102] Reddy, M. V., Devi, M. P., Chandrasekhar, K., Goud, R. K., and Venkata, M. S. V. (2011). Aerobic remediation of petroleum sludge through soil supplementation: Microbial community analysis. *Journal of Hazardous Materials*, 197, 80-87. doi: 10.1016/j.jhazmat.2011.09.061
- [103] He, Z., Wagner, N., Minteer, S. D., and Angenent, L. T. (2006). An upflow microbial fuel cell with an interior cathode: Assessment of the internal resistance by impedance spectroscopy. *Environmental Science and Technology*, 40, 5212-5217. doi: 10.1021/es060394f
- [104] Nordstorm, D. K., and Alpers, C. N. (1999). Geochemistry of acid mine waters. The environmental geochemistry of mineral deposits. *Part A: Process Technology Health Issues*, 6, pp. 133-160. doi: 10.5382/Rev.06.06
- [105] Shuler, M. L., and Kargi, F. (2002). The Basics of Biology: An Engineer's Perspective. *Bioprocess Engineering - Basic Concepts* (pp. 49-52). New Jersey, USA: Pearson Education Incorporation
- [106] Capodaglio, A. G., Molognoni, D., Dallago, E., Liberale, A., Cella, R., Longoni, P., and Pantaleoni, L. (2013). Microbial fuel cells for direct electrical energy recovery from urban wastewaters. *The Scientific World Journal*, pp. 1-8. doi: 10.1155/2013/634738
- [107] Zhu, F. Y., Wang, Q. Q., Zhang, X. S., Hu, W., Zhao, X., and Zhang, X. H. (2014). 3D nanostructure reconstruction based on the SEM imaging principle, and applications. *Nanotechnology*, 25 (18), p. 185705. doi: 10.1088/0957-4484/25/18/185705
- [108] Zaidi, S. R., and Sitepu, H. (2011). Characterization of Corrosion Products in Oil and Gas Facilities using X-ray Powder Diffraction. *NACE- International Corrosion Conference and Exposition*, p. 11393. Retrieved from <https://www.researchgate.net/publication/265596705>
- [109] Mohan, S. V., Mohanakrishna, G., Srikanth, S., and Sarma, P. N. (2008). Harnessing of bioelectricity in microbial fuel cell (MFC) employing aerated cathode through anaerobic treatment of chemical wastewater using selectively enriched hydrogen producing mixed consortia. *Fuel*, 87, pp. 2667-2676. doi: 10.1016/j.fuel.2008.03.002

- [110] Serway, A. R. (1998). *Principles of Physics* (p. 602). Fort Worth, Texas, USA: Saunders College Publication
- [111] Liu, H., Cheng, S., and Logan, B.E. (2005). Power generation in fed-batch microbial fuel cells as a function of ionic strength, temperature, and reactor configuration. *Environmental Science and Technology*, 39(14), p. 5488. doi: 10.1021/es050316c
- [112] Chaudhuri, S. L., and Lovely, D. R. (2003). Electricity generation by direct oxidation of glucose in mediatorless microbial fuel cells. *Nature Biotechnology*, 21 (10), p. 1229. doi: 10.1038/nbt867
- [113] Uddin, I., Ahmer, F. M., and Asiri, A. M. (Eds.). (2019). *Microbial fuel cells: Materials and applications* (pp. 53-74). Millersville, USA: Material Research Foundation
- [114] Zhou, M., Chi, M., Luo, J., He, H., and Jin, T. (2011). An overview of electrode materials in microbial fuel cells. *Journal of Power Sources*, 196, pp. 4427-4435. doi: 10.1016/j.jpowsour.2011.01.012
- [115] Goldstein, J., Newbury, D. E., Joy, D.C., Lyman, C. E., Echlin, P., Lifshin, E., Sawyer, L., and Michael, J.R. (2007). *Scanning Electron Microscopy and X-Ray Microanalysis* (3rd ed.). New York, USA: Springer
- [116] Bergstrom, J. (2015). Experimental characterization techniques. *Mechanics of Solid Polymers*, pp. 19-114. doi: 10.1016/B978-0-323-31150-2.00002-9
- [117] Ali, M. R., Nishikata, A., and Tsuru, T. (2001). Electrodeposition of cobalt-chromium alloys from cobalt chloride-N-(n butyl) pyridinium chloride molten salt. *Indian Journal of Chemical Technology*, 8, pp. 44-50. doi: 10.1016/S0013-4686(96)00382-9
- [118] Dongol, M., El-Denglawey, A., Abd EL Sadek, M. S., and Yahia, S. I. S. (2015). Thermal annealing effect on the structural and the optical properties of nano CdTe films. *Optik*, 126 (14), pp. 1352-1357. doi: 10.1016/j.ijleo.2015.04.048

APPENDIX

APPENDIX

A.1 Sample Calculation of Cell Performance for Synthetic Wastewater (SWW)

$$\begin{aligned}\text{Fuel Cell Performance (max. power density)} &= \frac{(\text{Power})_{\text{sww}}}{(\text{Volume})_{\text{cell}}} = \\ &= \frac{(\text{Voltage} \times \text{Current})_{\text{sww}}}{(\text{Volume})_{\text{cell}}} \\ &= \frac{659.3 \text{ mV} \times 397.1 \text{ } \mu\text{A}}{1200 \times 10^{-6} \text{ m}^3} = \frac{659.3 \times 10^{-3} \times 397.1 \times 10^{-6}}{1200 \times 10^{-6}} \text{ W m}^{-3} = 218.17 \text{ mW m}^{-3}\end{aligned}$$

$$\therefore \text{Maximum Power Density i.e. Cell Performance for SWW} = 218.17 \text{ mW m}^{-3}$$

Time to reach maximum value during 10 days of batch operation was 72×3600 sec

Therefore, maximum electric energy recovered for synthetic wastewater unit volume,

$$E_{\text{recovered}} = \text{Maximum Power Density} \times \text{Time} = 218.17 \times 10^{-3} \text{ W m}^{-3} \times 72 \times 3600 \text{ s}$$

$$\therefore E_{\text{recovered}} = 56550.53 \text{ W s m}^{-3} = 56550.53 \text{ Js}^{-1} \text{ s m}^{-3} = 56.55 \text{ kJ m}^{-3}$$

A.2 Sample Calculation of Cell Performance for Textile Wastewater (TWW)

$$\begin{aligned}\text{Fuel Cell Performance (max. power density)} &= \frac{(\text{Power})_{\text{tww}}}{(\text{Volume})_{\text{cell}}} = \\ &= \frac{(\text{Voltage} \times \text{Current})_{\text{tww}}}{(\text{Volume})_{\text{cell}}} \\ &= \frac{1100.1 \text{ mV} \times 733.4 \text{ } \mu\text{A}}{1200 \times 10^{-6} \text{ m}^3} = \frac{1100.1 \times 10^{-3} \times 733.4 \times 10^{-6}}{1200 \times 10^{-6}} \text{ W m}^{-3} = 672.3445 \text{ mW m}^{-3}\end{aligned}$$

$$\therefore \text{Maximum Power Density i.e. Cell Performance for TWW} = 672.3445 \text{ mW m}^{-3}$$

Time to reach maximum value during 10 days of batch operation was 120×3600 sec

Therefore, maximum electric energy recovered for textile wastewater unit volume,

$$E_{\text{recovered}} = \text{Maximum Power Density} \times \text{Time} = 672.3445 \times 10^{-3} \text{ W m}^{-3} \times 120 \times 3600 \text{ s}$$

$$\therefore E_{\text{recovered}} = 290452.80 \text{ W s m}^{-3} = 290452.80 \text{ Js}^{-1} \text{ s m}^{-3} = 290.453 \text{ kJ m}^{-3}$$

A.3 Sample Calculation of Coulombic Efficiency for Synthetic Wastewater

In case of Synthetic Wastewater,

$I = I_{\max} = 397.1 \times 10^{-6} \text{ A}$, $V = 1.2 \text{ L}$, $F = 96500 \text{ C}$, time to reach the maximum value during 10 days of batch operation was, $t = 72 \times 3600 \text{ sec}$

$(\text{COD})_{\text{initial}} = 512 \text{ mg/L} = 512 \times 10^{-3} \text{ g/L}$; COD at maximum current generation,
 $(\text{COD})_t = 409 \text{ mg/L} = 409 \times 10^{-3} \text{ g/L}$

$$\Delta\text{COD} = (\text{COD})_{\text{initial}} - (\text{COD})_t = (512 - 409) \times 10^{-3} \text{ g/L}$$

∴ Coulombic Efficiency of Synthetic Wastewater,

$$C_{E(\text{SWW})} = \frac{8 \int_0^{72 \times 3600} (397.1 \times 10^{-6}) dt}{96500 \times 1.2 \times (512 - 409) \times 10^{-3}} \times 100\%$$

$$\therefore C_{E(\text{SWW})} = \frac{8 \times 397.1 \times 10^{-6} \times (72 \times 3600 - 0)}{96500 \times 1.2 \times (512 - 409) \times 10^{-3}} \times 100\% = 6.90\%$$

A.4 Sample Calculation of Coulombic Efficiency for Textile Wastewater

In case of Textile Wastewater,

$I = I_{\max} = 733.4 \times 10^{-6} \text{ A}$, $V = 1.2 \text{ L}$, $F = 96500 \text{ C}$, time to reach the maximum value during 10 days of batch operation was, $t = 120 \times 3600 \text{ sec}$

$(\text{COD})_{\text{initial}} = 1544 \text{ mg/L} = 1544 \times 10^{-3} \text{ g/L}$; COD at maximum current generation,
 $(\text{COD})_t = 1310 \text{ mg/L} = 1310 \times 10^{-3} \text{ g/L}$

$$\Delta\text{COD} = (\text{COD})_{\text{initial}} - (\text{COD})_t = (1544 - 1310) \times 10^{-3} \text{ g/L}$$

∴ Coulombic Efficiency of Synthetic Wastewater,

$$C_{E(\text{TWW})} = \frac{8 \int_0^{120 \times 3600} (733.4 \times 10^{-6}) dt}{96500 \times 1.2 \times (1544 - 1310) \times 10^{-3}} \times 100\%$$

$$\therefore C_{E(\text{TWW})} = \frac{8 \times 733.4 \times 10^{-6} \times (120 \times 3600 - 0)}{96500 \times 1.2 \times (1544 - 1310) \times 10^{-3}} \times 100\% = 9.35\%$$

A.5 Sample Calculation of COD Removal for Textile and Synthetic Wastewater

Though the transmission of electrical power is low, the overall process reduces the total amount of organic compounds in the anodic chamber and hence decrease the COD of the sample. The result obtained from treating synthetic wastewater (SWW) and the textile wastewater (TWW) for 10 days are given below:

A.5.1 Sample Calculation of COD Removal for Synthetic Wastewater

Concentration of blank Sample (calibrated) = 0 mg/L

Multiplying factor of HACH machine for COD measurement = $\frac{1200}{527}$

Initial COD (raw wastewater) = $225 \times \frac{1200}{527}$ mg/L ≈ 512 mg/L

Final COD (treated wastewater) = $120 \times \frac{1200}{527}$ mg/L ≈ 273 mg/L

\therefore % COD removal = $\frac{(\text{COD})_{\text{initial}} - (\text{COD})_{\text{final}}}{(\text{COD})_{\text{initial}}} \times 100\% = \frac{512 - 273}{512} \times 100\% = 46.67\%$

A.5.2 Sample Calculation of COD Removal for Textile Wastewater

Concentration of blank Sample (calibrated) = 0 mg/L

Multiplying factor of HACH machine for COD measurement = $\frac{1200}{527}$

Initial COD (raw wastewater) = $678 \times \frac{1200}{527}$ mg/L ≈ 1544 mg/L

Final COD (treated wastewater) = $324 \times \frac{1200}{527}$ mg/L ≈ 738 mg/L

\therefore % COD removal = $\frac{(\text{COD})_{\text{initial}} - (\text{COD})_{\text{final}}}{(\text{COD})_{\text{initial}}} \times 100\% = \frac{1544 - 738}{1544} \times 100\% = 52.20\%$

A.6 Sample Calculation of Total Chromium Removal for Textile and Synthetic Wastewater

Percentage removal of total chromium can be obtained by utilizing the total chromium concentrations of the raw and treat sample of wastewater simultaneously. The result obtained from treating SWW and TWW for 10 days are given below:

A.6.1 Calculation of Total Chromium Removal for Synthetic Wastewater

Concentration of blank Sample (calibrated) = 0 mg/L

Initial concentration of Total Chromium (raw wastewater) = 0.03 mg/L

Final concentration of Total Chromium (treated wastewater) = 0.02 mg/L

$$\therefore \% \text{ Chromium removal} = \frac{(\text{Cr})_{\text{initial}} - (\text{Cr})_{\text{final}}}{(\text{Cr})_{\text{initial}}} \times 100\% = \frac{0.03 - 0.02}{0.03} \times 100\% = 33.33\%$$

A.6.2 Calculation of Total Chromium Removal for Textile Wastewater

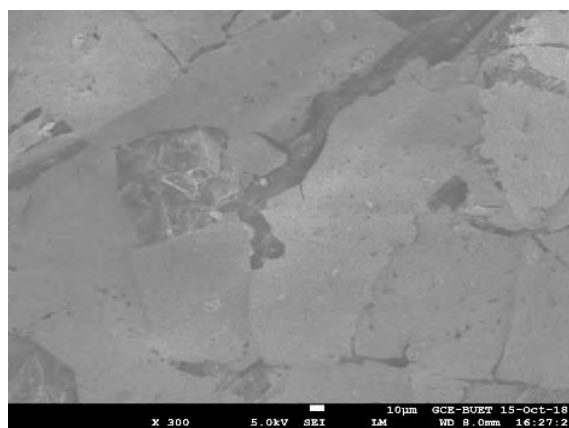
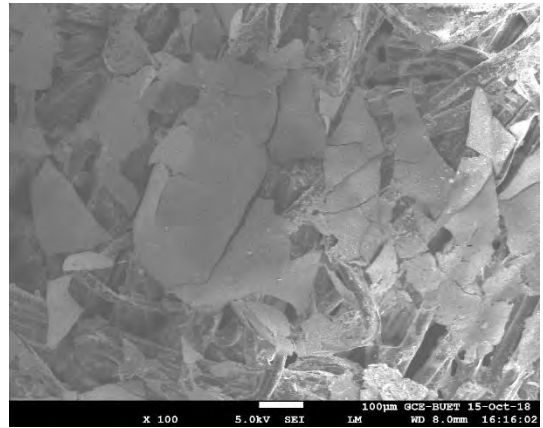
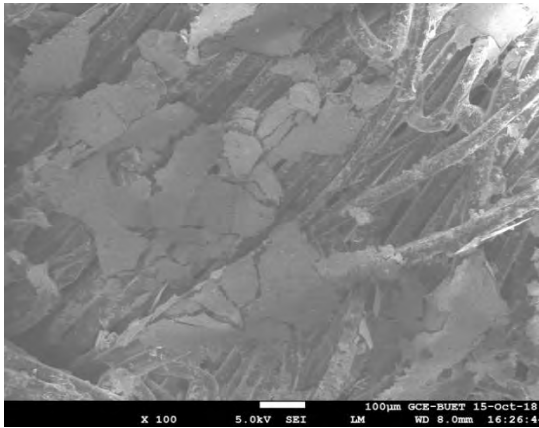
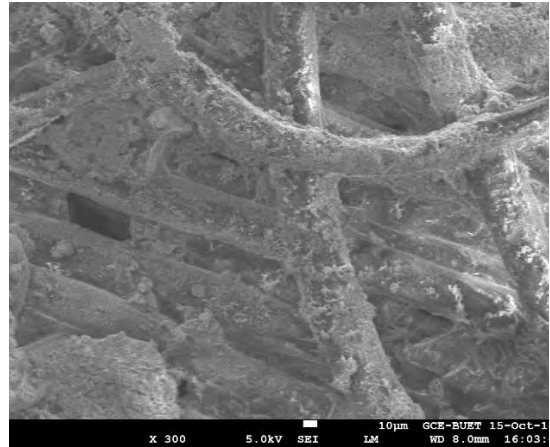
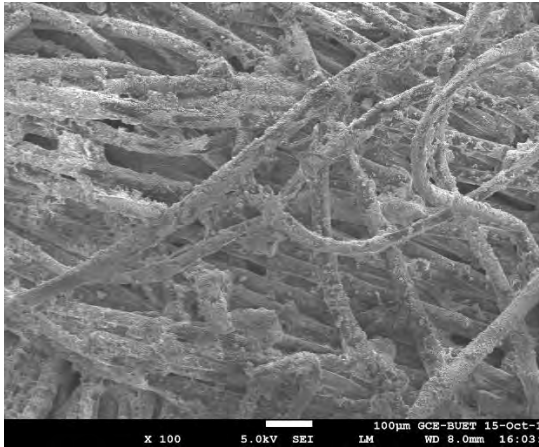
Concentration of blank Sample (calibrated) = 0 mg/L

Initial concentration of Total Chromium (raw wastewater) = 0.08 mg/L

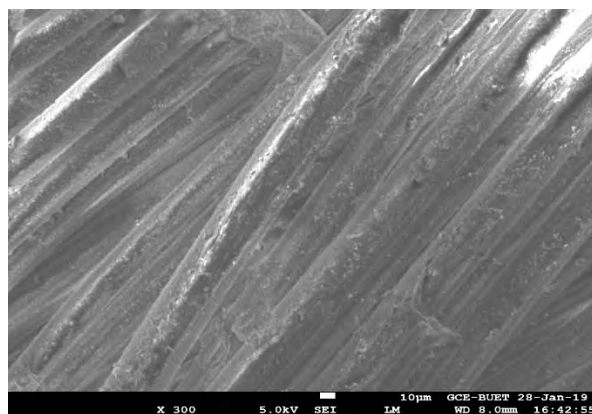
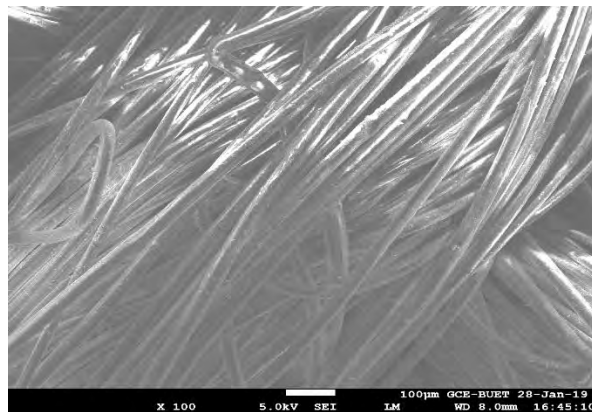
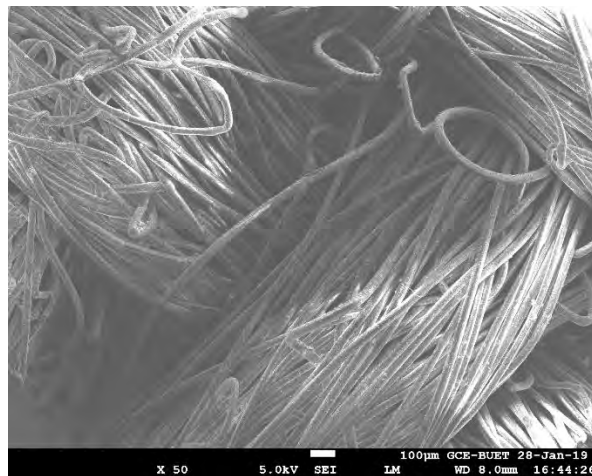
Final concentration of Total Chromium (treated wastewater) = 0.037 mg/L

$$\therefore \% \text{ Chromium removal} = \frac{(\text{Cr})_{\text{initial}} - (\text{Cr})_{\text{final}}}{(\text{Cr})_{\text{initial}}} \times 100\% = \frac{0.08 - 0.037}{0.08} \times 100\% = 53.75\%$$

A.7 Additional SEM reports of treated carbon cloth for synthetic wastewater (SWW)

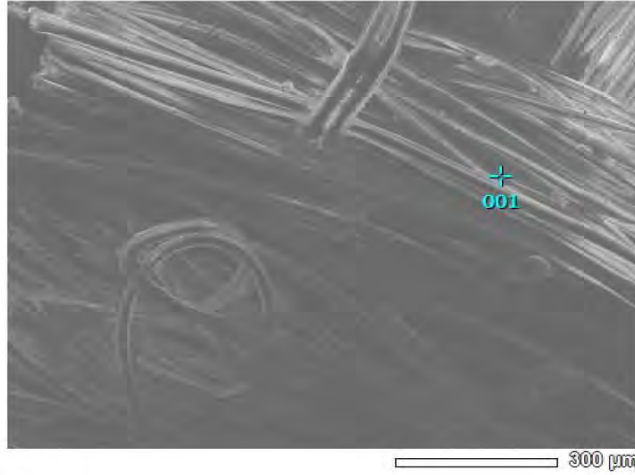


A.8 Additional SEM Reports of treated carbon cloth for textile wastewater (TWW)



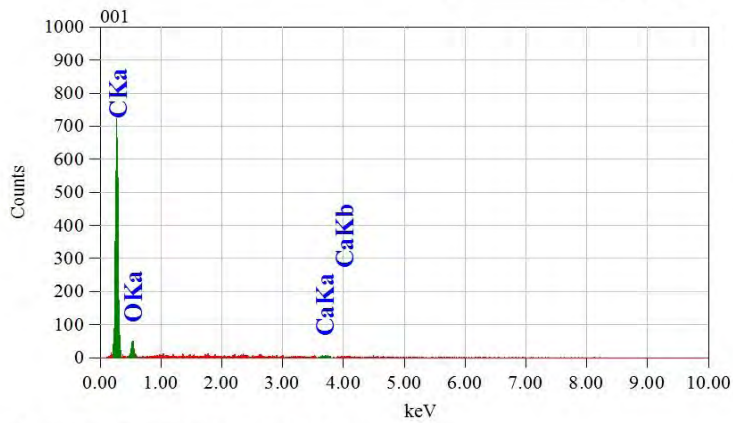
A.9 Additional SEM – EDX reports of raw carbon

View000



JEOLUSER 1/1

Title : IMG1
 Instrument : 7600F
 Volt : 5.00 kV
 Mag. : x 100
 Date : 2018/10/15
 Pixel : 512 x 384



Acquisition Parameter
 Instrument : 7600F
 Acc. Voltage : 10.0 kV
 Probe Current: 1.00000 nA
 PHA mode : T3
 Real Time : 30.07 sec
 Live Time : 30.00 sec
 Dead Time : 0 %
 Counting Rate: 194 cps
 Energy Range : 0 - 20 keV

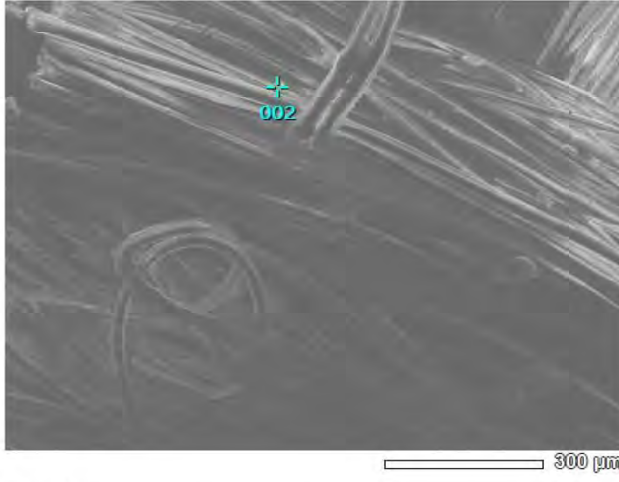
ZAF Method Standardless Quantitative Analysis

Fitting Coefficient : 0.1127

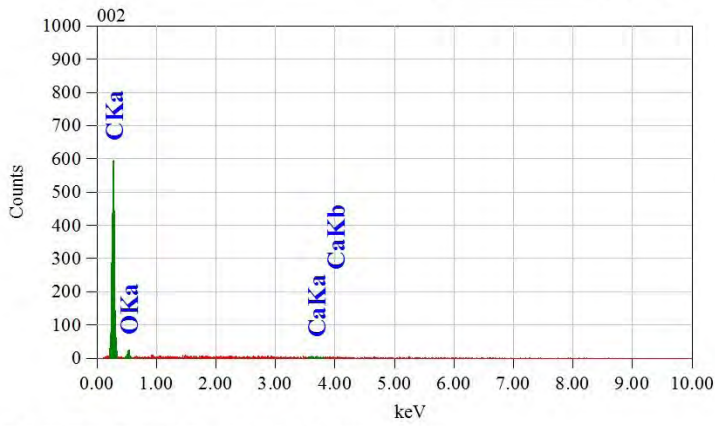
Element	(keV)	Mass%	Sigma	Atom%	Compound	Mass%	Cation	K
C K	0.277	86.27	0.13	89.77				91.8640
O K	0.525	12.69	0.26	9.91				6.9231
Ca K*	3.690	1.04	0.18	0.32				1.2129
Total		100.00		100.00				

View000

JEOLUSER 1/1



Title : IMG1
 Instrument : 7600F
 Volt : 5.00 kV
 Mag. : x 100
 Date : 2018/10/15
 Pixel : 512 x 384



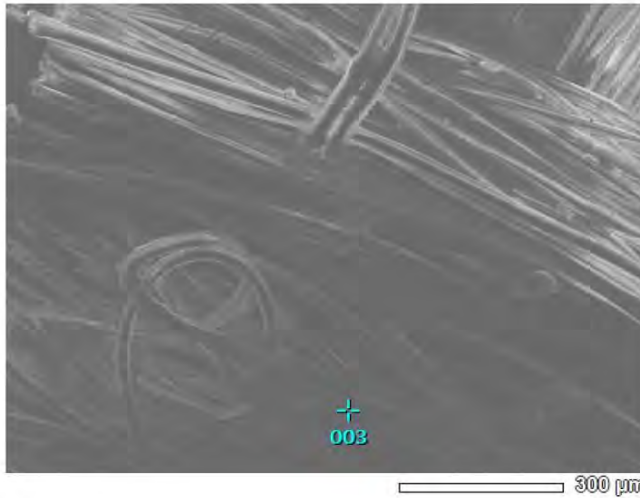
Acquisition Parameter
 Instrument : 7600F
 Acc. Voltage : 10.0 kV
 Probe Current: 1.00000 nA
 PHA mode : T3
 Real Time : 30.05 sec
 Live Time : 30.00 sec
 Dead Time : 0 %
 Counting Rate: 168 cps
 Energy Range : 0 - 20 keV

ZAF Method Standardless Quantitative Analysis
 Fitting Coefficient : 0.1129

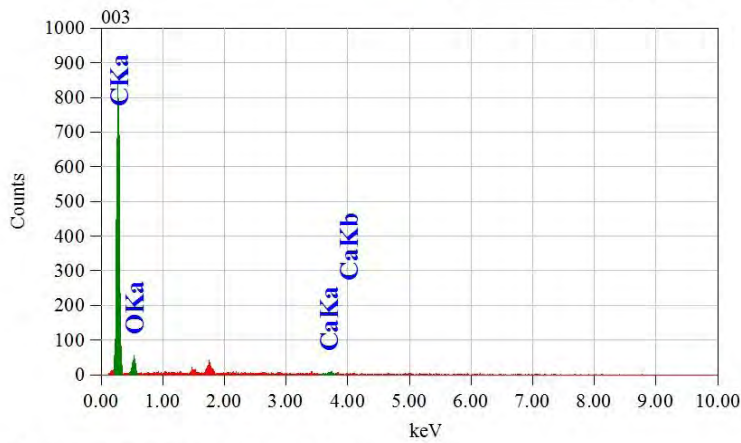
Element	(keV)	Mass%	Sigma	Atom%	Compound	Mass%	Cation	K
C K	0.277	92.27	0.16	94.19				96.0712
O K	0.525	7.47	0.24	5.73				3.6403
Ca K*	3.690	0.26	0.23	0.08				0.2885
Total		100.00		100.00				

View000

JEOLUSER 1/1



Title : IMG1
 Instrument : 7600F
 Volt : 5.00 kV
 Mag. : x 100
 Date : 2018/10/15
 Pixel : 512 x 384



Acquisition Parameter
 Instrument : 7600F
 Acc. Voltage : 10.0 kV
 Probe Current: 1.00000 nA
 PHA mode : T3
 Real Time : 30.07 sec
 Live Time : 30.00 sec
 Dead Time : 0 %
 Counting Rate: 240 cps
 Energy Range : 0 - 20 keV

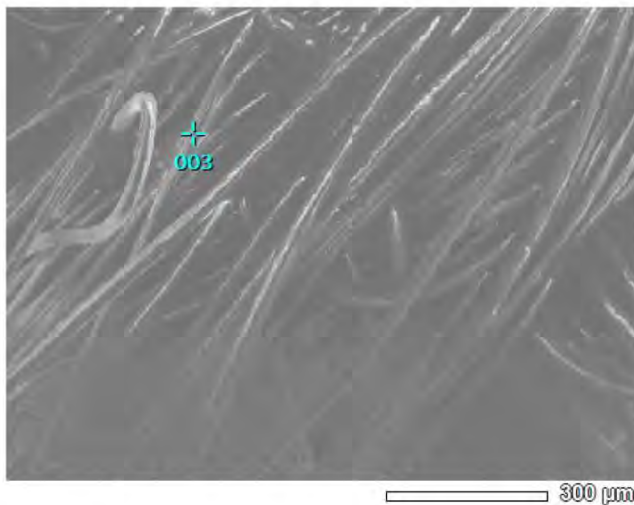
ZAF Method Standardless Quantitative Analysis

Fitting Coefficient : 0.1190

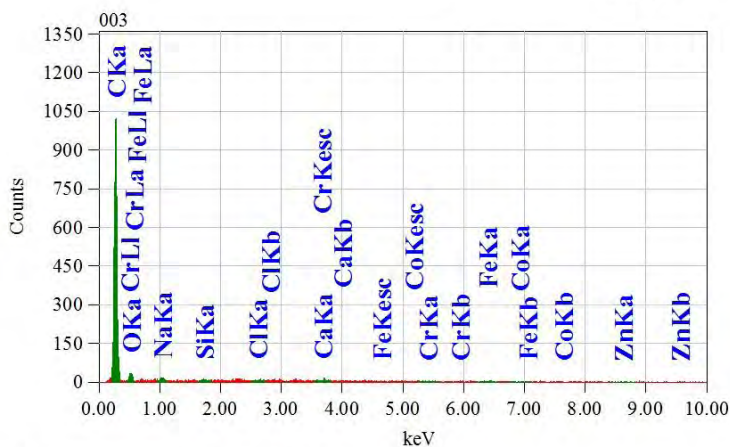
Element	(keV)	Mass%	Sigma	Atom%	Compound	Mass%	Cation	
C K	0.277	87.88	0.12	90.91				93.1309
O K	0.525	11.43	0.24	8.88				6.0779
Ca K*	3.690	0.69	0.16	0.21				0.7912
Total		100.00		100.00				

View000

JEOLUSER 1/1



Title : IMG1
 Instrument : 7600F
 Volt : 5.00 kV
 Mag. : x 100
 Date : 2019/01/28
 Pixel : 512 x 384



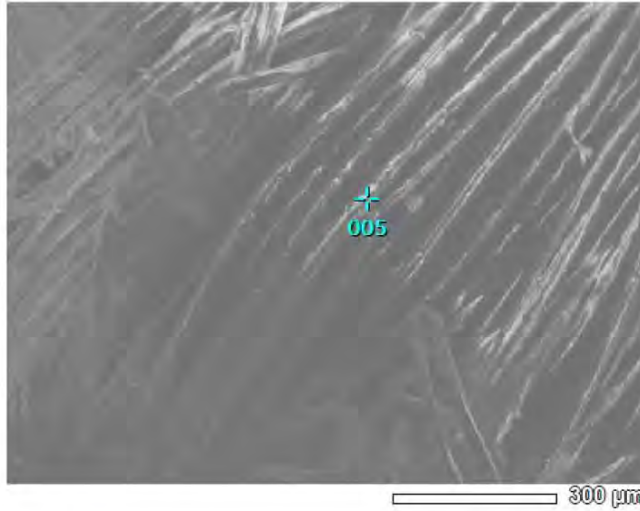
Acquisition Parameter
 Instrument : 7600F
 Acc. Voltage : 15.0 kV
 Probe Current: 1.00000 nA
 PHA mode : T3
 Real Time : 30.08 sec
 Live Time : 30.00 sec
 Dead Time : 0 %
 Counting Rate: 308 cps
 Energy Range : 0 - 20 keV

ZAF Method Standardless Quantitative Analysis
 Fitting Coefficient : 0.1028

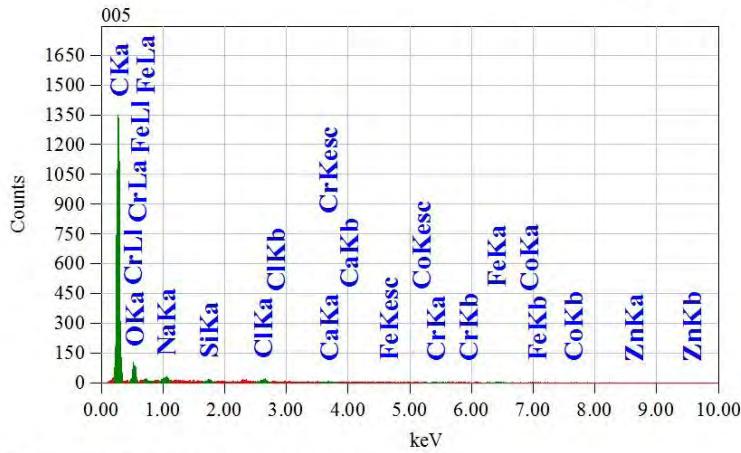
Element	(keV)	Mass%	Sigma	Atom%	Compound	Mass%	Cation	K
C	0.277	94.60	0.12	97.12				96.0883
O	0.525	2.79	0.08	2.15				1.0272
Na	1.041	0.40	0.05	0.22				0.4065
Si	1.739	0.07	0.04	0.03				0.0838
Cl	2.621	0.15	0.04	0.05				0.2078
Ca	3.690	0.33	0.07	0.10				0.4593
Cr								
Fe	6.398	0.58	0.11	0.13				0.6374
Co								
Zn	8.630	1.08	0.23	0.20				1.0897
Total		100.00		100.00				

View001

JEOLUSER 1/1



Title : IMG1
 Instrument : 7600F
 Volt : 10.00 kV
 Mag. : x 100
 Date : 2019/01/28
 Pixel : 512 x 384



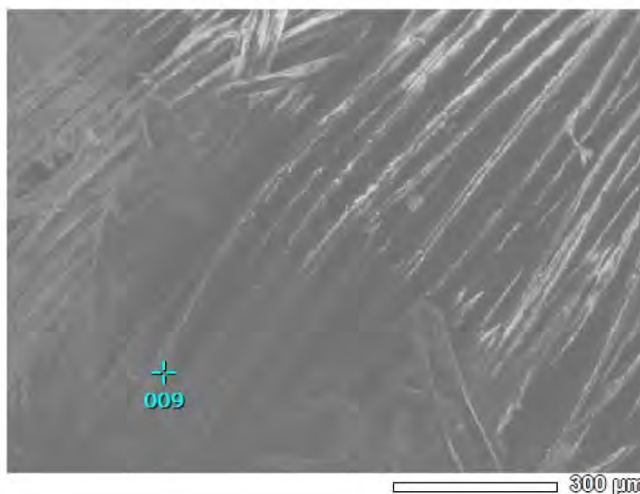
Acquisition Parameter
 Instrument : 7600F
 Acc. Voltage : 10.0 kV
 Probe Current: 1.00000 nA
 PHA mode : T3
 Real Time : 30.09 sec
 Live Time : 30.00 sec
 Dead Time : 0 %
 Counting Rate: 363 cps
 Energy Range : 0 - 20 keV

ZAF Method Standardless Quantitative Analysis
 Fitting Coefficient : 0.1037

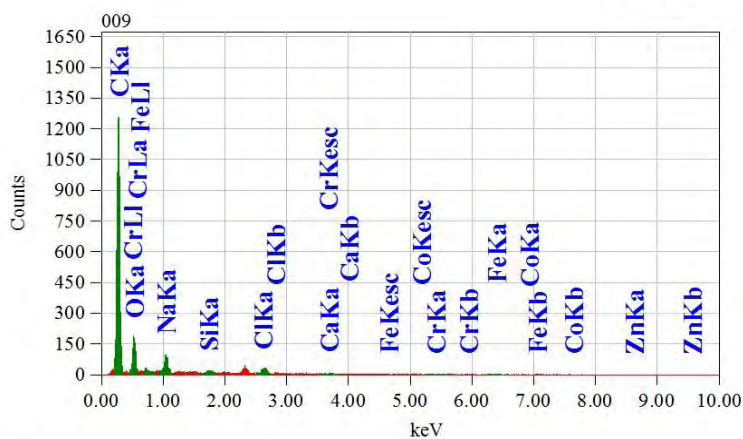
Element	(keV)	Mass%	Sigma	Atom%	Compound	Mass%	Cation	K
C	0.277	85.16	0.48	89.70				88.8733
O	0.525	11.52	0.44	9.11				7.0957
Na	1.041	0.68	0.07	0.37				0.7726
Si	1.739	0.45	0.07	0.20				0.5966
Cl	2.621	0.81	0.10	0.29				1.1184
Ca	3.690	0.08	0.08	0.02				0.0974
Cr	5.411	0.46	0.19	0.11				0.5225
Fe	6.398	0.85	0.36	0.19				0.9234
Co								
Zn								
Total		100.00		100.00				

View001

JEOLUSER 1/1



Title : IMG1
 Instrument : 7600F
 Volt : 10.00 kV
 Mag. : x 100
 Date : 2019/01/28
 Pixel : 512 x 384



Acquisition Parameter
 Instrument : 7600F
 Acc. Voltage : 10.0 kV
 Probe Current: 1.00000 nA
 PHA mode : T3
 Real Time : 30.11 sec
 Live Time : 30.00 sec
 Dead Time : 0 %
 Counting Rate: 407 cps
 Energy Range : 0 - 20 keV

ZAF Method Standardless Quantitative Analysis

Fitting Coefficient : 0.1015

Element	(keV)	Mass%	Sigma	Atom%	Compound	Mass%	Cation
C K	0.277	76.42	0.45	83.25			K
O K	0.525	17.44	0.48	14.26			78.6678
Na K*	1.041	2.22	0.11	1.26			13.2148
Si K*	1.739	0.30	0.06	0.14			2.8069
Cl K*	2.621	1.59	0.12	0.59			0.4453
Ca K	3.690	0.26	0.09	0.09			2.4857
Cr K*	5.411	0.04	0.15	0.01			0.3938
Fe K*	6.398	1.39	0.39	0.32			0.0568
Co L*	0.776	0.34	0.35	0.07			1.7082
Zn L*							0.2307
Total		100.00		100.00			

